2017-10-13

Regulation of the FGF/ERK Signaling Pathway: Roles in Zebrafish Gametogenesis and Embryogenesis

Jennifer M. Maurer
University of Massachusetts Medical School

REGULATION OF THE FGF/ERK SIGNALING PATHWAY: ROLES IN ZEBRAFISH GAMETOGENESIS AND EMBRYOGENESIS

A Dissertation Presented

By

JENNIFER M. MAURER

Submitted to the Faculty of the

University of Massachusetts Graduate School of Biomedical Sciences, Worcester

in partial fulfillment of the requirements for the degree of

DOCTOR OF PHILOSOPHY

October 13, 2017

Department of Biochemistry and Molecular Pharmacology

REGULATION OF THE FGF/ERK SIGNALING PATHWAY: ROLES IN ZEBRAFISH GAMETOGENESIS AND EMBRYOGENESIS

A Dissertation Presented

By

JENNIFER M. MAURER

This work was undertaken in the Graduate School of Biomedical Sciences
Department of Biochemistry and Molecular Pharmacology
under the mentorship of

Charles Sagerström, Ph.D., Thesis Advisor

Peter Pryciak, Ph.D., Member of Committee

Jaime Rivera, Ph.D., Member of Committee

Alonzo Ross, Ph.D., Member of Committee

Kellee Siegfried-Harris, Ph.D., External Member of Committee

Roger Davis, Ph.D., Chair of Committee

Anthony Carruthers, Ph.D.,
Dean of the Graduate School of Biomedical Sciences

October 13, 2017

DEDICATION

To my loving husband Matthew – you have been by my side since the very beginning of graduate school and I would never have been to do this without you. Like we always say, you are the best part of my life, and I am so grateful for all of your love and support.

And to my parents – your encouragement and understanding was essential to my completion of this degree. Thank you for always listening to the ups and downs of my experiments and being ready to offer advice. I love you and thank you for your support throughout my education.

ACKNOWLEDGEMENTS

First and foremost, I would like to thank Charles. His mentorship has allowed me to grow as a scientist much more than I could have imagined when I first joined his lab as a rotation student. He created a productive lab environment where I was able to learn and develop more than just experimental skills. He has devoted so much time over the years to discussing and interpreting data with me and guiding my ideas for future experiments. I always left our Monday morning meetings encouraged to tackle the next week's experiments. And as I approached the completion of my degree, he has always been supportive of my future career goals.

Perhaps the most important people to thank are my fellow Sagerstöm lab members. You guys have seen entire course of this project, including all of the failed experiments and frustrations. I would never have been able to complete this work without our helpful discussions and intense troubleshooting. Priya and Özge – you ladies have become some of my closest friends over the years and I've loved working with you (even if we were always complaining about *in situs*). Will – your computer skills and ability to always make us laugh in the lab have been invaluable to me. Franck – you are a wonderful post-doc mentor and I appreciate all the time you took to explain protocols and concepts to me. I also have to thank Denise and Steve who were both here during my early days in the lab. Their guidance got me started on the right foot – Denise taught me everything there is to know about zebrafish and Steve assisted with my early

CRISPR work. You all have made this lab a wonderful place to do my graduate work, and I cannot thank you guys enough.

I would like to thank my TRAC – Roger Davis, Peter Pryciak, Jaime Rivera, and Alonzo Ross – for their years of attending my talks and meetings. I appreciate all of their helpful ideas, discussions, and time. I'd also like to thank Kellee Siegfried-Harris for joining my DEC and taking time to come to Worcester for my defense.

Finally, I must thank my family. Thank you to my husband Matthew for providing me with support even during the hardest times. Thank you to my parents and sister for your unconditional love and encouragement. You made this possible for me, and I can never thank you enough.

ABSTRACT

Signaling cascades, such as the extracellular signal-regulated kinase (ERK) pathway, play vital roles in early vertebrate development. Signals through these pathways are initiated by a growth factor or hormone, are transduced through a kinase cascade, and result in the expression of specific downstream genes that promote cellular proliferation, growth, or differentiation. Tight regulation of these signals is provided by positive or negative modulators at varying levels in the pathway, and is required for proper development and function. Two members of the dual-specificity phosphatase (Dusp) family, *dusp6* and *dusp2*, are believed to be negative regulators of the ERK pathway and are expressed in both embryonic and adult zebrafish, but their specific roles in gametogenesis and embryogenesis remain to be fully understood.

Using CRISPR/Cas9 genome editing technology, we generated zebrafish lines harboring germ line deletions in *dusp6* and *dusp2*. We do not detect any overt defects in *dusp2* mutants, but we find that approximately 50% of offspring from homozygous *dusp6* mutants do not proceed through embryonic development. These embryos are fertilized, but are unable to proceed past the first zygotic mitosis and stall at the one-cell stage for several hours before dying by 10 hours post fertilization. We demonstrate that *dusp6* is expressed in the gonads of both male and female zebrafish, suggesting that loss of *dusp6* causes defects in germ cell production. Notably, the 50% of homozygous *dusp6* mutants that complete the first cell division appear to progress through embryogenesis normally and give rise to fertile adults.

The fact that offspring of homozygous *dusp6* mutants stall at the one-cell stage, prior to activation of the zygotic genome, suggests that loss of *dusp6* affects gametogenesis. Further, since only approximately 50% of homozygous *dusp6* mutants are affected, we postulate that ERK signaling is tightly regulated and that *dusp6* is required to keep ERK signaling within a range that is permissive for gametogenesis. Lastly, since *dusp6* is expressed throughout zebrafish embryogenesis, but *dusp6* mutants do not exhibit defects after the first cell division, it is possible that other feedback regulators of the ERK pathway compensate for loss of *dusp6* at later stages.

TABLE OF CONTENTS

LIST OF FIGURES

LIST OF TABLES

CHAPTER I: INTRODUCTION

The process of embryonic development involves complex communication between cells as they proliferate and differentiate. A wide range of methods for communicating signals between cells exist in eukaryotes, but some of the most ubiquitous are the mitogen-activated protein (MAP) kinase signal transduction pathways. These central pathways allow cells to process and respond to multiple simultaneous inputs, including those from growth factors, hormones, cytokines, and environmental stresses. Activation of a MAP kinase pathway results in increased morphological organization and cellular diversity by coordinating cell-specific activities such as gene expression, cell cycle control, apoptosis, motility, survival, and metabolism. The proper timing and management of these cellular events is critical to successful development, thus making MAP kinase pathways significant contributors to gametogenesis and embryogenesis.

The ERK Signaling Pathway

In eukaryotic cells, there are three primary MAP kinase signaling pathways: c-Jun N-terminal kinase (JNK), p38 mitogen-activated protein kinase (p38), and extracellular regulated kinase (ERK). The JNK pathway has been extensively studied in response to stress conditions, such as DNA damage, inflammatory cytokines, and UV irradiation, and also has known roles in transducing apoptotic and survival signals (reviewed in [1]). Similarly, the p38 kinase pathway has a minimal and inconsistent response to growth factors, but strongly responds to stress signals. In the context of the immune system where it

has been extensively studied, the p38 pathway modulates neutrophil and macrophage response and T cell differentiation (reviewed in [1]). In contrast to the JNK and p38 pathways, the ERK pathway strongly responds to growth factors and has a very large number of target substrates, including transcription factors, membrane proteins, and cytoskeletal components. During embryonic development, the ERK pathway activates proteins involved in cell proliferation, angiogenesis, cell migration, cell cycle regulation, and survival (reviewed in [1]). Many outcomes of the ERK pathway have been extensively studied, including its crosstalk interactions with the other MAP kinase pathways, but certain aspects of its regulation and role in early patterning of the embryo remain unclear. Accordingly, the remainder of this work will focus on the ERK pathway, the proteins responsible for its regulation, and its ability to control developmental processes from gamete production to neuronal differentiation.

Activation and components of the ERK signaling pathway

Cell surface receptors for various signaling molecules lie upstream of the ERK signaling pathway. Secreted ligands, such as fibroblast growth factors (FGFs), epidermal growth factors (EGFs), platelet-derived growth factors (PDGFs), bone morphogenetic proteins (BMPs), and WNTs, can act over large distances to promote intracellular signaling through MAP kinase pathways in appropriate cells. While all of these morphogens have well-studied roles in embryonic development and patterning, FGF signaling is particularly interesting due to its presence in key areas of the developing zebrafish embryo, including

the hindbrain, eye, and tailbud, and its predominant signaling through the ERK pathway. The majority of this work will discuss FGF-dependent activation of the ERK pathway (Figure 1.1).

The receptors for many signaling ligands, including FGFs, are receptor tyrosine kinases. There are four FGF receptors (FGFRs) in vertebrates, all of which have a similar structure. Each contains three ligand-binding Ig-like domains, an acidic box, a heparin-binding domain, a single transmembrane domain, and an intracellular tyrosine kinase domain (reviewed in [2]). These receptors will dimerize and trigger auto-phosphorylation upon binding of the ligand to the extracellular domain. This phosphorylation then recruits several adaptor proteins including Frs2 and Grb2. These proteins facilitate the activation of the small G-protein Ras, which in turn, transduces the signal to the ERK pathway. In the same manner as the JNK and p38 pathways, the core of the ERK signaling pathway consists of a tri-level kinase cascade. Following Ras activation, a MAP kinase kinase kinase called Raf phosphorylates and activates a MAP kinase kinase called MEK. MEK then phosphorylates and activates the MAP kinase ERK. These three kinases are highly conserved evolutionarily and provide various levels for signal amplification and regulation (reviewed in [3]).

Upon activation, ERK moves into and accumulates in the cell nucleus. This movement allows access to a large number of substrates to promote downstream outcomes.

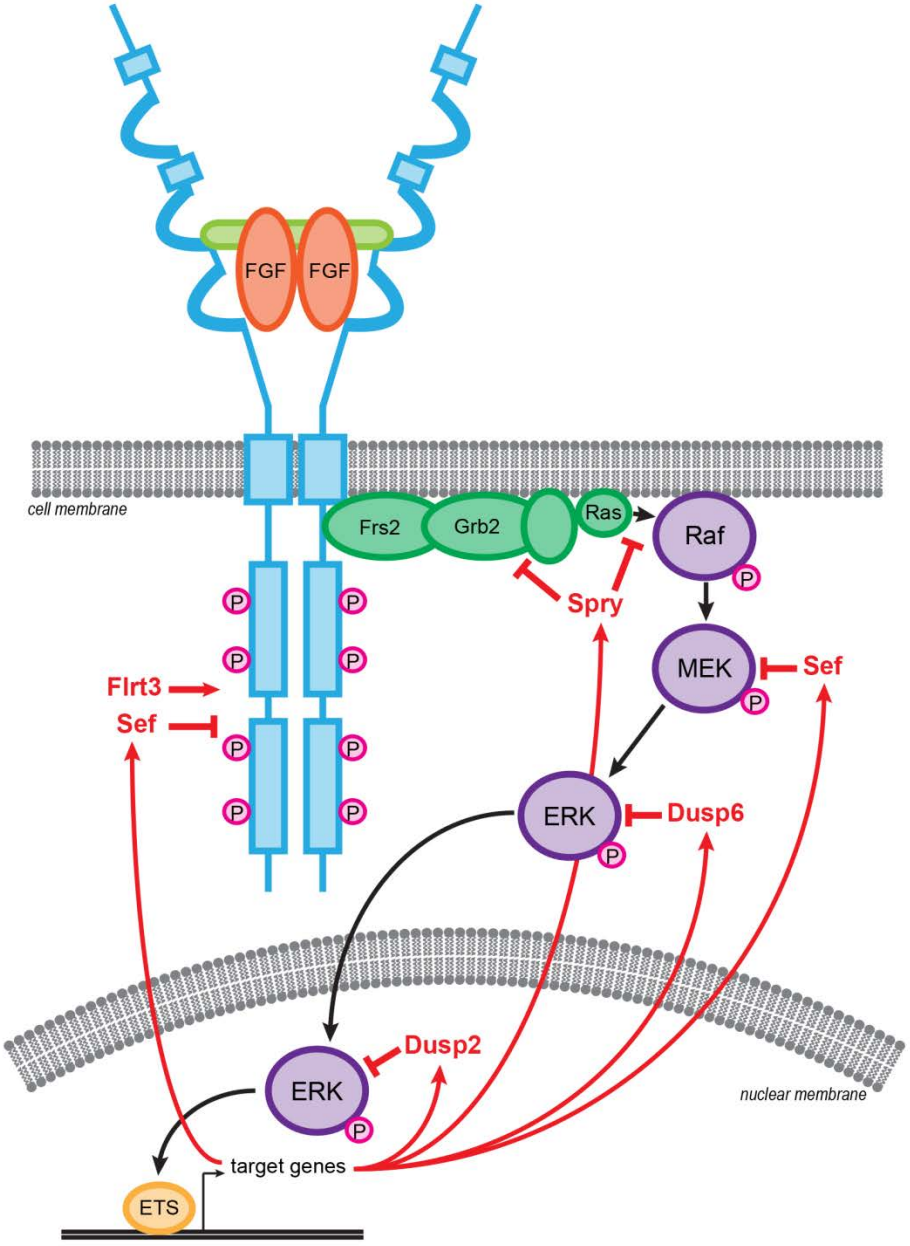

Figure 1.1. The FGF/ERK signaling pathway and its regulation
Schematic of the FGF and ERK signaling pathways. The transmembrane protein represents the FGFR (blue), which dimerizes upon binding to the FGF ligand (orange). Activation of this receptor recruits several adaptor proteins (green). These initiate the kinase cascade (purple), which results in the activation of ERK and its translocation to the cell nucleus. ERK then activates transcription factors, including those of the ETS family (yellow), to drive downstream gene expression. Many of the genes expressed downstream of the pathway provide positive or negative modulation on the pathway (red).

Downstream targets of FGF/ERK signaling

ERK is capable of phosphorylating and activating a vast number of targets in the nucleus. Many direct targets of ERK are transcription factors, and these proteins have their own unique targets that can be specific to different cell types or activating growth factors. As mentioned above, these targets facilitate and promote various cellular processes required for proper development, including proliferation, survival, apoptosis, differentiation, and migration. This allows ERK signaling to impact numerous aspects of development.

One of the most studied classes of proteins targeted by ERK is the ETS family. This family of transcription factors is defined by a highly conserved DNA-binding domain that structurally forms a winged-helix-loop-helix element and is unique to metazoans [4]. Following phosphorylation by active ERK, these proteins undergo a conformational change, exposing the DNA-binding domain (reviewed in [5]). ETS proteins have well-defined roles in directing signals from the ERK MAP kinase to specific target genes by interacting directly with gene promoters or with additional transcription factors. In the zebrafish, two examples of predominant ETS family members are Pea3 and Erm. These proteins are expressed downstream of FGF signaling in the early embryo, have partially redundant functions, and directly bind to the promoters of specific target genes [6–9].

Another group of proteins targeted by ERK consists of regulators of the FGF/ERK pathway. As with any other vital signaling pathway, the ERK pathway is held under many levels of regulation [2,10–15]. A subset of the proteins

responsible for this regulation is actually induced by the pathway and function as part of feedback loops. This group has been termed the ‘FGF-synexpression group’ as their expression patterns match the regions where FGF signaling is most active [2,10–16].

Regulation of the ERK signaling pathway

Due to the wide range of downstream outcomes of FGF/ERK signaling, it is logical that this pathway must be held under tight regulation. Signals must be able to be triggered and attenuated accordingly to ensure proper timing, duration, and location of downstream effects. Much of this regulation is provided by members of the FGF-synexpression group, with their expression being dependent on the same pathway they regulate (reviewed in [10,15,16]). This establishes a system of feedback loops.

The majority of the members of the FGF-synexpression group modulate the pathway by participating in negative feedback loops [2,10–16]. The first negative regulator, Sprouty (Spry), was discovered in *Drosophila* as an inhibitor of the Breathless FGF receptor during tracheal development [17]. Vertebrates have four Spry proteins homologous to the singular Spry in *Drosophila*. Additional studies in other species have confirmed the ability of Spry proteins to antagonize receptor tyrosine kinase signaling [18–25], although it remains unclear if all Spry proteins act at the same level in the pathway [17–20,24,25]. The role of Spry in zebrafish development is discussed in detail in Appendix A.

A second protein family that negatively regulates the FGF/ERK pathway is the dual-specific phosphatases (Dusps). The Dusp family proteins, also known as the MAP kinase phosphatases, remove phosphates from activated MAP kinases, resulting in their deactivation. There are at least ten Dusp proteins identified in vertebrates, all of which have different MAP kinase specificities and also belong to a larger family of protein phosphatases (reviewed in [26–30]). Some Dusp proteins are localized to the nucleus while others are present in the cytoplasm, implying that ERK is under their regulation in both cellular compartments. The cytoplasmic Dusps, including Dusp6/MKP3, are selective for ERK over the other MAP kinases, while the nuclear Dusps, including Dusp1/MKP1 and Dusp2/PAC-1, have varying specificities depending on the cellular environment. The Dusp proteins are discussed in further detail below.

Sef is an additional negative regulator of the FGF/ERK pathway. The Sef protein is believed to be a transmembrane protein and is conserved among vertebrates [31,32]. Work in zebrafish suggests that Sef acts at the level of MEK [32], while mammalian studies indicate that Sef interacts with the intracellular domain of the FGF receptor [31]. Loss of function and gain of function experiments demonstrate that Sef specifically antagonizes FGF/ERK signaling [32].

In contrast to the negative regulators, Flrt3 is a final member of the FGF-synexpression group and is believed to be a positive regulator of the pathway. A study in *Xenopus* shows that loss of function Flrt3 produces the same phenotypes as loss of FGF signaling [33]. Interestingly, this does not appear to

be true in zebrafish where there is evidence that Flrt3 is not connected to the FGF signaling pathway [16].

In addition to modulation supplied by feedback loops of the FGF-synexpression group, the FGF/ERK pathway also receives input from other signaling pathways through crosstalk. It is believed that the different MAP kinase pathways exist in a dynamic balance by modulating each other [1,34]. It has also been shown that several pathway components can activate more than one MAP kinase, further complicating downstream signals. In addition to the MAP kinase pathways, other signaling pathways, such as PI3K/AKT, mTOR, WNT, and NFκB, can also contribute to the regulation of ERK signaling.

Known roles of FGF/ERK signaling in development across species

The FGF/ERK signaling pathway has been extensively studied in the context of embryonic development in many vertebrate species. The majority of roles for the pathway are very similar among species due to the high evolutionary conservation of the pathway components and targets. Species-specific genetic events, such as the genome duplications in zebrafish, have resulted in minor variations among roles for specific FGF ligands. Regardless of which ligand triggers the signal, many of the biological outcomes remain conserved.

Mice carrying null alleles have been generated for nearly all of the FGF ligands. Many of these mutations are lethal, with some individuals not surviving to birth or weaning. Of those knockouts that are viable, most have some developmental abnormalities, including defects in heart and muscle repair,

ineffective metabolism of vitamins and lipids, and impaired development of the kidneys, inner ear, hair, facial features, hindbrain, and other organs (reviewed in [35]). Knockouts of the FGFRs result in defects in mesoderm and endoderm specification in the early embryo and lead to embryonic lethality before E9.5 (reviewed in [36]). A role for the pathway has even been identified in pre-implantation cell fate choices in cows and humans [37]. Additionally, mice carrying null alleles for ERK1/2 are viable, but completely infertile [38,39]. Activating mutations in Ras have been shown to impair ovulation and decrease fertility [40]. The wide range of phenotypes seen with these mutations demonstrates the broad involvement of FGF signaling in many mammalian developmental processes.

In *Xenopus*, chick, and zebrafish, disruptions to either FGF ligands or the FGFRs result in defects in gastrulation, mesoderm specification, somitogenesis, axis definition, spinal cord elongation, and muscle development (reviewed in [36]). As an example, the treatment of zebrafish embryos with a pharmacological inhibitor of FGFRs results in an imbalance between ERK and WNT signaling in the tailbud causing defects in axis elongation and segmentation [41]. In these non-mammalian species, recent investigations have emphasized the role of FGF/ERK signaling in neurodevelopment. The processes of neural plate patterning, maintenance of neural stem cells, axon pathfinding, and synapse formation have all been linked to the FGF pathway (reviewed in [42,43]). As an example, the expression of dominant negative FGFR4 or the knockdown of FGF8 by anti-sense morpholino oligo (MO) in *Xenopus* blocks neural induction

and reduces the size of the hindbrain [44,45]. The pharmacological inhibition of FGFRs in chick similarly prevents neural development [46]. In the zebrafish, FGF signaling disruptions result in severe patterning and neuronal defects in the hindbrain [47,48]. The role of FGF/ERK signaling specifically in the zebrafish hindbrain will be discussed in further detail below.

In humans, FGF signaling mutations contribute to a variety of congenital disorders and metabolic diseases. Loss of function mutations in the FGF ligands have been associated with specific mental retardation diseases, neurodegenerative disorders, microtia and microdontia, hypogonadotropic hypogonadism, cleft palate, and aplasia of the salivary glands (reviewed in [35]). Conversely, fatty liver disease, type 2 diabetes, obesity, Cushing's syndrome, and renal failure have been connected to inappropriate increases in signaling through the FGF/ERK pathway (reviewed in [35]). Additionally, activating mutations of the ERK pathway play a critical role in the development of many cancers due to the stimulation of cancer cell proliferation and metastasis (reviewed in [49]). The range and severity of these disorders further illustrates the importance of the FGF/ERK signaling pathway throughout the animal kingdom.

The Role of FGF/ERK Signaling in Developing Hindbrain of the Zebrafish

The hindbrain is responsible for controlling vital functions such as heartbeat, respiration, and blood pressure. It also gives rise to the cranial nerves

that control the eye, jaw, and face. Hindbrain structure is highly conserved among vertebrate species at the morphological and gene expression level. Shortly after gastrulation in the zebrafish, the presumptive hindbrain segments into eight compartments, called rhombomeres (r) (reviewed in [50]). Each rhombomere is genetically distinct and will develop a unique combination of mature neurons. The *hox* genes are major drivers of early hindbrain patterning, but signaling pathways including FGF, retinoic acid, BMP, WNT, and sonic hedgehog also make significant contributions (reviewed in [50–53]).

Emergence of the r4 FGF signaling center

As the hindbrain develops, the rhombomeres do not appear in an anterior-to-posterior order, but instead form as specific genetic events occur in each compartment. In the zebrafish, the center of the hindbrain is specified early, causing r4 to arise first, followed by the r5 (reviewed in [50]). The anterior rhombomeres are defined next, and finally the more posterior compartments are the last to form. At the onset of these segmentation events, the two predominant FGF species, *fgf3* and *fgf8*, are strongly expressed in presumptive r4 [54]. The four FGFRs are expressed throughout the central hindbrain region at the same time [55], and the downstream signals triggered by these ligands promote the development of the surrounding rhombomeres by regulating specific transcription factors [47,54,56]. This abundance of signaling has earned r4 recognition as a local organizer and signaling center of the early embryo (reviewed in [43]). Additional organizing centers emerge at the anterior neural ridge and the mid-

hindbrain boundary (MHB), which contribute to the development of the telencephalon and the cerebellum respectively.

Mis-patterning of the hindbrain in the absence of FGF/ERK signaling

Based on the early understanding of the importance of FGF signaling and the strong presence of FGF ligands in presumptive r4, many studies have examined the effects of removing FGF signaling from the hindbrain. The zebrafish mutant *acerebellar* expresses a null *fgf8* allele, as a point mutation in a splice site results in the exclusion of exon 2 from the *fgf8* transcript [57]. These mutants have only mild patterning phenotypes, despite severe cognitive impairment seen in embryos older than two days. A similar mutant line for *fgf3* has not been generated, so several groups have combined the use of the *acerebellar* line and an anti-sense MO targeted against *fgf3* to remove both ligands [54,58]. Others have utilized two separate MOs, one inhibiting *fgf8* and one inhibiting *fgf3* [47,58,59], a dominant negative FGFR [59], or a pharmacological inhibitor of FGFRs [47] to block the signaling pathway. These studies conclude that signaling triggered by these ligands is required for proper rhombomere patterning (Figure 1.2). In the absence of signaling, the territories of r5 and r6 are lost and r3 is reduced [47,54,58,59]. The neurons that are normally born in these regions are also absent. In the place of r5 and r6, there is an anterior shift of the more posterior hindbrain structures, including the T interneurons and the facial, glossopharyngeal, and vagal cranial nerves of r7 [47,54]. Interestingly, the size, gene expression, and neurons of r4 are unaffected

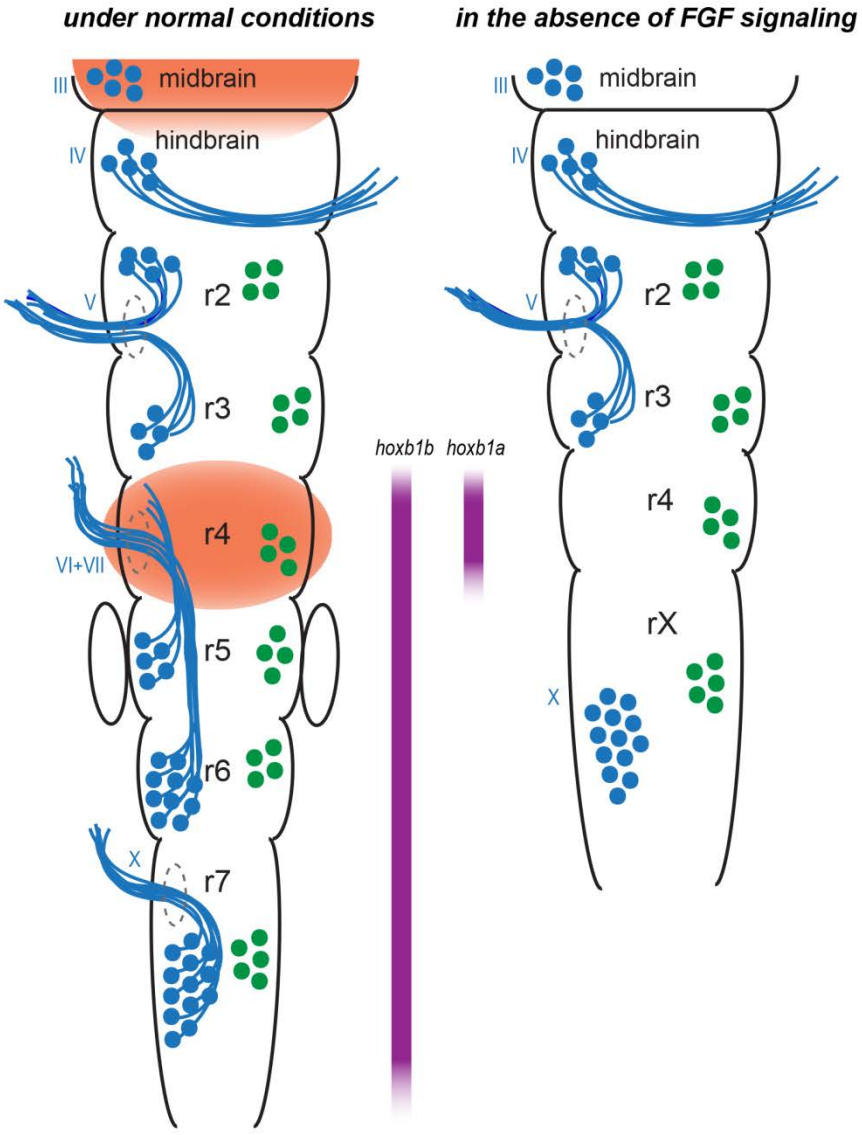

Figure 1.2. Proper hindbrain patterning depends on the FGF signaling pathway
Schematic of the zebrafish hindbrain, divided into rhombomeres and showing the mature neurons that will develop in each compartment. The reticulospinal neurons (green) develop as one cluster in each rhombomere. The cranial motor neurons (blue) develop throughout the hindbrain, with their projections exiting in specific rhombomeres (III, oculomotor; IV, trochlear; V, trigeminal; VI+VII, abducens and facial motor neurons; X, vagus). FGF ligands are expressed at signaling centers in r4 and at the MHB (orange). The *hox* genes, *hoxb1b* and *hoxb1a*, are expressed in the caudal hindbrain and r4 respectively (as represented by purple bars). Left panel shows proper hindbrain patterning under normal conditions. Right panel shows defective hindbrain patterning when FGF signaling is absent.

by the loss of signaling. Similar studies have shown that this is also true in chick [60]. This implies that while FGF ligands emanating from r4 are required for patterning the surrounding rhombomeres, the pathway is not required within r4. This is further discussed in Appendix B. The severity of this patterning defect demonstrates the significance of proper regulation of the FGF/ERK signaling pathway specifically in the hindbrain.

Dual-Specific Phosphatases and Their Regulation of the FGF/ERK Pathway

As mentioned above, the Dusp proteins dephosphorylate and inactivate ERK, and are thus key regulators of the FGF/ERK pathway.

The Dusp family

The Dusp family is unique among protein phosphatases as they are capable of dephosphorylating both serine/threonine and tyrosine residues on the same substrate. Since ERK activation requires dual phosphorylation on a conserved T-X-Y motif by MEK (reviewed in [61]), Dusp proteins are well-suited to modulate ERK activity. The ten Dusp proteins that act on MAP kinases can be sorted in three subfamilies based on cellular localization and target specificity (reviewed in [26,29,62]). The first includes Dusp1/MKP1, Dusp2/PAC-1, Dusp4/MKP2, and Dusp5, which are all localized to the nucleus and are induced by mitogen and stress signals. The second group contains Dusp6/MKP3, Dusp7/MKPX, and Dusp9/MKP4, which are all cytoplasmic proteins shown to

have substrate preference for ERK over the other MAP kinases. The final group includes Dusp8, Dusp10/MKP5, and Dusp16/MKP7, which are all selective for JNK and p38 kinases.

Regardless of subfamily, all of the Dusp proteins share a common domain structure. The N-terminal portion contains an inactive rhodanese homology domain [63,64] and kinase interaction motif (reviewed in [27–29]). The positively charged arginine residues within the kinase interaction motif are believed to interact with the negative aspartic acid residues of the MAP kinase docking site to facilitate binding [65]. This physical arrangement of these charged residues varies between the MAP kinases, allowing Dusp proteins to selectively interact with them.

The C-terminal portion of Dusp proteins contains the dual-specific phosphatase catalytic domain. This highly conserved domain is similar to that of other protein phosphatases. It contains critical cysteine, arginine, and aspartic acid residues that initiate catalysis and stabilize the intermediate (reviewed in [27,29]). However, this domain creates a unique catalytic pocket that is shallow and wide, allowing it to accommodate two phosphorylated residues simultaneously [66]. For several Dusp proteins, binding to substrate significantly increases the catalytic activity of the phosphatase (reviewed in [26,29]).

As previously discussed, several Dusp proteins are expressed downstream of the FGF/ERK pathway and are part of the FGF-synexpression group. Due to their expression in fundamental regions of the zebrafish body and

minimal understanding of their role in embryonic development, Dusp2 and Dusp6 will be the focus of the remainder of this work.

Dusp2

Dusp2 was first identified in peripheral blood T cells activated by mitogens and in other T cells activated by antigen presentation [67]. It was previously called PAC-1 for phosphatase of active cells for this reason. Initial immunofluorescent staining showed Dusp2 localized to the nucleus and was very strongly expressed in T cells approximately four hours after antigen-activation [67]. This expression was later shown to be dependent on ERK signaling [68]. Subsequent *in vitro* studies showed that Dusp2 selectively acts on ERK and that this activity is specific, as Dusp2 did not dephosphorylate other tyrosine- or serine/threonine-phosphorylated proteins, including MEK [69]. Further *in vitro* work confirmed ERK as the substrate preference for Dusp2 and demonstrated that the catalytic activity of Dusp2 is significantly increased following the binding of Dusp2 and ERK [70]. Interestingly, the specificity of Dusp2 appears to vary based on cellular context, as there is evidence that Dusp2 is able to act on p38 *in vitro* [71] and on JNK *in vivo* in mouse bone marrow-derived mast cells [72].

Consistent with its expression in activated T cells, *Dusp2*$^{-/-}$ mice have a significantly reduced inflammatory response, and this is suggested to be the result of mis-regulated crosstalk between ERK and JNK pathways [72]. Despite this involvement in inflammatory response, Dusp2 has been shown to play no role in obesity-associated inflammation [73].

Although *Dusp2* expression is undetectable in the mouse brain [67], *dusp2* is strongly expressed in a rhombomere-specific pattern in the zebrafish hindbrain [7,74]. *In situ* RNA hybridization experiments performed in a time course show that *dusp2* is restricted to r4 of the zebrafish hindbrain between 10 and 14 hours post fertilization (hpf) (Figure 1.3). Since *dusp2* expression is downstream of ERK signaling, and the primary method of ERK activation in the early hindbrain is through the FGF pathway, it is likely that *dusp2* is also downstream of FGF. Additionally, *dusp2* was found to be induced by over-expression of *hoxb1b*, a transcription factor of the *hox* family and a key driver of embryonic patterning and development in the zebrafish [74]. Further details regarding regulation of *dusp2* expression are discussed in Appendix C. While this suggests a role for *dusp2* in hindbrain development, there is no supporting evidence at this time.

Dusp6

Dusp6, previously known as MKP3, was first identified in skin and kidney fibroblast cells as one of the first dual-specific phosphatases [75]. The original study immediately noted that Dusp6 is not inducible by stress, is localized in the cytoplasm, and shows substrate preference for ERK over JNK and p38 kinases [75]. More recent studies have confirmed the selective action of Dusp6 on ERK [76,77], have demonstrated the requirement of FGF/ERK signaling for Dusp6 induction [77–79], and have extensively investigated the mechanism of recognition and activation upon binding ERK (reviewed in [29]). Similar to Dusp2, there is evidence that Dusp6 can act on JNK in specific cellular contexts, as was

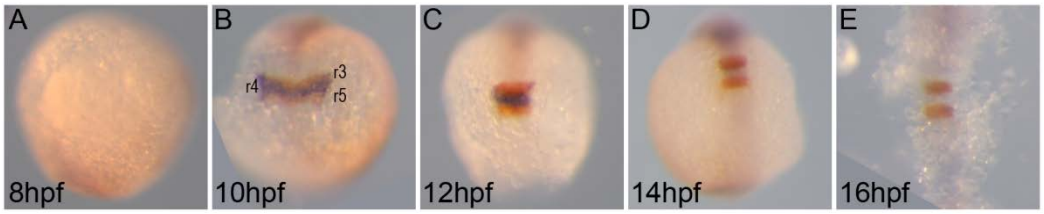

Figure 1.3. Expression of *dusp2* in the zebrafish hindbrain
Wildtype embryos were assayed by *in situ* hybridization for *dusp2* (blue stain) and *krox20* (red stain) marking r3 and r5 at 8hpf (**A**), 10hpf (**B**), 12hpf (**C**), 14hpf (**D**), and 16hpf (**E**). All embryos are in dorsal view of the hindbrain with anterior to the top.

shown in cultured rat astrocytes [80]. *Dusp6* expression in both mice and zebrafish overlaps with regions of the embryo that are known to contain active FGF/ERK signaling, including the pharyngeal arches, limb buds, somites, and otic vesicle in the mouse [81] and the forebrain, MHB, r4 of the hindbrain, and tailbud in zebrafish [82].

Consistent with this role of Dusp6 dephosphorylating ERK, loss of function *Dusp6* mice exhibit increased phospho-ERK (pERK) and expression of Erm [81,83]. *Dusp6*$^{-/-}$ mutant mice also show increased postnatal lethality, with a significant decrease in homozygous mutant pups surviving to weaning age, skeletal dwarfism, craniosynostosis, hearing loss, and increased heart size [81,83]. Many of these defects are also characteristic of FGFR activating mutations.

Loss of function *dusp6* zebrafish have also been studied with the use of MOs, but their phenotypes differ from those seen in the mouse mutant. Embryos injected with MO targeted to *dusp6* exhibit a dorsalization phenotype, marked by decreased expression of ventral marker *bmp4*, increased expression of dorsal marker *chordin*, expansion of neural domains, and a loss of trunk structures [84]. These embryos phenocopy embryos over-expressing the *fgf8* ligand [85], providing evidence that the role of Dusp6 in negatively modulating FGF/ERK signaling is conserved in zebrafish. However, recent studies have questioned the reliability of MOs [86–89], and thus, these phenotypes will need to be confirmed in mutant lines.

Due to its specific control of the ERK signaling pathway, DUSP6 has been extensively studied in relation to human cancer progression. *DUSP6* mutations have been associated with leukemias, melanomas, lung cancers, and pancreatic cancers, in which the absence of DUSP6 commonly occurs with activating Ras mutations, resulting in hyperactivation of the ERK pathway (reviewed in [62]). Additionally, *DUSP6* mutations have been connected to congenital hypogonadotropic hypogonadism [90]. This rare disorder is marked by gonadotropin deficiency and low levels of follicle stimulating hormone (FSH) and luteinizing hormone (LH), resulting in abnormal pubertal development and infertility. While this disorder is genetically heterogeneous, most of the associated genes encode modulators of FGF/ERK signaling.

Here in this work, I will study the role of *dusp6*, as well as *dusp2*, in modulating the FGF/ERK signaling pathway during gametogenesis and embryogenesis in the zebrafish by creating germ line mutants using the CRISPR/Cas9 genome editing system.

Use of the CRISPR/Cas9 Genome Editing System in Zebrafish

The recent use of the CRISPR/Cas9 system has allowed zebrafish research groups to efficiently generate mutations in their gene of interest [91]. The system was adapted from bacteria and archaea who use clustered, regularly interspaced, short palindromic repeats (CRISPRs) to guide CRISPR-associated system (Cas) endonucleases to foreign genetic material as part of their innate immune system. The CRISPR/Cas9 system has greatly increased the ease of

use and transmission of germ line mutations over previous genome editing systems, namely zinc-finger nucleases (ZFNs) and transcription activator-like effector nucleases (TALENs). At this time, the system has been used extensively in zebrafish and is continually being optimized further for greater efficiently and reduced off-target effects.

CRISPR guide RNAs can be targeted to any genomic sequence and only require the presence of a protospacer adjacent motif. Upon binding of the guide RNA to the target sequence, the Cas9 nuclease will introduce a double strand DNA break. In many cases, this lesion is then repaired through non-homologous end joining (NHEJ), but this method is error-prone and may create small indel mutations leading to shifts in the reading frame. A single indel mutation that results in a premature stop codon is usually sufficient to generate a loss of function allele. Moreover, the idea of utilizing two target sites within the same gene to cause large-scale whole-gene deletions has been suggested, and this is the approach presented in this work.

Contribution of this Work to the Field

Despite extensive study of the FGF/ERK signaling pathway and its proper regulation by Dusp proteins, specific roles for *dusp2* and *dusp6* in zebrafish embryonic development have not been clearly defined. The severity of defects observed when FGF/ERK signaling is disrupted proves that tight regulation of this pathway is vital to successful development. Understanding how the

modulators of this pathway function and interact with each other is of particular interest due to the pathway's association with various human congenital disorders and cancers.

The only known role for Dusp2 is within the context of the immune system and inflammatory response, yet it is strongly expressed in the early hindbrain under the potential control of one of the *hox* genes. Its rhombomere-restricted expression pattern suggests a role in patterning r4, but this remains to be demonstrated. The role of Dusp6 has been studied to a greater extent compared to Dusp2, but it is still not clear what effect loss of function *dusp6* will have on zebrafish embryos. There are significant differences between the phenotypes seen in genetic mice mutants and zebrafish morphants. Additionally, the role of these regulators in adult zebrafish is also not fully understood.

Here, through the use of germ line deletions in the *dusp2* and *dusp6* coding sequences, I aimed to discover functions for these phosphatases in the hindbrain or elsewhere in the developing embryo. Following the generation of these zebrafish lines, I find that only approximately 50% of offspring from homozygous *dusp6* mutants survive to the segmentation stages. In contrast, I do not detect any overt defects in the *dusp2* mutants. Further characterization of the *dusp6* mutant embryos shows that those that do not survive are fertilized, but arrest during the first zygotic mitosis and stall at the one-cell stage for several hours before dying. Remarkably, the 50% of mutants that are able to complete the first cell division appear healthy and continue through embryogenesis without any defects.

Since this defect occurs prior to the activation of the zygotic genome, I suggest that the loss of *dusp6* is actually affecting gametogenesis in the adults. I further demonstrate the presence of *dusp6* in both male and female gonads, supporting this idea. As only half of the offspring are affected, I hypothesize that ERK signaling is tightly regulated in the gonads, as in other regions of the body, and that *dusp6* is required to keep ERK signaling within a permissive range for successful gametogenesis. I also discuss the ability of other feedback regulators of the ERK pathway to compensate for the loss of *dusp6* at later stages of embryogenesis. Taken together, the work presented here provides new insight into the roles of these two phosphatases both in the embryo, where it appears they are not essential, and in the adult during gametogenesis, where these results suggest *dusp6* is required.

CHAPTER II:
A REQUIREMENT FOR DUAL-SPECIFICITY PHOSPHATASE 6 IN ZEBRAFISH GAMETOGENESIS

Jennifer M. Maurer and Charles G. Sagerström

This chapter has been submitted as a manuscript to BMC Developmental Biology and is currently under review.

BACKGROUND

The extracellular signal-regulated kinase (ERK) pathway is a major signaling cascade that promotes proliferation and differentiation in many different cell types. As one of the mitogen-activated protein (MAP) kinase pathways, the canonical ERK pathway receives signals from receptors for a growth factor or hormone, such as fibroblast growth factor (FGF), epidermal growth factor (EGF), and platelet-derived growth factor (PDGF), which then activates a MAP kinase kinase kinase (Raf), a MAP kinase kinase (MEK), and finally the MAP kinase ERK. Phosphorylated and activated ERK then moves into the cell nucleus, where it can activate transcription factors to initiate target gene expression. During early development, ERK signaling is active in several critical regions of the zebrafish embryo. For example, ERK signaling works cooperatively with Wnt signaling to promote trunk elongation and the formation of somites in the tailbud [41], and triggers the differentiation of lens fiber cells in the developing eye [92]. It has been demonstrated that ERK signaling is required for proper patterning, especially within the hindbrain, where the cascade is initiated by the FGF pathway, defines the forming rhombomere boundaries, and sets up the anterior-posterior axis [47,60,93,94]. Zebrafish embryos treated with an inhibitor of the FGF receptors upstream of ERK lack the fifth and sixth rhombomere (r5 and r6) of the hindbrain and the neurons that normally develop in those regions [47]. Similar to other major signaling pathways, the ERK pathway is able to induce the expression of its own regulators. Many such proteins, including members of the

dual-specificity phosphatase (Dusp) and Sprouty (Spry) families, Sef, and Flrt, are expressed downstream of the pathway [16]. These proteins interact with upstream pathway components or with ERK itself, and provide positive or negative feedback to modulate the signaling pathway [29,60,62,95].

Early embryonic patterning is also driven by the *hox* genes, a key family of homeodomain-containing transcription factors that control cell fate specification [96,97]. Notably, a microarrary screen identified a Dusp family member, *dusp2* (also called PAC-1 or wu:fj40g04), as a *hoxb1b*-inducible gene in zebrafish [74]. The Dusp family comprises a group of proteins that remove phosphates from both serine/threonine and tyrosine residues of MAP kinases, resulting in their inactivation. Previous work has shown that Dusp2 is an inducible, nuclear protein that has a strong specificity for ERK [29,67,69–72,98]. There is also evidence that Dusp2 is capable of dephosphorylating p38 *in vitro* [71] and JNK *in vivo* [72]. In accordance with it being *hoxb1b*-regulated, *dusp2* is expressed in rhombomere 4 (r4) of the hindbrain, a region that requires *hoxb1b* function. A very similar protein, Dusp6 (also called MKP3), is expressed in several regions of the early embryo, including in r4 where its expression overlaps with *dusp2* and *hoxb1b* [84]. In contrast to Dusp2, Dusp6 is a cytoplasmic protein and has confirmed roles in developmental signaling, including axial patterning, limb development, organ size regulation, and somite formation [78,81,84]. The fact that *dusp2* and *dusp6* are co-expressed with *hoxb1b* in r4, and that *dusp2* is *hoxb1b* inducible, suggests a potential role for *hox* genes in controlling ERK signaling. Loss of function *dusp2* mice were reported to develop normally, but

this was not analyzed in detail [72]. Loss of function *dusp6* mice and morphant zebrafish have been analyzed, and the effects in these animals mimic mutations that inappropriately active FGF receptors [81,84]. However, these phenotypes differ significantly between the two species. Notably, the analysis in zebrafish made use of anti-sense morpholino oligos (MOs), whose reliability has recently been called into question [86,87].

Here we used the CRISPR/Cas9 genome editing system to generate loss of function zebrafish mutants for both *dusp2* and *dusp6*. We do not detect any developmental defects in *dusp2* mutants, but find that embryos derived from homozygous *dusp6* mutant parents have reduced viability. These embryos are unable to undergo the first cell division and stall at the one-cell stage. Our results indicate that this phenotype is independent of the zygotic genome, and instead suggest that the gametes produced by adult *dusp6* mutants are defective.

METHODS

Zebrafish care

Wildtype Ekkwill and mutant zebrafish lines were raised in the University of Massachusetts Medical School Zebrafish Facility. All embryos were staged according to morphological criteria and hours or minutes post fertilization [99].

Zebrafish embryonic injections

Embryos were collected from natural matings immediately following fertilization. Collected embryos were aligned on an agarose mold and injected

with 1-2nl of injection mix using a borosil needle, micromanipulator, and dissecting microscope. For the injections of *fgf8* mRNA, a plasmid containing the full coding sequence of *fgf8* was *in vitro* transcribed. This mRNA was diluted in water and phenol red to a final concentration of 5-500ng/µl and injected into one-cell embryos.

Generation and injection of CRISPR guide RNAs

CRISPR target sites were selected based on their proximity to the start and stop codons of the coding sequence of the targeted gene, and also by the requirement for a protospacer adjacent motif (PAM) sequence (NGG) at the 3′ end of target site. We created and annealed oligos containing a T7 promoter sequence, the target sequence, and an additional constant region to create the template for the guide RNAs (Table 2.1). These templates were transcribed *in vitro* using T7 RNA polymerase (Promega) in a reaction containing transcription buffer (Promega), RNase inhibitor (Promega), and rNTPs. A linearized plasmid encoding Cas9 [100] was also transcribed *in vitro* using the Sp6 mMessage mMachine Kit (Ambion). The two guide RNAs targeting each gene were combined with *cas9* mRNA and phenol red, and 1-2nl of this mixture was injected into the cell of early one-cell stage embryos.

Table 2.1. Sequences of oligos to generate CRISPR guide RNAs

CRISPR	Target sequence [a]	PAM [b]	First oligo [c]	Second oligo [d]
dusp6-5′	GAGCCTCATGCTCCGGCGAC	GGG	TTAATACGACTCACTATAGGTCGCCGGAGCATGAGGCTCGGGGTTTTAGAGCTAGAAATAGCAAG	AAAAAAGCACCGACTCGGTGCCACTTTTTCAAGTTGATAACGGACTAGCCTTATTTTAACTTGCTATTTCTAGCTCTAAAAC
dusp6-3′	CTCGAGTCCACGTGAGGTCC	AGG	TTAATACGACTCACTATAGGACCTCACGTGGACTCGAGAGGGTTTTAGAGCTAGAAATAGCAAG	AAAAAAGCACCGACTCGGTGCCACTTTTTCAAGTTGATAACGGACTAGCCTTATTTTAACTTGCTATTTCTAGCTCTAAAAC
dusp2-5′	GGCGACCCTCTCGAGATCTC	AGG	TTAATACGACTCACTATAGGCGACCCTCTCGAGATCTCAGGGTTTTAGAGCTAGAAATAGCAAG	AAAAAAGCACCGACTCGGTGCCACTTTTTCAAGTTGATAACGGACTAGCCTTATTTTAACTTGCTATTTCTAGCTCTAAAAC
dusp2-3′	ACACTGTGACAGATCTACAA	AGG	TTAATACGACTCACTATAGACACTGTGACAGATCTACAAAGGGTTTTAGAGCTAGAAATAGCAAG	AAAAAAGCACCGACTCGGTGCCACTTTTTCAAGTTGATAACGGACTAGCCTTATTTTAACTTGCTATTTCTAGCTCTAAAAC

[a] Genomic sequence targeted by the guide RNA
[b] Protospacer adjacent motif (PAM) sequence in the genomic DNA recognized by Cas9
[c] Sequence of the first oligo used to create the guide template containing the T7 promoter sequence
[d] Sequence of the second oligo used to create the guide template containing the constant region

Identification of germ line mutations and genotyping

For both *dusp6* and *dusp2* mutants, the embryos injected with the guide RNAs and *cas9* mRNA mixture were raised as the F0 generation. At three months of age, these fish were individually crossed to a wildtype fish (Figure 2.3B-C). Half of each resulting clutch was raised to adulthood as the F1 generation. Genomic DNA was extracted from the embryos in the remaining half of the clutch to confirm activity of the guide RNAs. This genomic DNA was screened for deletions by PCR using primers that flank the region between the two guide RNA target sites (Figure 2.3A-C, Table 2.2). Amplification from mutant sequences containing large deletions will produce 400-600bp products (Figure 2.3B-C, Table 2.2, Table 2.3). In contrast, amplification from wildtype sequences

will produce products greater than 1kb and these fragments may not amplify well under the PCR conditions used. F1 adults derived from positive clutches were individually genotyped with fin clip DNA using the same PCR primers. To confirm that these fish were heterozygous, a second set of primers was used to amplify only the wildtype sequence where one or both primers were placed inside the deletion (Figure 2.3A, Table 2.2). F1 heterozygous fish were then crossed to generate homozygous mutants.

Table 2.2. Primer sequences to genotype mutants

Gene	PCR primers to detect mutant allele (F/R) [a]	Size of mutant band [b]	PCR primers to detect WT allele (F/R) [c]	Size of WT band [d]
dusp6	CGGTAGAGTGGCTGAAGGAG/ TCCCAAAAACAGGCAAGTCT	~564bp	GTTCCTCAAGCAGCAGTTCC/ AGAGGTTCTGGCTCCAGTGA	345bp
dusp2	GGAACAATATTGATTTGTGTCACC/ GTAGAGGTTCGGGGACACG	~392bp	CTTTCTTTTCCTGGGCAGTG/ GTAGAGGTTCGGGGACACG	811bp

[a] Sequence of the forward and reverse primers used to detect deletion alleles
[b] Approximate expected size of the PCR band if a CRISPR-induced deletion occurred
[c] Sequence of the forward and reverse primers used to detect the wildtype allele
[d] Expected size of the PCR band for the wildtype allele

Table 2.3. Characteristics of CRISPR guide RNAs targeting *dusp6* and *dusp2*

CRISPR guide	Target coordinate [a]	Target sequence [b]	Strand [c]	Size of mutant PCR band [d]	Mutagenesis rate [e]
dusp6-5'	Chr25:18233489	GAGCCTCATGCTCCGGCGAC	-	~564bp	2/23
dusp6-3'	Chr25:18231243	CTCGAGTCCACGTGAGGTCC	-		
dusp2-5'	Chr8:40589831	GGCGACCCTCTCGAGATCTC	+	~392bp	3/23
dusp2-3'	Chr8:40592681	ACACTGTGACAGATCTACAA	+		

[a] Target coordinate defined by the first nucleotide of the target sequence
[b] Genomic sequence targeted by the guide RNA
[c] Strand of genomic DNA which is targeted by the guide RNA
[d] Approximate expected size of the PCR band if a CRISPR-induced deletion occurred
[e] The number of F0 germ line positive founders identified out of those screened

Anti-sense morpholino oligo knockdowns

An anti-sense morpholino oligo (MO) was designed to the *dusp6* translation start site with the sequence 5′-TACCGTGAGACCTTAAAACTGCGGA -3′. A MO targeted to the *dusp2* translation start site with the sequence 5′-GTCGCCGATACCCATGATGCCCTCT-3′ was also designed. As a control, a 5-mismatch control oligo was designed with the sequence 5′-GTCcCCcATAgCCATcATcCCCTCT-3′. All MOs were generated by Gene Tools, LLC and re-suspended in distilled water for a stock solution of 3mM. The stock solution was further diluted with water and phenol red and 1-2nl was injected into the yolk of one-cell stage embryos.

RNA-seq library preparation

Total RNA was extracted from pools of dechrionated, deyolked wildtype and *dusp2*$^{um287/um287}$*;dusp6*$^{um286/um286}$ embryos at 18hpf using the RNeasy Mini Kit (Qiagen). Three libraries from wildtype embryos and three libraries from *dusp2*$^{um287/um287}$*;dusp6*$^{um286/um286}$ embryos were then generated from 3µg RNA using the TruSeq Stranded mRNA Library Prep Kit (Illumina). All libraries were analyzed for quality on a bioanalyzer prior to sequencing (Agilent 2100 BioAnalyzer).

Processing and analysis of RNA-seq data

Fastq files containing strand-specific and filtered reads were processed using the University of Massachusetts Medical School Dolphin web interface

[101]. Reads were quality checked using FastQC and aligned to the DanRer7 zebrafish transcriptome using RSEM. After filtering out ribosomal RNA read counts, differentially-expressed genes were identified as those with a greater than 2-fold change in expression between the wildtype and *dusp2*$^{um287/um287}$;*dusp6*$^{um286/um286}$ samples.

In situ RNA hybridization, immunostaining, and nuclear staining

For *in situ* hybridization, embryos were fixed at the appropriate time point in 4% paraformaldehyde and stored in 100% methanol at -20°C. RNA hybridization was performed as described and was followed by a color reaction using NBT/BCIP or INT/BCIP in 10% polyvinyl alcohol [102]. RNA probes for the following genes were produced by cloning a 900-1000bp fragment of the coding sequence into a vector and transcribing an anti-sense transcript: *dusp6*, *dusp2*, *krox20*, *hoxb1a*, *six7*, *pea3*, *erm*, *fgf3*, *fgf8*, *valentino*, *bmp2b*, *bmp4*, *chordin*, and *noggin1*. The *otx5* probe was purchased from the Zebrafish International Resource Center.

For whole-mount immunostaining, embryos were fixed in 4% paraformaldehyde/8% sucrose/1x PBS. Fluorescent antibody staining was performed as described previously [103]. Commercially-available primary antibodies used: mouse 3A10 (1:100; Developmental Studies Hybridoma Bank [DSHB]), mouse anti-Islet1/2 (39.4D5; 1:100; DSHB), rabbit anti-phospho-p44/42 MAPK ERK1/2 (1:250; Cell Signaling Technology 4370), rabbit anti-phospho-histone H3 (1:200; Abcam 5176), mouse RMO-44 (1:100; Fisher Scientific 13-

0500), and mouse anti-Zn8 (1:1000; DSHB). An antibody against Valentino was generated by immunizing rabbits with a GST-tagged full-length zebrafish Valentino protein. This antibody was purified using an IgG Purification Kit (Dojindo Molecular Technologies) and used at a concentration of 1:100. Secondary antibodies used: goat anti-mouse Alexa Fluor 488 (1:200; Molecular Probes A11001), goat anti-rabbit Alex Fluor 568 (1:200; Molecular Probes A110011), and goat anti-rabbit IgG-HRP (1:1000; Abcam 6789; detected with PerkinElmer's TSA Plus Fluorescein System).

For nuclear staining, embryos were fixed in 4% paraformaldehyde and stored in 100% methanol at -20°C. Rehydrated whole embryos were stained with 0.5µg/ml DAPI solution in distilled water for 15 minutes, and then washed for several hours.

For imaging, embryos older than 24hpf were dissected from the yolk and flat-mounted in 70% glycerol for imaging on bridged coverslips. Images were captured using a Nikon Eclipse E600 microscope equipped with a Nikon 20x Plan Fluor objective and a Zeiss Axiocam 503 color camera. Embryos between 1hpf and 24hpf were suspended in 3% methyl cellulose for imaging. Images were captured using a Leica M165 FC microscope equipped with a Leica DFC310 FX camera. Embryos younger than 1hpf were mounted in 70% glycerol in depression slides for imaging. All images were imported into Adobe Photoshop and adjustments were limited to contrast, levels, and cropping; all adjustments were applied to the entire image.

Quantitative PCR

Total RNA was extracted from whole embryos, or from dissected organs of the adult fish, using the RNeasy Mini Kit (Qiagen). At least 100ng of RNA was used to reverse transcribe cDNA using the High Capacity cDNA Reverse Transcription Kit (Applied Biosystems). The qPCR reaction was carried out using SYBR Green qPCR Master Mix (BioTool) on an Applied Biosystems 7300 PCR System. Results were normalized to those of a housekeeping gene (*b-actin* or *odc1*).

RESULTS

Knockdown of dusp6 and dusp2 via MO results in a hindbrain phenotype

We initially used anti-sense morpholino oligos (MOs) to assess the function of *dusp6* and *dusp2* by designing MOs to the translation start site to prevent synthesis of Dusp6 and Dusp2 proteins (Figure 2.1B). Since *dusp6* and *dusp2* are both expressed in rhombomere 4 (r4) of the hindbrain (Figure 2.1A), possibly by acting downstream of *hoxb1b* [74], we examined hindbrain development in MO-injected embryos. r4 is characterized by formation of the Mauthner neurons, a pair of large reticulospinal neurons found in fish and amphibians that are responsible for the escape response (Figure 2.1C). We find that a large percentage of *dusp6* and *dusp2* morphants are missing one or both Mauthner cells (Figure 2.1E-J), while a control MO has no effect (Figure 2.1D). Furthermore, injecting a combination of both MOs results in an increase in the

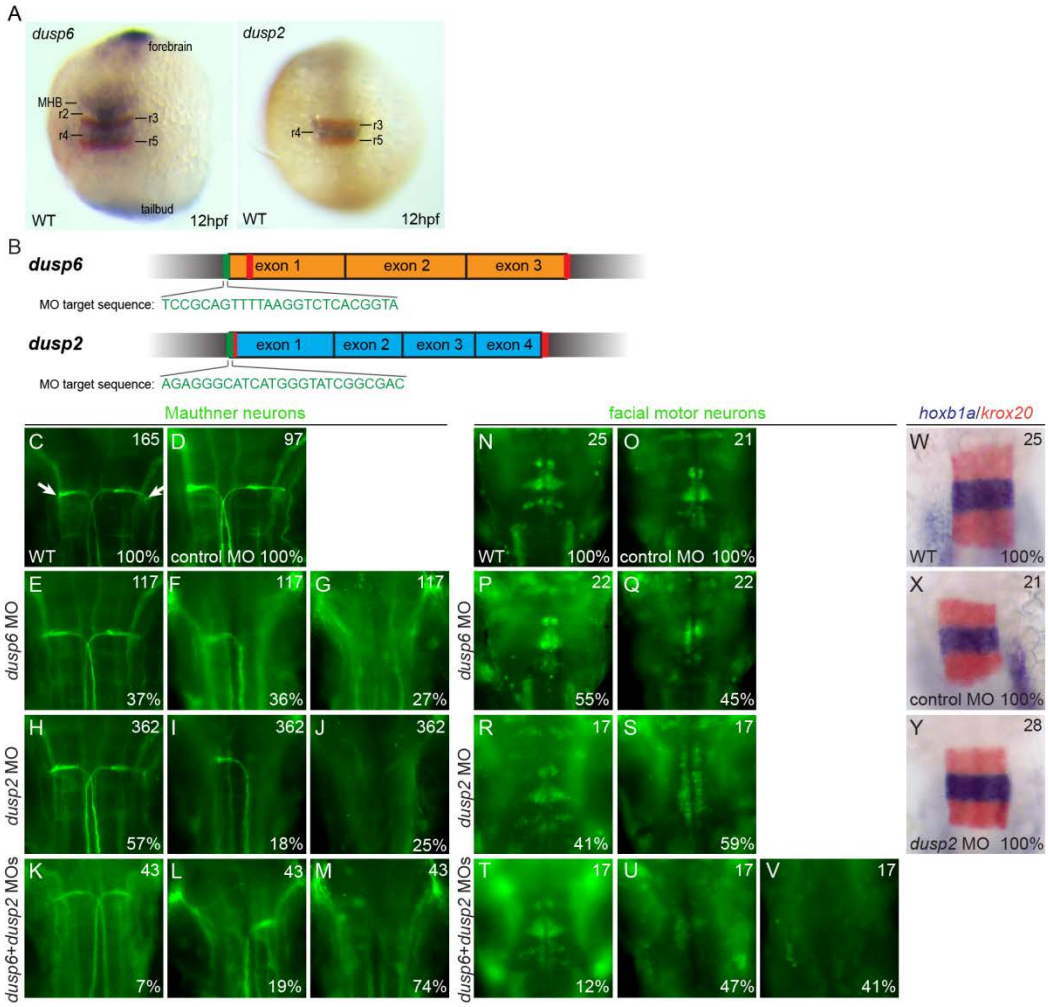

Figure 2.1. Knockdown of *dusp2* and *dusp6* via MO yields a hindbrain phenotype
A. 12hpf wildtype embryos were assayed by *in situ* hybridization for expression of *krox20* (red stain) and *dusp6* (blue stain in left panel) or *dusp2* (blue stain in right panel). **B**. Schematic of genomic sequence for *dusp6* and *dusp2*. Red vertical lines indicate CRISPR target sites and green vertical lines indicate MO target sites. **C-V**. 48hpf wildtype (**C, N**), control MO-injected (**D, O**), *dusp6* MO-injected (**E-G, P-Q**), *dusp2* MO-injected (**H-J, R-S**), and *dusp6+dusp2* MO-injected (**K-M, T-V**) embryos were assayed by immunostaining for differentiation of Mauthner neurons (3A10 staining in **C-M**) and facial motor neurons (Islet1/2 staining in **N-V**). **W-Y**. 18hpf wildtype (**W**), control MO-injected (**X**) and *dusp2* MO-injected (**Y**) embryos were assayed by in situ hybridization for expression of *krox20* (red stain) and *hoxb1a* (blue stain). Numbers in top right corner of each panel indicate the total number of embryos assayed for that condition. Numbers in bottom right corner indicate percent of embryos with the phenotype shown. All embryos are in dorsal view with anterior to the top. Embryos in **A** are whole-mounts, while embryos in **C-Y** are flat-mounted and show only the central hindbrain region.

occurrence of this phenotype (Figure 2.1K-M). Additionally, we notice a minor defect in the patterning of the facial motor neurons that normally migrate from r4 to distinct clusters in the caudal rhombomeres of the hindbrain (Figure 2.1N-O). The patterning and clustering of these cells is disrupted in the morphants (Figure 2.1P-S). Again, the combination of both MOs results in a more severe phenotype, with some morphants lacking detectable facial motor neurons (Figure 2.1T-V). Despite these neuronal defects, the expression of two genes involved in patterning of the early hindbrain appears normal in the morphants (Figure 2.1W-Y). Additional neurons and markers were examined in the *dusp2* morphants, including the reticulospinal neurons, pERK, *pea3*, *erm*, *fgf8*, *valentino*, and the abducens motor neurons, with no defects (Figure 2.2). These results demonstrate that MOs targeting *dusp6* and *dusp2* disrupt the formation and migration of neurons originating in r4 of the hindbrain.

Generation of dusp6 and dusp2 germ line mutants

To investigate the roles of *dusp6* and *dusp2* in zebrafish development in greater detail, we set out to generate germ line mutants using the CRISPR/Cas9 genome editing system. We designed two guide RNAs for each gene – one targeted to the 5′ end of the coding sequence and one targeted to the 3′ end (Figure 2.3A, Table 2.1, Table 2.3) – with the intention of co-injecting them to delete the sequence between the two target sites. Dusp proteins contain a C-terminal catalytic domain required for substrate recognition and binding [104], as well as an N-terminal rhodanese-homology domain. Although the latter domain is

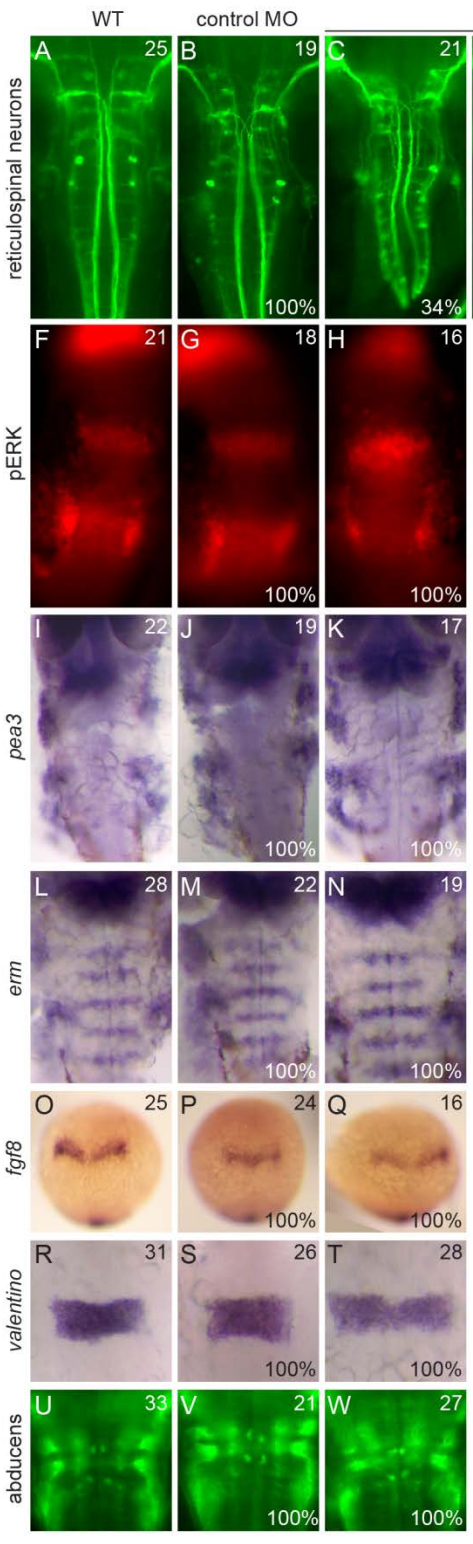

Figure 2.2. Additional neuronal and patterning markers examined in *dusp2* morphants

Wildtype (**A, F, I, L, O, R, U**), control MO-injected (**B, G, J, M, P, S, V**), and *dusp2* MO-injected (**C-E, H, K, N, Q, T, W**) embryos were assayed by immunostaining for formation of reticulospinal neurons at 48hpf (RMO44 antibody in **A-E**), for pERK staining at 14hpf (**F-H**) and for formation of abducens neurons (Zn8 antibody in **U-W**) at 48hpf, as well as by in situ hybridization for expression of *pea3* at 24hpf (**I-K**), *erm* at 24hpf (**L-N**), *fgf8* at 10hpf (**O-Q**), and *valentino* at 12hpf (**R-T**). All embryos are in dorsal view with anterior to the top. Numbers in top right corner of each panel indicate the total number of embryos assayed for that condition. Numbers in bottom right corner indicate percent of embryos with the phenotype shown.

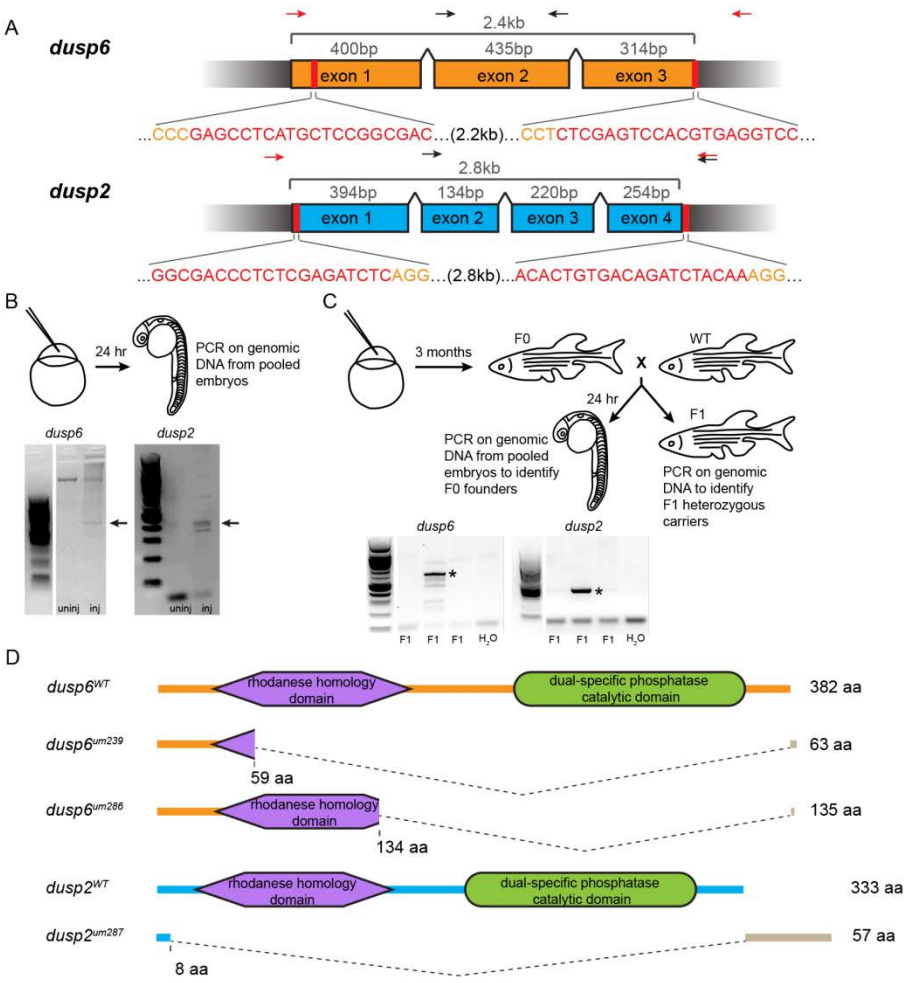

Figure 2.3. CRISPR genome editing yields loss of function mutants for *dusp6* and *dusp2*
A. Schematic of the genomic sequence for *dusp6* and *dusp2* with the length of each exon and total coding sequence indicated. Black wedges represent introns. Vertical red lines and red nucleotides denote the CRISPR target sequence, and orange nucleotides indicate PAM sequence. Arrows above each schematic indicate the approximate locations of genotyping primers used to detect CRISPR-induced deletion alleles (red arrows) and wildtype alleles (black arrows). **B**. Identification of active guide RNAs. Genomic DNA was extracted from pools of injected embryos and PCR-amplified to detect CRISPR-induced deletions. Arrows point to PCR products resulting from successful deletions. **C**. Identification of F0 founder fish. Adult F0 fish were crossed to wildtype and the resulting offspring genotyped as in **B**. Asterisks indicate F0 fish transmitting deletions to their offspring. **D**. Predicted peptide sequences of the identified mutant alleles for *dusp6* and *dusp2*. The large dashed wedges represent the location of CRISPR-induced deletions, and the gray bars represent residues that are read out of frame prior to a stop codon. Amino acid numbers below each peptide sequence indicate the residue affected by the deletion, and the numbers to the right indicate the length of the peptide.

catalytically inactive [63,64], we nevertheless elected to delete both domains with the goal of generating null alleles. Hence, guide RNA target sequences were chosen based on their proximity to the start and stop codons of the coding sequence, and also by the requirement for a protospacer adjacent motif (PAM) sequence (NGG) at the 3′ end of each target site (Figure 2.3A, Table 2.1, Table 2.3).

We injected *in vitro* transcribed guide RNAs and mRNA encoding Cas9 into early one-cell stage embryos to test if the guide RNAs were functional. To this end, we prepared genomic DNA from pools of injected embryos at 24hpf and analyzed the target sites by PCR. Using primers that anneal outside the guide RNA target sites (Figure 2.3A, Table 2.2), we detected bands of approximately 400-600bp (Figure 2.3B), indicating the presence of large deletions created by both the *dusp6* and *dusp2* guide RNA pairs. Each guide RNA pair was then injected into several hundred embryos that were raised to adulthood as the F0 generation (Figure 2.3C). This F0 generation is mosaic and each individual fish may carry more than one mutant allele for the same gene. We therefore identified founder fish carrying germ line mutations by crossing F0 individuals to wildtype fish and screening for deletions in the resulting offspring using the same PCR primers (Figure 2.3C). F0 founders that were positive for germ line mutations were crossed to wildtype fish and the offspring raised to adulthood followed by genotyping to identify heterozygous F1 carriers.

For *dusp6*, two F0 founders with germ line mutations were identified out of 23 fish tested (Table 2.3). One founder (*dusp6*^{um239}) carried a mutant allele with a

2.2kb deletion within the coding sequence of the *dusp6* gene (Table 2.4). The exact nucleotides deleted were determined by sequencing of the genomic DNA and cDNA (Figure 2.4). This large deletion appears to be the product of two double strand breaks as was expected. Conceptual translation of this sequence predicts a 63-amino-acid protein with no known protein domains (Figure 2.3D). This founder transmitted this mutation to 13% of its offspring (Table 2.4). A second founder (*dusp6*^{um286}) carried a mutant allele with a 1.3kb deletion spanning exons 2 and 3 of the *dusp6* gene (Table 2.4). We suspect that the 5′ guide RNA did not cause a break in this case, and instead the 3′ guide RNA generated a cut that was not properly repaired resulting in a smaller deletion. The translation of the resulting sequence predicts a 135-amino-acid protein that lacks the catalytic domain (Figure 2.3D). This founder transmitted this mutation to 24% of its offspring (Table 2.4).

For *dusp2*, three F0 founders with germ line mutations were identified out of 23 fish tested (Table 2.3). Each of these founders arose from an independent injection, but interestingly, all three carried the same mutant allele containing a 2.8kb deletion within the coding sequence (Table 2.4). Again, the exact nucleotides deleted were determined by sequencing of the genomic DNA (Figure 2.4). The mutant allele translates to produce a 57-amino-acid protein that lacks any known protein domains (Figure 2.3D). The first *dusp2*^{um287} founder transmitted this mutation to 18% of its offspring (Table 2.4). The two additional founders were positive for a deletion by PCR, but we were unable to identify any

Figure 2.4. Sequences of *dusp6* and *dusp2* mutants
Standard Sanger sequencing of PCR-amplified regions shows the WT, *dusp6* mutant alleles (**A**), and *dusp2* mutant allele (**B**) nucleotide sequences. Regions spanning the deletion site were amplified using primers that anneal outside the CRISPR target sites (see red arrows in Figure 2.3). Lowercase nucleotides are outside of the coding region in the UTR. Green and red nucleotides indicate the translation start and stop sites respectively. Ellipses (…) indicate the continuation of WT sequence, dashes (---) indicate deleted nucleotides, and blue nucleotides indicate insertions. The predicted protein sequences are also shown for both WT and all mutant alleles. The purple box indicates the residues of the rhodanese homology domain and the green box indicates the residues of the catalytic domain. Asterisks (*) represent the stop codon. Orange residues are non-WT amino acids caused by deletion of the natural stop codon and translation of the UTR sequence. For *dusp6*, endpoint PCR shows that *dusp6*^{um239} and *dusp6*^{um286} transcripts are produced. Sequences of these transcripts were identical to those of the genomic DNA.

heterozygous carriers from their offspring. Hence, we have generated two *dusp6* and one *dusp2* alleles that are predicted to lack phosphatase activity.

Table 2.4. Characteristics of *dusp6* and *dusp2* mutant alleles

Allele ID	Transmission frequency [a]	Size of deletion [b]
dusp6^{um239}	13.3%	2263bp
dusp6^{um286}	23.8%	1308bp
dusp2^{um287}	18.2%	2855bp

[a] Percentage of F1 fish identified as heterozygous carriers of CRISPR-induced deletions
[b] Total number of nucleotides deleted from the genomic sequence

Both dusp6 and dusp2 are not required for early zebrafish embryogenesis

While breeding the mutant lines, we found that both *dusp6* and *dusp2* homozygous mutants are viable. Furthermore, crosses of double heterozygous (*dusp2*$^{um287/+}$;*dusp6*$^{um286/+}$) carriers produced off-spring at the expected ratios, including of double homozygous (*dusp2*$^{um287/um287}$;*dusp6*$^{um286/um286}$) animals that could be raised to adulthood (Figure 2.5A). We took advantage of this to establish a double homozygous mutant line and used this line for RNA-seq analysis to identify global changes in gene expression resulting from simultaneous loss of *dusp6* and *dusp2.* Since *dusp6* and *dusp2* are expressed in multiple tissues at segmentation stages, we extracted RNA from pools of 18hpf whole embryos to generate RNA-seq libraries (Figure 2.5B).

RNA-seq analysis yielded 673 genes that are differentially-expressed between wildtype and mutant embryos out of 23150 total genes with mapped reads. Of those that are differentially-expressed, 334 are up-regulated and 339

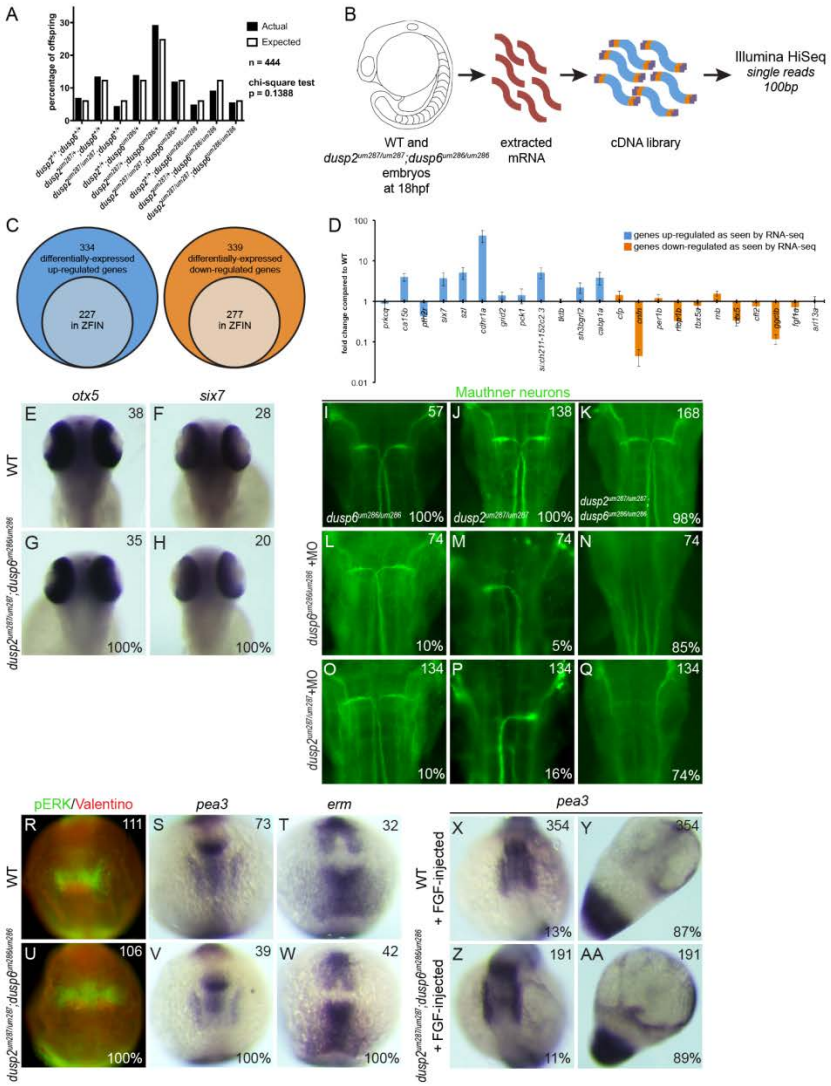

Figure 2.5. Loss of *dusp6* and *dusp2* does not impact early development

A. Offspring from crosses of *dusp2*$^{um287/+}$;*dusp6*$^{um286/+}$ fish were raised to adulthood and genotyped in order to determine the percentage of each possible genotype in surviving fish. A chi-square test indicates no significant statistical difference between the actual and expected Mendelian ratios. **B**. Outline of RNA-seq library production. **C**. Diagrams representing the number of differentially expressed up-regulated (left circles) and down-regulated (right circles) genes in *dusp2*$^{um287/um287}$;*dusp6*$^{um286/um286}$ mutants versus wildtype. Inner circles indicate the subset of genes annotated in ZFIN. **D**. 23 genes identified as differentially expressed by RNA-seq were re-examined by qPCR on wildtype versus *dusp2*$^{um287/um287}$;*dusp6*$^{um286/um286}$ cDNA. **E-H**. 48hpf wildtype (**E, F**) and *dusp2*$^{um287/um287}$;*dusp6*$^{um286/um286}$ mutant (**G, H**) embryos were assayed for changes in *otx5* (**E, G**) and *six7* (**F, H**) expression by *in situ* hybridization. **I-Q**. Uninjected *dusp6*$^{um286/um286}$ (**I**), *dusp2*$^{um287/um287}$ (**J**), and *dusp2*$^{um287/um287}$;*dusp6*$^{um286/um286}$ (**K**) mutants, as well as *dusp6* MO-injected *dusp6*$^{um286/um286}$ mutants (**L-N**) and *dusp2* MO-injected *dusp2*$^{um287/um287}$ mutants (**O-Q**) were assayed by immunostaining with 3A10 antibody to detect the Mauthner neurons at 48hpf. **R-W**. 12hpf wildtype (**R, S, T**) and *dusp2*$^{um287/um287}$;*dusp6*$^{um286/um286}$ (**U, V, W**) embryos were assayed by immunostaining for pERK (green in **R, U**; red counterstain detects the Valentino transcription factor), as well as by *in situ* hybridization for expression of *pea3* (**S, V**), and *erm* (**T, W**). **X-AA**. Wildtype (**X, Y**) and *dusp2*$^{um287/um287}$;*dusp6*$^{um286/um286}$ (**Z, AA**) embryos were injected with *fgf8* mRNA and the expression pattern of *pea3* visualized by *in situ* hybridization. All embryos are in dorsal view with anterior to the top. Numbers in top right corner of each panel indicate the total number of embryos assayed for that condition. Numbers in bottom right corner indicate percent of embryos with the phenotype shown.

are down-regulated in the mutants (Figure 2.5C). We selected 23 differentially-expressed genes for validation by quantitative PCR (qPCR) on independently prepared cDNA samples collected from sibling embryos. We find that the expression changes observed by RNA-seq are confirmed by qPCR analysis for 18 of these genes (78%; Figure 2.5D).

Next, we narrowed the number of candidate genes down to 504 by pursuing only those with a Zebrafish Information Network (ZFIN, [105]) gene ID number, as these have available information regarding their expression pattern. For this list of differentially-expressed genes, we examined whether there is an enrichment in genes that function within particular pathways, specifically the ERK signaling pathway or another MAPK pathway. Although the PANTHER gene ontology classification system [106–108] grouped 124 of the up- and down-regulated genes into 44 different pathways, there is no clear enrichment for any singular pathway (Figure 2.6). We next reasoned that genes expressed in the same regions as *dusp6* and/or *dusp2* would be the best candidates for genes affected in the mutant lines. Using ZFIN's gene expression database for wildtype fish [109], we analyzed the body structures in which the candidate genes are expressed, with a focus on the regions containing *dusp6* and *dusp2*. Of the 504 genes, 97 are expressed in 25 different structures that overlap with *dusp6* and *dusp2* expression (Table 2.5). We selected two genes (*otx5* and *six7*) that are expressed in the same regions of the forebrain as *dusp6* and *dusp2* and that were also validated by qPCR, but we were unable to detect any change in expression of these genes using *in situ* hybridization (Figure 2.5E-H).

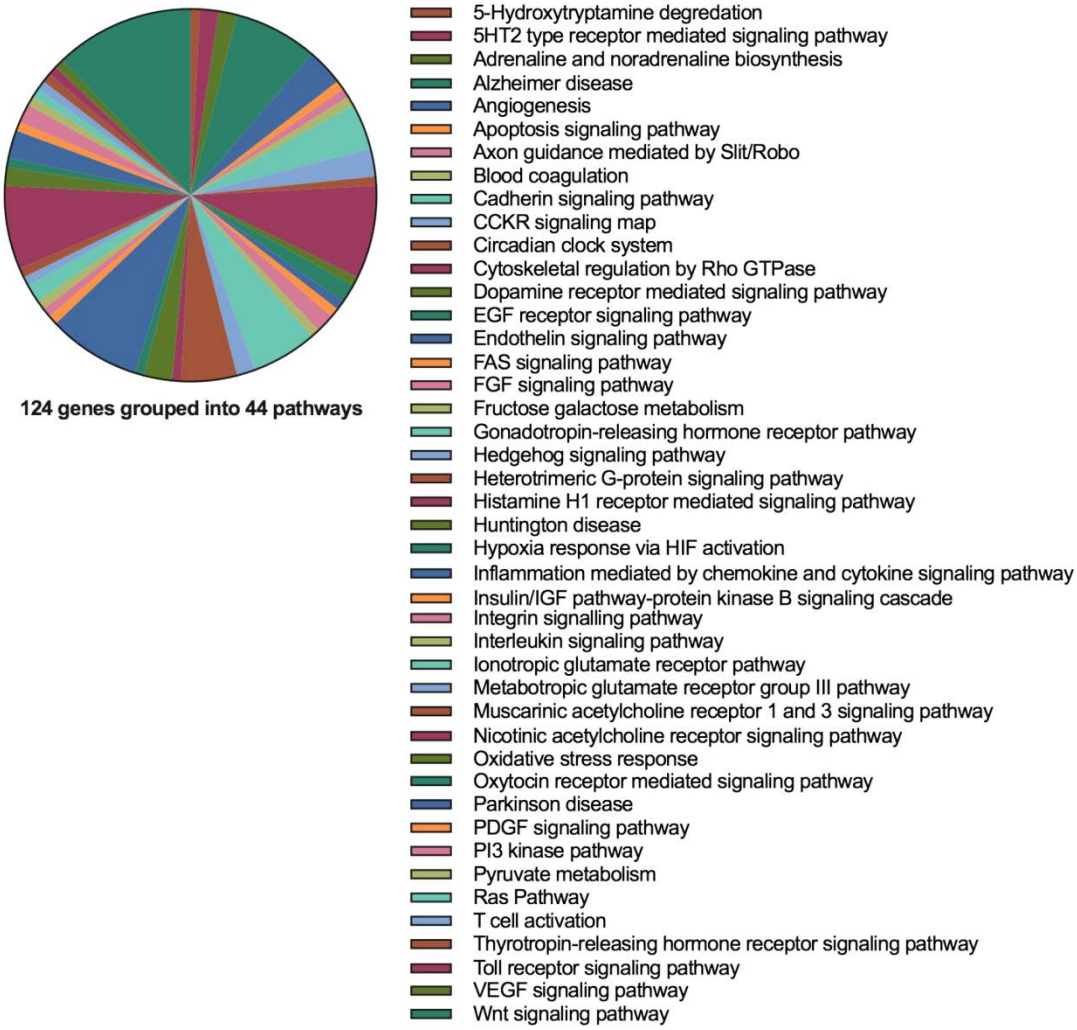

Figure 2.6. Gene ontology grouping of differentially-expressed genes
Representation of gene ontology grouping of 124 differentially-expressed genes into 44 different signaling pathways performed by Panther.

Table 2.5. Differentially-expressed genes in the same body structures as *dusp6* and *dusp2*

Regions of the fish where *dusp6* and/or *dusp2* are expressed [a]	**Differentially-expressed genes also found in those regions** [b]
axial hypoblast	*gsc*
blastodisc	*nanos3*
	gsc
brain	*gria2a*
	nupr1
	slc14a2
	def6a
	ca15b
	irf8
	cabp1a
	prkcq
	sult6b1
	s100z
	kiss1rb
	tmie
	rbp7a
	kiss1
	duox2
	ptger3
	dbh
diencephalon	*kiss1rb*
	kiss1
	gsc
forebrain	*dock8*
	pth2r
hindbrain	*grid2*
	kiss1rb
	kiss1
	sst1.2
	dbh
	pth2r
hindbrain neural plate	*si:ch211-152c2.3*
hypothalamus	*gria2a*
	mchr1b
	kiss1rb
	sst1.2
margin	*egln3*
	im:7138239
	mespab
	gsc
midbrain	*pck1*
	dock8
	kiss1rb
	kiss1
	pth2r
mucus secreting cell	*zgc:92066*
	cabp1a
neuron	*dbh*
optic vesicle	*pth2r*
otic vesicle	*si:ch211-152c2.3*
	zgc:92066
	cabp1a
	tmie
	agbl4
	gsc
	pth2r
pectoral fin	*gpib*
	def6a
	ptgr1
	mxra8a
	gsc

pectoral fin bud	*gsc*
peripheral olfactory organ	*zgc:92066*
	sult6b1
	s100z
	agbl4
pharyngeal arch	*gpib*
	def6a
	gsc
	pth2r
presumptive telencephalon	*gsc*
regenerating fin	*lcp1*
retina	*pck1*
	sh3bgrl2
	ptgr1
	six7
	pth2r
segmental plate	*zgc:92066*
	im:7138239
	mespab
shield	*gsc*
somite	*acta2*
	cpa4
	zgc:92066
	mxra8a
	mespab
tail bud	*szl*
	sult6b1
	abcc6a
telencephalon	*gria2a*
	grid2
	sult6b1
	kiss1rb
	kiss1
	sst1.2
	gsc
trunk	*bco2l*
	lcp1

[a] Structures of the zebrafish in which *dusp6* and/or *dusp2* is expressed
[b] Genes identified by RNA-seq that are expressed in those regions

The lack of an apparent phenotype in *dusp* germ line mutants led us to examine if the *dusp6*$^{um286/um286}$ and *dusp2*$^{um287/um287}$ mutants recapitulate the loss of Mauthner cells observed in *dusp* morphants (Figure 2.1E-M). Strikingly, Mauthner neurons form normally in *dusp6*$^{um286/um286}$, *dusp2*$^{um287/um287}$, and *dusp2*$^{um287/um287}$*;dusp6*$^{um286/um286}$ mutants (Figure 2.5I-K). To examine the cause of this discrepancy further, we injected MOs into the respective mutant line and find that Mauthner cells are lost (Figure 2.5L-Q). Since these mutant embryos derive from homozygous mutant parents and lack the sequences encoding each

phosphatase, the MOs cannot affect *dusp* gene expression, but likely have an off-target effect. Because a previous study reported defective *bmp4* and *chordin* expression in *dusp6* morphants [84], we also examined a variety of other genes involved in early embryonic patterning, including *krox20*, *fgf3*, *fgf8*, *bmp2b*, *bmp4*, *chordin*, and *noggin1*, but detect no changes in expression in *dusp2*$^{um287/um287}$*;dusp6*$^{um286/um286}$ germ line mutants (Figure 2.7). We conclude that zebrafish dorsoventral patterning and Mauthner cell formation is independent of *dusp6* and *dusp2* activity.

To further address the absence of a phenotype, we next investigated the level of pERK (the primary substrate for both *dusp6* and *dusp2*) during early segmentation, when both phosphatases are expressed. Double mutant embryos stained with an anti-pERK antibody, and counter-stained with an anti-Valentino antibody marking r5 and r6 of the hindbrain, show no differences in intensity or location of pERK within the hindbrain or other regions of the embryo compared to wildtype embryos (Figure 2.5R, U). We also examined the expression patterns of two ERK target genes, *pea3* and *erm*, of which neither is affected in the mutants (Figure 2.5S-T, V-W). Since key signaling pathways, such as the ERK signaling pathway, are held under many levels of regulation [10–14,16], we considered the possibility that other forms of control could be compensating for the loss of *dusp6* and *dusp2*. Accordingly, we hypothesized that challenging the pathway by exposure to higher levels of ligand might expose a defect in the mutants. To test this, we injected wildtype and mutant embryos with *fgf8* mRNA, raised them to the early segmentation stages, and then examined the expression pattern of the

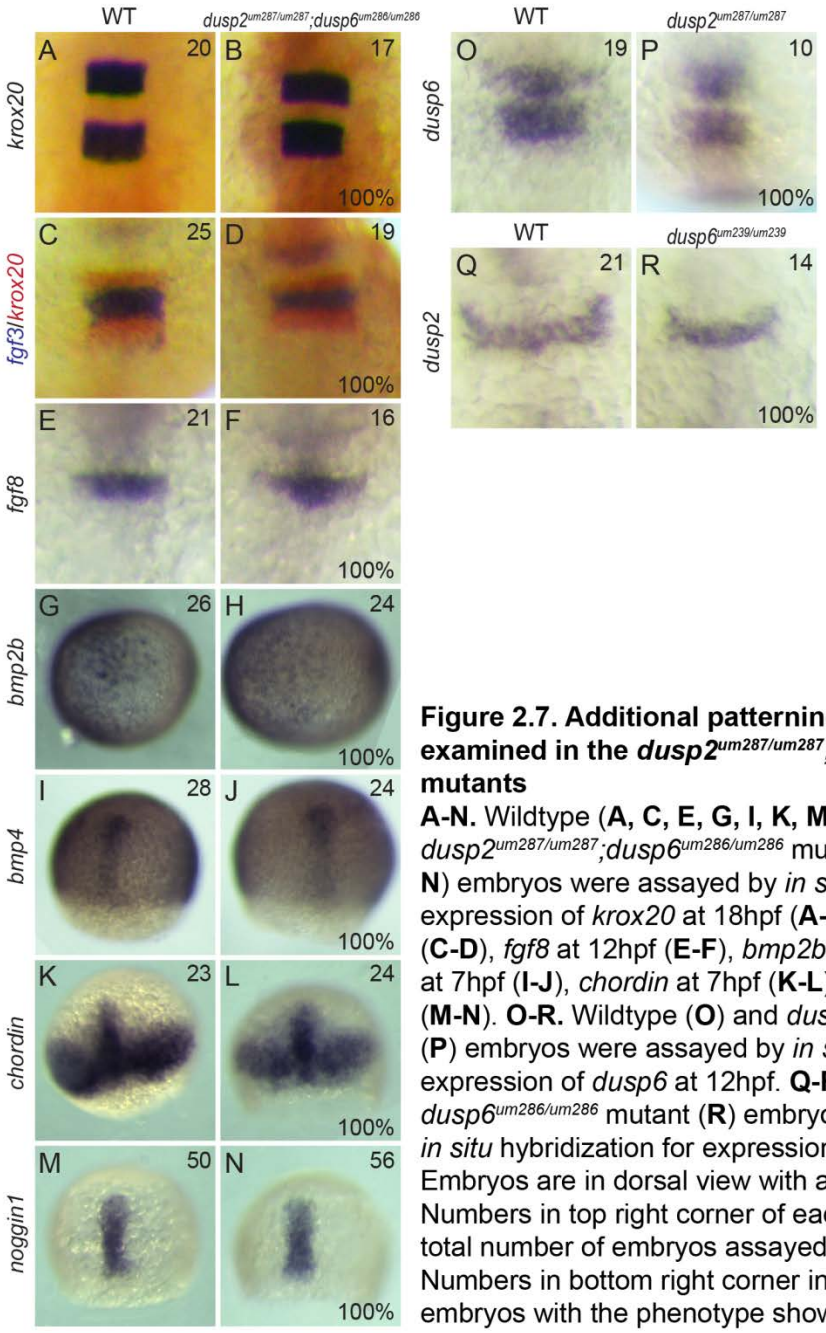

Figure 2.7. Additional patterning markers examined in the *dusp2*$^{um287/um287}$;*dusp6*$^{um286/um286}$ mutants

A-N. Wildtype (**A, C, E, G, I, K, M**) and *dusp2*$^{um287/um287}$;*dusp6*$^{um286/um286}$ mutant (**B, D, F, H, J, L, N**) embryos were assayed by *in situ* hybridization for expression of *krox20* at 18hpf (**A-B**), *fgf3* at 14hpf (**C-D**), *fgf8* at 12hpf (**E-F**), *bmp2b* at 7hpf (**G-H**), *bmp4* at 7hpf (**I-J**), *chordin* at 7hpf (**K-L**), *noggin1* at 7hpf (**M-N**). **O-R.** Wildtype (**O**) and *dusp2*$^{um287/um287}$ mutant (**P**) embryos were assayed by *in situ* hybridization for expression of *dusp6* at 12hpf. **Q-R.** Wildtype (**Q**) and *dusp6*$^{um286/um286}$ mutant (**R**) embryos were assayed by *in situ* hybridization for expression of *dusp2* at 12hpf. Embryos are in dorsal view with anterior to the top. Numbers in top right corner of each panel indicate the total number of embryos assayed for that condition. Numbers in bottom right corner indicate percent of embryos with the phenotype shown.

ERK target gene *pea3*. While excess *fgf8* proved to have a gross effect on early embryonic development and morphology, we did not observe a difference in the effect between wildtype and mutant embryos (Figure 2.5X-AA). We conclude that, despite validated gene expression changes in the mutants, disrupting *dusp6* and *dusp2* function does not produce defects in early zebrafish embryogenesis.

Homozygous dusp6 mutant embryos have reduced viability through gastrulation

During our analysis, we noticed that the offspring of *dusp6* homozygous mutants have reduced viability during the first 10 hours after fertilization. To examine this effect further, wildtype and *dusp6*$^{um239/um239}$ clutches were collected and the number of live embryos counted at 1hpf and 10hpf. We routinely observe that a small percentage (approximately 5%) of wildtype embryos die by the end of gastrulation, but the homozygous *dusp6*$^{um239/um239}$ embryos show a significant decrease in viability with only approximately 50% of embryos surviving to 10hpf (Figure 2.8A). We also examined the viability of *dusp2*$^{um287/um287}$*;dusp6*$^{um286/um286}$ double homozygous mutants. These clutches show a decrease in viability comparable to *dusp6*$^{um239/um239}$ mutants (Figure 2.8B), suggesting that loss of *dusp2* does not decrease viability further. This also demonstrates that both *dusp6* mutant alleles exhibit the same phenotype. Lastly, we examined if one parent is responsible for the reduced survival phenotype. To address this, we crossed a wildtype female to a *dusp2*$^{um287/um287}$*;dusp6*$^{um286/um286}$ male or a wildtype male to a *dusp2*$^{um287/um287}$*;dusp6*$^{um286/um286}$ female. The survival of embryos from these crosses, while somewhat variable from clutch to clutch, is

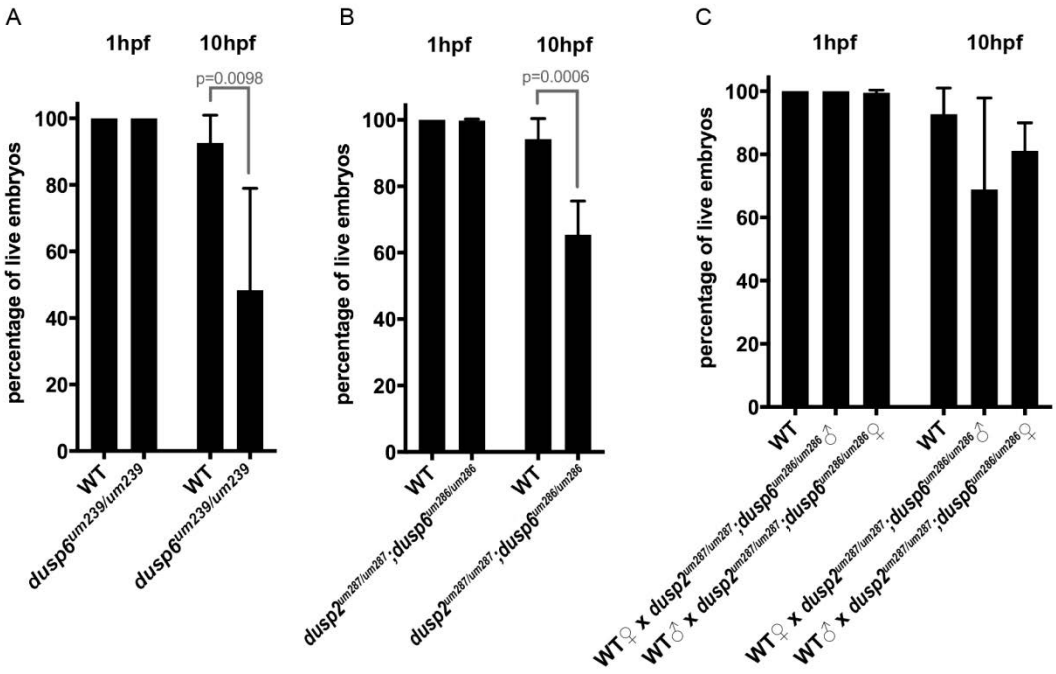

Figure 2.8. *dusp6* homozygous mutant embryos have reduced viability through gastrulation

A, B. Comparison of the percent live embryos at 1hpf and 10hpf between wildtype and *dusp6*$^{um239/um239}$ clutches (**A**), and wildtype and *dusp2*$^{um287/um287}$*;dusp6*$^{um286/um286}$ mutant clutches (**B**). Statistical significance was determined by t-test and the p-value is indicated. **C**. Comparison of the percent live embryos at 1hpf and 10hpf in clutches derived from wildtype male crossed to wildtype female, wildtype female crossed to *dusp2*$^{um287/um287}$*;dusp6*$^{um286/um286}$ mutant male, and wildtype male crossed to *dusp2*$^{um287/um287}$*;dusp6*$^{um286/um286}$ mutant female. ANOVA analysis did not reveal a statistically significant difference. A minimum of three clutches was analyzed for each cross with the mean percentages displayed ± SD.

not statistically different than that of wildtype embryos (Figure 2.8C), indicating that reduced viability is observed only when both parents are mutant.

A fraction of homozygous dusp6 mutant embryos stall at the first cell division

To further characterize the reduced viability of *dusp6* mutants, we collected clutches of wildtype and homozygous *dusp6*$^{um239/um239}$ embryos and monitored them throughout the cleavage, blastula, and gastrula stages (Figure 2.9A). For the *dusp6*$^{um239/um239}$ clutches, we again found that 50% of embryos die by 10hpf. However, in contrast to wildtype embryos that had all undergone at least one round of cell division by 1hpf, approximately 40-50% of *dusp6*$^{um239/um239}$ embryos remained at the one-cell stage at 1hpf. We refer to these as 'stalled' embryos and we monitored their development for the subsequent stages. We find that all of the stalled embryos remain at the one-cell over the next 8 to 10 hours until they eventually die. We noticed that some of the stalled embryos proceed to develop a slight cleavage furrow, but they appear to be unable to complete the process of cell division, and will later return to the smooth cellular surface typically seen at the one-cell stage. We again find that clutches of *dusp2*$^{um287/um287}$*;dusp6*$^{um286/um286}$ embryos behave similarly to *dusp6*$^{um239/um239}$ clutches (Figure 2.9A), indicating that loss of *dusp2* does not further decrease viability. This again demonstrates that both *dusp6* mutant alleles have the same phenotype. We also examined clutches from a wildtype female crossed to a *dusp2*$^{um287/um287}$*;dusp6*$^{um286/um286}$ male and a wildtype male crossed to a *dusp2*$^{um287/um287}$*;dusp6*$^{um286/um286}$ female. These exhibited less severe profiles

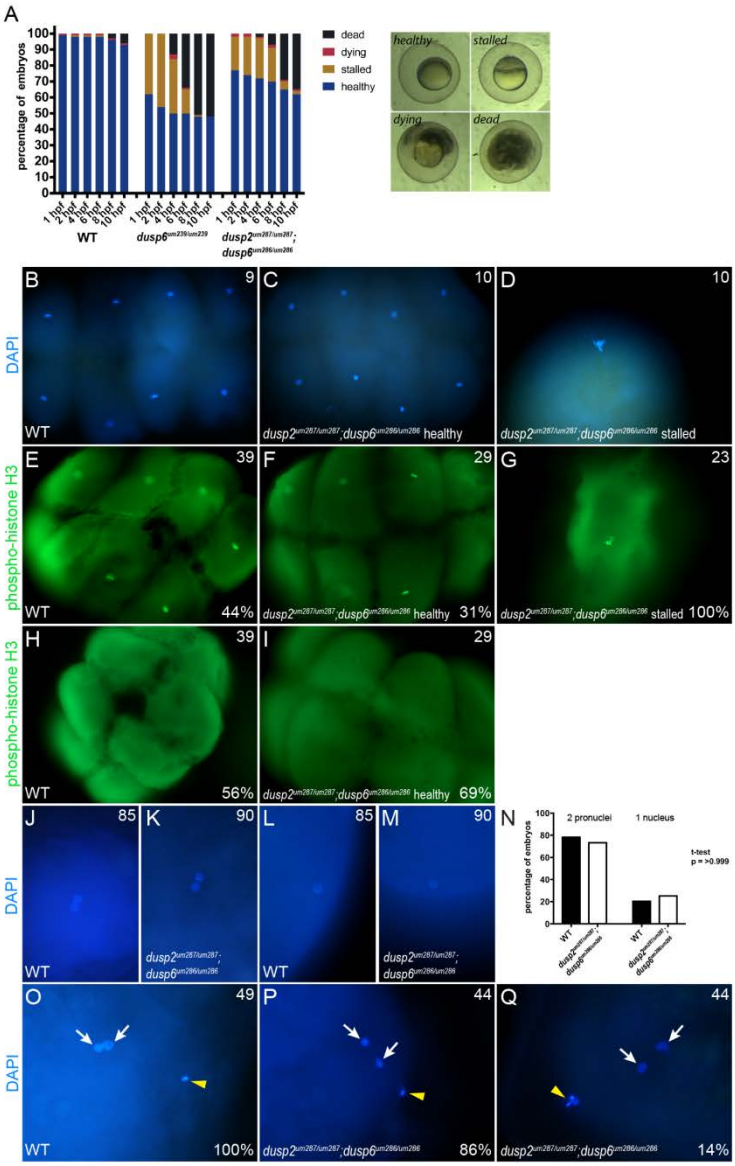

Figure 2.9. A fraction of *dusp6* homozygous mutant embryos stall at the first cell division
A. Embryos from wildtype, *dusp6*$^{um239/um239}$, and *dusp2*$^{um287/um287}$;*dusp6*$^{um286/um286}$ clutches were monitored throughout early development and the health of each embryo scored at each time point according to the brightfield images to the right (a minimum of three clutches were scored for each cross). Average cumulative counts are shown. **B-D**. DAPI staining on 1hpf embryos to visualize the nuclei. **E-I**. Immunostaining for phospho-histone H3 to visualize mitotic nuclei. **J-M**. DAPI staining at 10 minutes post fertilization to visualize the early pronuclei and determine if embryos are fertilized. **N**. Quantification of wildtype and *dusp2*$^{um287/um287}$;*dusp6*$^{um286/um286}$ mutant embryos containing one or two pronuclei. A t-test yields a p-value of >0.999 indicating no significant statistical difference. **O-Q**. DAPI staining to detect polar bodies in embryos at 10 minutes post fertilization. White arrows indicate pronuclei and yellow arrowheads indicate polar bodies. Numbers in top right corner of each panel indicate the total number of embryos assayed for that condition. Numbers in bottom right corner indicate percent of embryos with the phenotype shown.

(Figure 2.10), further supporting our previous conclusion that both parents need to be mutant to significantly affect embryo viability.

Although the stalled embryos appear unable to complete cell division, it is unclear if they are progressing through the cell cycle. To address this, we visualized the nuclei of embryos using DAPI at 1hpf. At this time point, wildtype and healthy *dusp2*$^{um287/um287}$*;dusp6*$^{um286/um286}$ embryos are entering the 8-cell stage, while the stalled embryos remain at the one-cell stage. Accordingly, wildtype and healthy *dusp2*$^{um287/um287}$*;dusp6*$^{um286/um286}$ embryos contain eight DAPI-positive nuclei with varying degrees of condensation likely depending on their position in the cell cycle at the time of fixation (Figure 2.9B-C). In contrast, the stalled embryos contain a single large and disorganized DAPI-positive nucleus (Figure 2.9D). We conclude that the stalled *dusp2*$^{um287/um287}$*;dusp6*$^{um286/um286}$ embryos are unable to complete the cell cycle.

To test at what point of the cell cycle the stalled embryos are arresting, we used a phospho-histone H3 antibody to detect mitotic nuclei. Histone H3 becomes phosphorylated at serine 11 during the end of the G2 phase and the early stages of mitosis [110]. Since the first several cell cycles in the developing zebrafish embryo lack G1 and G2 phases [111], positive staining with this antibody should indicate nuclei that are in mitosis and not in interphase. Notably, it is not possible to synchronize embryos in the cell cycle prior to fixation, so we expected to see some embryos in mitosis and some in interphase. At 1hpf, when normally developing embryos should enter the 8-cell stage, we find that 44% of wildtype embryos and 31% of healthy *dusp2*$^{um287/um287}$*;dusp6*$^{um286/um286}$ embryos

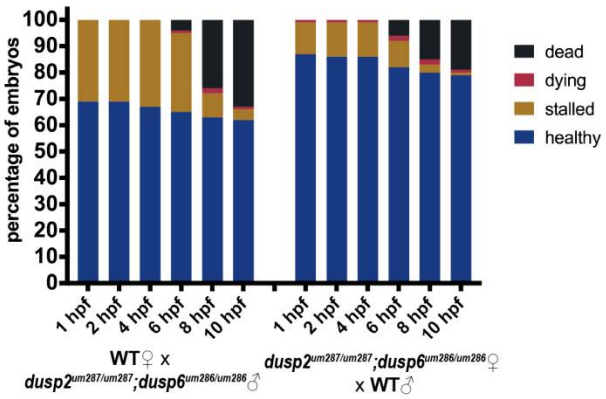

Figure 2.10. Offspring from a single mutant parent have a milder phenotype
Clutches of embryos from a wildtype female crossed to a *dusp2*$^{um287/um287}$;*dusp6*$^{um286/um286}$ male and a *dusp2*$^{um287/um287}$;*dusp6*$^{um286/um286}$ female crossed to a wildtype male were monitored throughout early development and the health of each embryo scored at each time point as in Figure 2.9A. A minimum of six clutches were scored from each cross. Average cumulative counts are shown.

are mitotic, while the remaining embryos are in interphase (Figure 2.9E-F, H-I). In contrast, at 1hpf all stalled embryos contained a single nucleus that is positively stained with the phospho-histone H3 antibody (Figure 2.9G). Since the first round of mitosis should have begun at approximately 30 minutes post fertilization, these embryos must have been stalled in mitosis for at least 30 minutes prior to fixation. Additionally, all of the stalled embryos contained only one nucleus, as seen by the DAPI and phospho-histone H3 staining, indicating that they do not proceed to anaphase when the sister chromatids are pulled apart. Indeed, separated chromatids are commonly seen in wildtype and healthy *dusp2*$^{um287/um287}$*;dusp6*$^{um286/um286}$ embryos at 1hpf (Figure 2.11), but are never observed in stalled embryos.

We next examined whether the stalled embryos are fertilized. In the few minutes following fertilization, the maternal and paternal pronuclei condense, migrate towards each other, and merge allowing the zygote to enter the cell cycle. Hence, the presence of two pronuclei indicates that an embryo has been fertilized. To visualize fertilization, we fixed embryos 10 minutes post fertilization and stained them with DAPI. However, since pronuclear fusion is very rapid and the embryos are collected from natural matings, it is difficult to catch all pronuclei prior to fusion. Accordingly, we find 79% of wildtype embryos contain two detectable pronuclei at 10 minutes post fertilization, indicating that these embryos are fertilized (Figure 2.9J, L, N). At this early time point, we cannot distinguish between *dusp2*$^{um287/um287}$*;dusp6*$^{um286/um286}$ embryos that are healthy and those that will stall at the one-cell stage. However, if the stalled embryos are

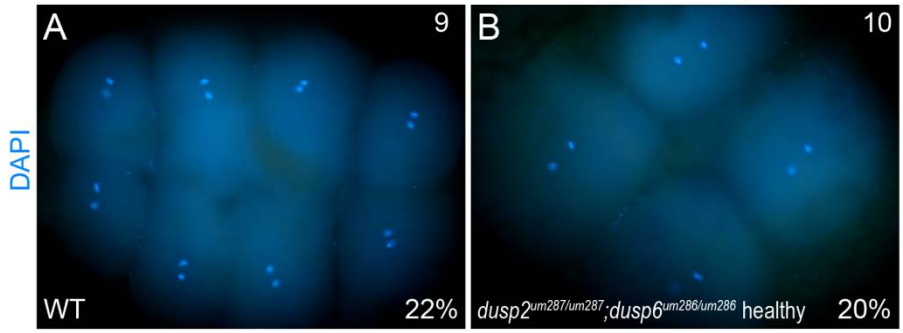

Figure 2.11. DAPI staining detects embryos undergoing mitosis
DAPI staining at approximately 1hpf shows that both wildtype (**A**) and healthy *dusp2*$^{um287/um287}$;*dusp6*$^{um286/um286}$ mutant (**B**) embryos can be detected at stages of mitosis when the chromatids are separated. Numbers in top right corner of each panel indicate the total number of embryos assayed for that condition. Numbers in bottom right corner indicate percent of embryos with the phenotype shown.

not fertilized, we would expect to see an approximate 50% reduction in *dusp2*$^{um287/um287}$*;dusp6*$^{um286/um286}$ embryos with two pronuclei, since we know that 50% of them will stall (Figure 2.9A). Instead, we find that 74% of *dusp2*$^{um287/um287}$*;dusp6*$^{um286/um286}$ embryos contain two detectable pronuclei (Figure 2.9K, M, N), indicating that these embryos are fertilized at the same rate as wildtype embryos. A t-test confirms that there is no significant difference in the fraction of embryos with two pronuclei from wildtype and *dusp2*$^{um287/um287}$*;dusp6*$^{um286/um286}$ clutches (Figure 2.9N).

DAPI staining at 10 minutes post fertilization also labels the polar bodies and we noticed that some *dusp2*$^{um287/um287}$*;dusp6*$^{um286/um286}$ mutants have large and disorganized polar bodies (Figure 2.9O-Q). The frequency of abnormal polar bodies (14%) is lower than the frequency of stalled embryos (approximately 50%) and the polar bodies appear to be degraded on time in *dusp2*$^{um287/um287}$*;dusp6*$^{um286/um286}$ mutants, likely ruling out a role for abnormal polar bodies in the stalling of mutant embryos.

We conclude that *dusp2*$^{um287/um287}$*;dusp6*$^{um286/um286}$ embryos are fertilized, but approximately 50% of them stall during mitosis of the first embryonic cell division. These embryos remain arrested in the early stages of mitosis for several hours until they die prior to the end of gastrulation.

dusp6 is expressed in zebrafish ovaries and testes

Our analysis revealed that approximately half of *dusp2*$^{um287/um287}$*;dusp6*$^{um286/um286}$ mutant embryos stall during the first embryonic

cell division. This event precedes activation of the zygotic genome, which occurs at 3-4hpf in zebrafish embryos, and must therefore be controlled by maternally deposited components supplied during oocyte maturation in the ovary. We therefore determined if *dusp6* transcripts are detectable in the ovary and in the early fertilized embryo. We find that *dusp6* is robustly expressed in the ovary, albeit at somewhat lower levels than in other adult tissues (Figure 2.12A). In contrast, *dusp6* is detected at very low levels at maternally controlled stages of embryogenesis (2.5hpf) relative to zygotically controlled stages (6hpf; Figure 2.12B), in agreement with a previous report that *dusp6* and *dusp2* transcripts are not maternally deposited in zebrafish [112]. In zebrafish, the large oocytes contribute the majority of cellular volume of the ovary while smaller granulosa cells surround the maturing oocytes and provide growth signals, maternal transcripts, and nutrients via gap junctions. Since *dusp6* is present at very low levels in fertilized oocytes (Figure 2.12B), it is likely that *dusp6* is primarily expressed in the granulosa cells. Interestingly, *dusp6* is also expressed in the adult testes (Figure 2.12A), consistent with our finding that decreased viability is only detected when both parents are homozygous mutants. Based on the current literature [113] and higher level of expression seen by qPCR, it is likely that *dusp6* is expressed in the sperm itself and the surrounding seminiferous tubules.

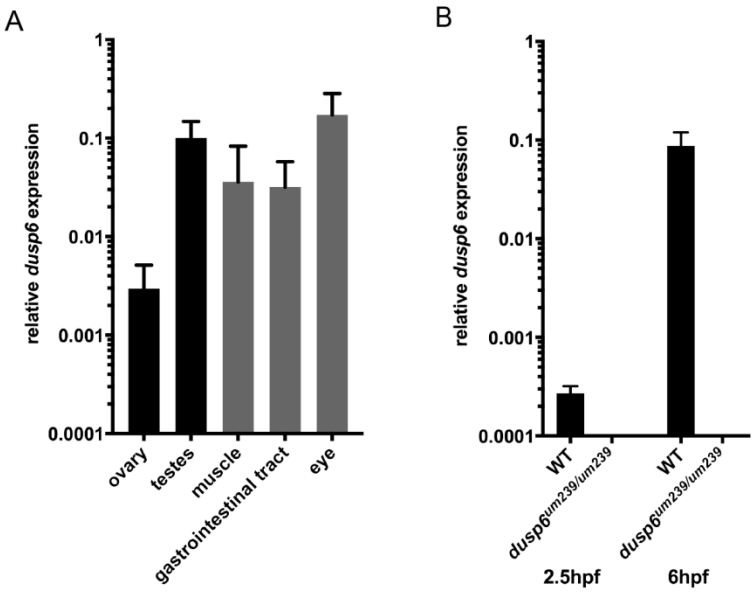

Figure 2.12. *dusp6* is expressed in ovaries and testes
dusp6 expression in wildtype adult zebrafish organs (**A**), as well as in wildtype and *dusp6*$^{um239/um239}$ mutant embryos at 2.5hpf and 6hpf (**B**), was assessed by quantitative RT-PCR. Results of three independent experiments were normalized to those of *b-actin* and displayed as the mean ± SD.

DISCUSSION

In order to identify a role for *dusp6* and *dusp2* in the developing zebrafish, we generated mutant lines carrying loss of function alleles for these two phosphatases, including a double homozygous mutant line. Our experiments show that a varying percentage of off-spring from homozygous *dusp6* mutants stall at the one-cell stage, unable to complete the process of cell division, and die within the first 10 hours after fertilization. Since the onset of mitotic arrest occurs very soon after fertilization in the affected embryos, we propose that loss of *dusp6* function prevents the proper production of zebrafish gametes in adult homozygous mutants. In contrast, loss of *dusp2* function does not affect embryo viability and we have been unable to identify a role for dusp2 in zebrafish embryogenesis.

Mis-regulated ERK signaling may disrupt development of female and male gametes in dusp6 mutants

Our results indicate that the decreased viability of *dusp6* mutant embryos is the result of defective gametes, but the underlying mechanism is not clear. Since *dusp6* acts as a feedback inhibitor of ERK signaling and is expressed during both oogenesis and spermatogenesis, *dusp6* mutants would be expected to have excess gonadal ERK activity. However, the fact that only a subset of mutant embryos is affected suggests that the effect on ERK signaling is subtle and since pERK staining in zebrafish is somewhat variable, it would be difficult to

assess this directly. However, work in other systems has shown that ERK signaling is essential for gametogenesis. In particular, two gonadotropins, luteinizing hormone (LH) and follicle stimulating hormone (FSH), are the primary drivers of ovarian follicle growth and stimulators of the granulosa cells surrounding the developing oocyte [114]. A study performed on rat granulosa cells demonstrated that DUSP6 in the granulosa cells keeps ERK inactivated in the absence of FSH [115]. Once maturation is initiated by FSH, PKA is activated through cAMP to inhibit DUSP6, thereby allowing active pERK to accumulate and drive downstream genes promoting oocyte maturation. For instance, cell cycle regulators, such as cyclins, *cdc2*, and *cdc25*, are transcribed downstream of activated ERK and allow the oocyte to proceed through the meiotic cell cycle [116]. Other genes activated by ERK, such as *has2* and *ptgs2*, are required for the expansion and growth of the granulosa cells within the ovarian follicle, creating space for the maturing oocyte [117,118]. Hence, zebrafish *dusp6* mutants may suffer from excess signaling in these pathways that could in turn affect expression of cell cycle regulators, perhaps causing oocytes to be released prematurely. Additionally, mis-regulated ERK signaling may result in oocytes that are lacking specific factors, transcripts, or proteins necessary for the early embryonic cell cycle.

The generation of healthy sperm in adult males also requires well-coordinated ERK signaling. Cell cycle regulators and condensation factors downstream of ERK are required for proper chromatid separation and condensation maintenance between rounds of meiosis [119–121]. Similar to the

granulosa cells of the ovary, Sertoli cells coordinate meiotic progression of the developing spermatocytes and their growth within the testes [122]. Genes downstream of ERK ensure the integrity of vital tight junctions between the Sertoli cells and spermatocytes during maturation [123]. ERK has also been detected in the tails of human sperm where it is required for proper sperm motility [124] and ERK within the sperm tails also has a role in the acrosome reaction that allows the sperm to penetrate the oocyte membrane [124]. Excessive ERK signaling in *dusp6* mutants could result in premature condensation of chromosomes or perhaps weaken the tight junctions with spermatocytes. Our results show that fertilization occurs normally with the *dusp6* mutant gametes, implying that the acrosome reaction is not effected, but similarly to the oocytes, these sperm may be lacking specific factors necessary for the early embryonic cell cycle.

Additionally, there is evidence that mis-regulation of ERK signaling within the mammalian reproductive system results in abnormal pubertal development and infertility. Female mice carrying a mutant allele for constitutively active RAS have defects in ovulation, and ERK1/2 mutant female mice are completely infertile [38,40]. Additionally, congenital hypogonadotropic hypogonadism in humans affects both males and females and has been linked to missense mutations in DUSP6 and other ERK regulators [90].

Dusp6 may act to maintain ERK signaling within a permissive range

A key observation regarding the stalling of *dusp6* mutant embryos is that only a portion of each clutch is affected (approximately 40-50%, Figure 2.8A-B, Figure 2.9A). This implies that not all oocytes and/or sperm produced by homozygous mutant adults are defective, but the basis of this variability is unclear. There is evidence of cell-to-cell variability in levels of protein kinase signaling, and negative feedback regulators such as Dusp proteins are thought to act to minimize the variation [125]. Differences in gene expression and protein concentrations contribute to variability in signaling intensity among individual cells [126,127], and studies in various cell types and signaling pathways have identified roles for redundant regulators in reducing signal noise [128,129]. We therefore hypothesize that *dusp6* is required to minimize variations in ERK signaling during gametogenesis and that when *dusp6* is lost, a fraction of oocytes and spermatocytes become exposed to ERK signaling outside a permissive range. Most oocytes and spermatocytes in the mutants would still be exposed to levels of ERK signaling that fall within the permissive range, but a percentage would receive excessive ERK signals leading to abnormal development, as discussed above. Since only half of the mutant embryos are affected, we also predict that the increase in signaling experienced by *dusp6* mutant gametes may be relatively subtle. In support of this model, the phenotype of *Dusp6* mutant mice is also incompletely penetrant [81], consistent with a general role for *dusp6* in maintaining a permissive range of ERK activity. However, the possibility remains that the incomplete penetrance displayed in these mutants may result

from other causes, such as variations in genetic background, epigenetic factors, individual variations in expressivity, or partial compensation from other regulators.

The role of Dusp6 as a negative regulator of ERK signaling is highly conserved throughout the animal kingdom. For instance, *Dusp6* mutant mice exhibit increased pERK and Erm expression, skeletal dwarfism, craniosynostosis, and hearing loss [81]. All of these defects are characteristic of FGF receptor activating mutations, alluding to the common role of Dusp6 as a negative regulator of ERK signaling. Similar to *dusp6* mutant zebrafish, *Dusp6* mutant mice have increased postnatal lethality, with a significant decrease in homozygous mutant pups surviving to weaning age. However, the mouse mutants die at later stages than the zebrafish mutants. Hence, there does not appear to be a comparable defect at the one-cell stage in mouse and zebrafish embryos. Furthermore, although we initially observed defects in *dusp6* morphants, these were not recapitulated in *dusp6* germ line mutants. Previous published analysis of *dusp6* morphants demonstrated dorsalization and expansion of neural domains [84], but these defects were also not observed in our germ line mutants. Several recent publications have found similar instances where germ line mutants do not have the same phenotype as the corresponding morphant [86,87]. While there may be several causes for these discrepancies, our finding that *dusp6* MOs produce a phenotype in *dusp6* mutants suggests that in our case the morphant phenotype is due to an off-target effect. Hence, *dusp6* mutant zebrafish that complete the first cell division do not display any overt

developmental phenotypes, although we cannot exclude the possibility of subtle phenotypes that we may have overlooked.

Other regulators of the ERK signaling pathway may compensate for the loss of dusp6

Multiple studies have noted that *dusp6* is expressed in many of the same regions of the zebrafish as FGF ligands [13,16,31,32,95]. Several other proteins known to regulate FGF signaling are also expressed in these regions, and for this reason they have been referred to as the FGF-synexpression group. This group includes other Dusp proteins and phosphatases, members of the Spry family, Sef, and Flrt [13,16,31,32]. Since these proteins are present in the same regions and modulate the same pathway, it is very likely that they are able to compensate for each other when necessary. To address possible compensation, we analyzed the list of differentially-expressed genes from our RNA-seq experiment to see if other negative ERK modulators of the FGF-synexpression group were up-regulated in *dusp6* and *dusp2* mutants. We did not detect significant changes in expression level of any of these genes, but it remains possible that factors regulated by post-translational modifications could compensate for the loss of Dusp function. Due to the redundancy of these modulators, it may be necessary to generate mutant lines with more than two loss of function alleles to observe changes in signaling levels and an overt developmental phenotype.

CONCLUSIONS

Our results presented here demonstrate a role for *dusp6* in gamete maturation in both female and male adult zebrafish. Tight regulation of ERK signaling is vital for these processes and a loss of function *dusp6* allele may result in a shift of active ERK levels. While some gametes develop under permissive conditions in the mutants, others may be exposed to elevated ERK levels and this may negatively impact their maturation. The embryos resulting from the union of a defective egg and defective sperm stall at the one-cell stage, unable to complete the first mitosis, and die by 10hpf. However, homozygous mutant embryos from unaffected gametes develop with no overt phenotypes, suggesting that other ERK regulators are able to compensate during embryonic development.

AVAILABILITY OF DATA AND MATERIALS

The RNA-seq dataset generated and analyzed in the present study is available in the GEO repository under the series entry GSE102793 at http://www.ncbi.nlm.nih.gov/geo/query/acc.cgi?acc=GSE102793.

AUTHORS' CONTRIBUTIONS

JMM participated in the design of the study, generated the germ line mutants, performed all phenotype analysis, and drafted the manuscript. CGS conceived the study, secured funding, participated in study design, and finalized the manuscript.

ACKNOWLEDGEMENTS

We are grateful to Dr. Scot Wolfe for advice regarding CRISPR/Cas9 mutagenesis, to Dr. Nathan Lawson for providing the Cas9 plasmid, and to the Sagerström lab for helpful discussions and ideas. The following monoclonal antibodies were obtained from the Developmental Studies Hybridoma Bank, created by the NICHD of the NIH and maintained at The University of Iowa, Department of Biology, Iowa City, IA 52242: Isl1/2 (39.4D5) antibody developed by T. M. Jessell and S. Brenner-Morton; 3A10 antibody developed by T. M. Jessell, J. Dodd, and S. Brenner-Morton; and Zn8 antibody developed by B. Trevarrow. This work was supported by NIH grant NS038183 to CGS.

CHAPTER III: DISCUSSION

The ERK signaling pathway has been studied extensively in regards to its kinase components, downstream targets, association with human disease, and regulation by various modulators. Clear roles have been defined for the pathway in many aspects of embryonic development, including early cell fate determination, axial patterning, organ growth, and metabolism. Despite this large field, the impact of individual regulators on the pathway, and on the developing embryo, is less understood.

Two such regulators, *dusp2* and *dusp6*, belong to the dual-specific phosphatase family and both inactivate ERK proteins by removing both phosphate groups. *dusp2* is expressed in a rhombomere-restricted expression pattern in the early hindbrain under control of one of the *hox* genes, suggesting a role in patterning this region, but this has not been previously investigated. Outside of the hindbrain, Dusp2 has a confirmed role in the inflammatory response and is up-regulated in activated T cells. In contrast, *dusp6* has been studied in different developmental roles, but it is not clear what effect loss of function *dusp6* will have on zebrafish embryos, as there are significant differences between the phenotypes seen in genetic mice mutants and zebrafish morphants. Additionally, the role of these regulators in adult zebrafish is also not fully understood.

In this work, I present the generation of mutant zebrafish lines carrying loss of function alleles for these two phosphatases, including a double homozygous mutant line, with the aim of identifying a role for these modulators of ERK signaling in the developing embryo. Following the generation of these lines,

I find that 50% of the offspring from homozygous *dusp6* mutants do not survive to the early segmentation stages. Further characterization showed that the non-viable embryos are fertilized, but arrest during the first zygotic mitosis and stalled at the one-cell stage for several hours before dying. Remarkably, the 50% of mutants that are able to complete the first cell division are healthy and continue without any defects. Interestingly, the *dusp2* mutants show no overt developmental or adult phenotypes.

In zebrafish, the zygotic genome is not active until approximately 4hpf, meaning that early development and patterning are controlled exclusively by maternal factors. The defect I observe in the *dusp6* mutants occurs much before the maternal to zygotic transition, and therefore suggests a defect in the parental contributions. To support this idea, I demonstrate that *dusp6* is expressed in both male and female gonads during gamete maturation. Based on my observations, I hypothesize that ERK signaling is kept in a permissive range by tight regulation in the gonads, and this could explain why only 50% of the embryos are affected when that regulation is not present. The mutant lines generated here provide insight into the vital role of this phosphatase in the adult during gametogenesis and into its non-essential role in the embryo.

Tightly-Regulated ERK Signaling Promotes the Proper Maturation of Gametes

The phenotypic stalling I describe in the *dusp6* mutants cannot be dependent on the zygotic genome as it occurs so rapidly after the fertilization event and prior to the activation of the zygotic genome. This indicates a probable defect in the gametes produced by the *dusp6* mutant parents.

I have demonstrated that *dusp6* is expressed in the ovaries and the testes under normal conditions. Without the negative regulation supplied by the phosphatase, *dusp6* mutants are expected to exhibit higher levels of active ERK signaling in the gonads. However, this effect is likely subtle. The fact that approximately 50% of the embryos continue through development to adulthood with no developmental phenotypes implies that any changes in ERK signaling during gametogenesis are unlikely to be extreme.

Work in mammalian systems has shown that gametogenesis and the maturation of oocytes and sperm requires ERK signaling. In adult females, an orchestrated series of events involving both the developing germ cell and the surrounding somatic cells allows primary oocytes to mature into fertilizable eggs. The oocytes must be released from arrest in meiotic prophase I after sufficient growth, undergo germinal vesicle breakdown and chromosome condensation, and continue through the second round of meiosis. Several studies have shown that ERK signaling is essential for these events. Two gonadotropins, luteinizing hormone (LH) and follicle stimulating hormone (FSH) are the primary drivers of

ovarian follicle growth and stimulators of the granulosa cells surrounding the developing oocyte [114]. A study performed on rat granulosa cells demonstrated that components of the pathway upstream of ERK, including EGFR, Ras, and MEK, are activated independently of the presence of FSH [115]. However, ERK is only phosphorylated and active when FSH is present. This study determined that the presence of Dusp6 in the granulosa cells keeps ERK inactivated until maturation is initiated by FSH. Then, PKA is activated through cAMP and inhibits Dusp6, allowing active ERK to accumulate and drive downstream genes promoting maturation. For example, expression of cell cycle regulators, such as cyclins, *cdc2*, and *cdc25*, is driven by the ERK pathway and allows the oocyte to proceed through the meiotic cell cycle [116]. Other downstream genes, including *has2* and *ptgs2*, are required for the expansion and growth of the granulosa cells within the ovarian follicle, creating space for the maturing oocyte [117,118].

In the mutant lines lacking the negative regulation supplied by Dusp6, I predict that levels of activated ERK are elevated, especially in the absence of FSH. In addition to a change in the amount of ERK signaling, the lack of negative regulation may also create a situation where ERK signals can be initiated without the proper trigger or during times when the pathway would normally be inactive. As such, if FSH is not required for Dusp6 inhibition and ERK activation, granulosa cells may be providing oocytes with an excess of cell cycle regulators. This could result in oocytes being released from arrest in prophase I prior to reaching the proper size or a reduction in genome copy number due to rapid progression through meiosis. Over-abundant ERK signals could also promote

improper nurturing and signaling to the oocyte, resulting in eggs containing too many or too few parental factors. I hypothesize that this change in signaling, even if subtle, could have severe impacts on the maturing oocytes.

To further support this idea, I observe more direct evidence of meiotic defects. In addition to the maturing oocytes, the asymmetrical cell divisions of meiosis give rise to small cells called polar bodies. These are normally not fertilizable, despite containing a full copy of the genome (reviewed in [130,131]). I observe large and disorganized polar bodies in a percentage of mutant embryos, presumably those that will go on to stall at the one-cell stage. These abnormal characteristics may be indications of defects in meiotic chromosomal segregation or polar body degradation. Both of these problems could result in the developing embryo carrying an improper genome copy number after fertilization. However, when mutants are later stained with DAPI at 1hpf, the polar bodies are no longer visible in both the healthy and stalled embryos. This suggests that while there may be a delay in their degradation, the polar bodies are eventually properly degraded or separated from the zygote.

Similar to oogenesis in adult females, the generation of healthy sperm in adult males also requires well-coordinated ERK signaling. At the beginning of meiotic metaphase I in the testes, cell cycle regulators are activated downstream of ERK signaling [119]. The phosphorylation of chromatin-binding factor HMGI-C by activated Nek2 causes release of DNA [120,121]. This allows condensation factors to bind chromatids and trigger their condensation in preparation of meiotic division. This mechanism also maintains condensation of chromosomes between

metaphase I and II to ensure the proper reduction of the genome from a diploid to a haploid state in the spermatids. Similarly to the granulosa cells of the ovary, Sertoli cells coordinate meiotic progression of the developing spermatocytes and their growth within the testes [122]. The maturation of spermatocytes requires the movement of the cells across the seminiferous epithelium and the blood-testis barrier. The hormones responsible for promoting this movement have been shown to activate ERK in the Sertoli cells, and downstream genes then ensure the integrity of vital tight junctions between the Sertoli cells and spermatocytes [123]. ERK signaling has also been detected in the tails of human sperm [124]. Its activation is required for proper sperm motility and hyperactivation within the female reproductive tract. It also appears to have a positive role in the acrosome reaction that allows the sperm to penetrate the oocyte membrane [124].

These demonstrated roles of ERK in proper spermatogenesis provide evidence that mis-regulation of this pathway could produce defective sperm. In the mutant lines containing loss of function *dusp6*, I again predict that levels of activated ERK are elevated. Excess ERK signaling could result in premature condensation of chromosomes and lead to improper genome copy numbers in the resulting sperm. The manipulation of ERK signaling in the Sertoli cells could also weaken the tight junctions with the spermatocytes, inhibiting proper movement and resulting in sperm carrying improper parental factors. Mis-regulation of ERK signaling in the mature sperm itself may also impact the acrosome reaction and prevent proper fertilization, although this does not seem to be the case in the *dusp6* zebrafish mutants.

Additionally, mis-regulation of ERK signaling in the mammalian reproductive system has previously been shown to cause abnormal pubertal development and infertility. Female mice carrying a mutant allele for constitutively active RAS have defects in ovulation and ERK1/2 mutant female mice are completely infertile [38,40]. In humans, congenital hypogonadotropic hypogonadism has been linked to missense mutations in *DUSP6* and other ERK regulators [90]. This disorder is characterized by gonadotropin deficiency, affects both males and females, and results in infertility.

Despite the evidence supporting the role of *dusp6* in modulating ERK signaling in the gonads during gametogenesis, this work has not identified a clear mechanism or nature of the resulting defect. These two caveats to this work are discussed below.

Is dusp6 expressed in granulosa and Sertoli cells?

As Figure 2.12B demonstrates, *dusp6* expression is detectable in both the ovaries and testes. However, the samples examined here were collected from whole ovaries and whole testes. This qPCR experiment clearly shows that *dusp6* is detectable in zebrafish gonads, but does not provide further information as to in which specific cell types. Previous work demonstrates that *Dusp6* is expressed in rat granulosa cells [115], in mouse epididymal cells [132], and in rat peritubular myoid cells of the testes [133], but I have not proven that *dusp6* is present in the corresponding cells of the zebrafish.

There are two direct approaches to determine the specific gonadal cell types expressing *dusp6* in the zebrafish. Histological sectioning techniques are commonly used to study tissue organization in zebrafish. Dissected ovaries and testes could be stained by *in situ* hybridization for *dusp6* and then mounted and cryosectioned. Similar techniques have been published and could serve as examples for identifying cell types within the section images [133–135]. Additionally, Michael Tsang's research group maintains a transgenic zebrafish line expressing destabilized green fluorescent protein (d2EGFP) under control of the *dusp6* promoter [82]. This line was originally generated as a FGF reporter line, but I could use this line to further characterize *dusp6* expression in adults. Similar cryosections of dissected ovaries and testes could be examined for fluorescence to determine the location of *dusp6* expression. This method would require that *dusp6* expression is fully recapitulated in *Tg(dusp6:d2EGFP)* adults and that the GFP fluorescence is visible from very thin tissue sections.

This question could be further explored in females utilizing a second transgenic line that expresses GFP under the control of the *cyp19a1a* promoter. This estrogen synthetase is strongly expressed in the granulosa cells surrounding maturing oocytes, and thus, the *TgBAC(cyp19a1a:EGFP)* line specifically fluoresces in granulosa cells [136]. A GFP-positive population of granulosa cells could be isolated by fluorescence activated cell sorting of cells from whole ovaries dissected from adult females of this line. The expression of *dusp6* in these cells could then be compared to that in the remaining ovarian cells by performing qPCR. This experiment would not only show if *dusp6* is

expressed in the granulosa cells, but would also indicate if *dusp6* could play a larger role in the ovary. This type of analysis could also be performed in the *Dr_gsdf:eGFP* line [137]. The zebrafish *gsdf* gene is expressed specifically in granulosa and Sertoli cells, and expression is increased in cells that are in closer proximity to the maturing gamete [137].

In what ways are gametes from dusp6 mutant adults defective?

The overt phenotype observed in *dusp6* mutants is that approximately 50% of offspring from homozygous parents arrest during the first zygotic mitosis, remain at the one-cell stage for several hours, and eventually die. This clearly demonstrates that a large portion of the gametes produced by the mutant adults are not capable of giving rise to a healthy embryo. However, as shown in Figure 2.9, these gametes are able to complete the fertilization process and the resulting pronuclei are able to migrate and merge. As mentioned above, I suggest that mis-regulated ERK signaling in the gonads could result in gametes that contain an inappropriate genome copy number or contain a defective parental factor. However, I have not identified the specific defect that prevents some gametes from developing into healthy embryos in this work.

Mammalian development is very sensitive to whole chromosome aneuploidies, and the gain or loss of any chromosome is embryonic lethal in mice [138]. In humans, somatic chromosome duplication results in severe congenital diseases, with the most widely known example being Down syndrome [138]. However, these aneuploid embryos are able to complete the first zygotic cell

cycle. Aneuploid zebrafish embryos also survive to the segmentation stages, albeit obvious morphological defects [139]. This is in contrast to the *dusp6* mutants that are not able to complete the first zygotic mitosis. While this suggests an additional defect in the *dusp6* mutant gametes, it may still be informative to determine if these gametes carry the correct number of chromosomes by quantifying the genomic DNA in individual oocytes or sperm. The isolation of oocytes and spermatocytes from zebrafish is straightforward and well-established [140]. Once isolated, standard flow cytometry following DNA labeling with propidium iodide could be used to quantify chromosomes [141]. If this method did not provide the necessary level of sensitivity, fluorescence *in situ* hybridization (FISH) could also be used to detect duplications or deletions of individual chromosomes [141]. Other standard techniques for quantification, such as qPCR, are technically challenging in gametes due to the extremely small amount of genetic material. New methods of detecting improper chromosomes have been tested in humans, as aneuploidy is a common cause of miscarriages and IVF failure. These involve advanced karyotyping and analysis of the genetic content of the polar body (reviewed in [142]). Recent advances in next generation sequencing have also been applied to gamete analysis, and could be used to identify aneuploidy [143].

Alternatively, the defect carried in gametes from *dusp6* homozygous mutant adults could be the lack or abundance of a specific parental factor. Maturating gametes and early zygotes are transcriptionally inactive, meaning early development is controlled by transcripts and proteins provided by the

parents. Translational control of these parental transcripts by adenylation factors is necessary for proper temporal and spatial protein expression (reviewed in [144]). Additional factors, such as non-coding RNAs, small RNAs, and microRNAs, and epigenetic modifications to histones and DNA methylation are also required in maturing gametes (reviewed in [145–149]). Mis-regulated ERK signaling in the gonadal cells that provide the maturing gametes with these factors could result in gametes that are defective in the factors required for embryonic development. Single-cell RNA-seq would provide information regarding all transcripts that are differentially expressed between wildtype and mutant gametes and might suggest a mechanism by which excess ERK signaling causes those defects. Single-cell techniques have recently been used to analyze the transcriptome of many cell types (reviewed in [150]), including oocytes from human patients [151]. Careful technical decisions would need to be considered to use this technique on germ cells, such as the method of mRNA isolation and ribosomal RNA removal. Additionally, ChIP-seq techniques could be used to compare epigenetic information between wildtype and *dusp6* mutant gametes.

Successful Gametogenesis Requires ERK Signaling to Fall Within a Permissive Range

An interesting observation regarding the phenotypic stalling in the *dusp6* mutant embryos is that only 40-50% of each clutch is affected. Likewise, I noticed significant inconsistency in the percentage of affected embryos among clutches

of embryos from different parents. I questioned the basis of this variability. These observations directly imply that not all gametes produced by homozygous mutant adults are defective, but do not suggest an explanation.

As discussed in previous chapters, there are natural examples of signaling variability in many pathways and cell types. Small differences in gene expression and protein concentrations among individual cells can be amplified in a pathway and can result in variable signal intensity [126,127]. For example, in a clonal population of mammalian cells, natural differences in protein expression within an apoptotic pathway allow some cells to survive while others succumb to apoptosis [126]. The recent use of genetic biosensors will allow further study of these variations among cells of different types and in different tissues [152]. The redundant roles of many negative regulators, such as Dusp proteins, are thought to minimize this variation and signal noise [125,128,129]. Additionally, there are various examples of phenotypes resulting from improper levels of signaling, as discussed earlier.

Considering this, I hypothesize that there is a range of acceptable levels of ERK signaling within the adult reproductive system. In wildtype fish, early stage oocytes and spermatocytes are exposed to levels of signaling that fall within this range and they mature normally (Figure 3.1). In contrast, the *dusp6* mutant adults lack a negative regulator and the range of ERK signaling within the gonads is presumably expanded and increased. This implies that some oocytes and spermatocytes in the mutants may still be exposed to levels of ERK signaling that fall within the normal permissive range, but many will sense excess

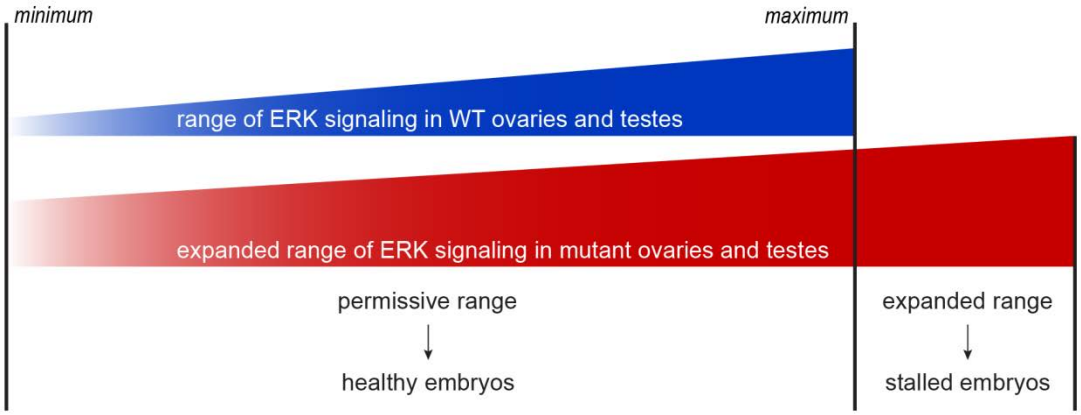

Figure 3.1. Model of permissive and expanded range of ERK signaling
A model illustrating the shifted and increased range of ERK signaling in the mutant fish lacking the negative regulation normally provided by Dusp6. Some embryos will still experience levels of signaling within the permissive range, but others will sense more, resulting in defective gametes and stalled embryos.

signaling. I hypothesize that these gametes will fail to give rise to healthy embryos, due to exposure to a level of ERK signaling that is higher than the permissive range. I also predict that the increase in signaling sensed by these gametes may not be overtly large, but my observations suggest that this change has a significant effect on the resulting embryos. Gametes derived from the same germ cell that remain connected by the syncytium will presumably respond to the same amount of ERK signaling, but this level may very within the gonad. The phenotype of *Dusp6* mutant mice is also incompletely penetrant [81], further supporting the idea of a role for *dusp6* in maintaining a permissive range of ERK activity. Conversely, the incomplete penetrance seen here could also be influenced by various other genetic modifiers.

The *dusp6* and *dusp2* Morphant Phenotype is Caused by an Unidentified Off-Target Effect

As presented in Chapter II, I had used MOs targeted against *dusp6* and *dusp2* to knock down their expression prior to the generation and analysis of the germ line mutant lines. MOs have a long history of use in zebrafish before genome editing techniques were widely available; however, recent discrepancies between reported MO-induced (morphant) and germ line mutant phenotypes in zebrafish have been highlighted in several publications [86–89].

With the rise of genome editing systems, such as CRISPR/Cas9, and the increased ease of generating targeted germ line mutations, many previously-

published morphant phenotypes can now be validated with genetic deletions. One study chose 20 different zebrafish genes with MO-induced phenotypes and generated a mutant line for each of them. Remarkably, ten of these mutants failed to recapitulate the morphant phenotype [86]. Further examination by the same group revealed that 80% of published morphant phenotypes are not observed in genetic mutants from the Sanger Zebrafish Mutation Project. These findings challenge the reliability of using MOs to achieve loss of gene function.

In light of these surprising comparisons, several explanations have been proposed. One possible cause may be that the mutant alleles are not completely loss of function, especially in cases where partial wildtype sequence remains in the mutant [88]. It is possible for a truncated polypeptide to be produced and retain some functionality, or for the translation machinery to make use of a secondary start site. This can be ruled out by quantifying mRNA expression and assaying for protein function in the mutant to ensure a null allele [88].

Second, the idea of a compensatory network has also been suggested. A recent study identified a set of genes up-regulated in mutants, but not in morphants, and revealed that such a network may exist to buffer against genetic deletions [87]. Since MOs only reduce the amount of translated protein, this compensation may not be triggered in the morphant, leading to a phenotype that is only observed in the morphant.

Another concern, which has been noted since the earliest MO knockdowns, is the activation of tumor suppressor p53. Non-specific toxicity and widespread apoptosis are common in embryos injected with MO, especially at

high doses. These effects are likely mediated by p53 and can be easily mistaken as a knockdown phenotype. Co-knockdown of p53 has been shown to rescue some MO-induced phenotypes, proving that they are not specific to the targeted gene [89].

Finally, perhaps the most obvious pitfall of using MOs is the potential for off-target effects. There is no standard dose appropriate for all MOs, and the chance of off-target binding increases with the amount injected [88]. It is also unclear what level of homology is required between the MO sequence and the target for efficient interference. The ideal method for minimizing off-target effects is to titrate the MO in a null background [88]. Since the transcript of the target gene would not be present, any additional phenotype observed would be clearly caused by the MO and would be an off-target effect. Notably, this could be difficult distinguish if the null has a complex phenotype. This method would determine an appropriate dose by identifying a concentration at which there are no additional effects in a null background and a phenotype is observed in a wildtype embryo.

This is the exact methodology I followed and is shown in Figure 2.5I-K. Following the observation of a Mauthner neuron phenotype in the *dusp6* and *dusp2* morphants on a wildtype background (Figure 2.1E-M), I observed the same phenotype when the MOs were injected into the respective germ line mutants. This proves that the MOs are binding to an off-target transcript. Remarkably, no other region of the zebrafish genome contains 100% sequence homology to my *dusp6* and *dusp2* MO sequences. It is possible that the MOs are

able to bind a region without complete sequence homology, and if this is the case, I account for the Mauthner neuron phenotype by predicting that they are knocking down a gene that functions in r4 of the hindbrain.

For these reasons, the zebrafish field has shifted away from the use of MOs and continues to emphasize the generation of germ line mutant lines.

Remaining Questions and Future Directions of this Work

The work presented here clearly demonstrates a requirement for *dusp6* during gametogenesis in female and male adult zebrafish. However, the mechanism and nature of the defect resulting from the loss of *dusp6* is not yet clear. To further investigate the role of *dusp6* and other regulators of the FGF/ERK pathway, there are several questions to address.

Do dusp6 mutants have additional or more subtle phenotypes?

As discussed in Chapter II, the offspring of two *dusp6* homozygous mutants that survive the first mitotic cell cycle continue through embryogenesis with no overt phenotypes. It is impossible to rule out other more subtle phenotypes without further characterization. Based on the data on *dusp6* mouse mutants, I suggest the examination of other organs and older embryos. *Dusp6*$^{-/-}$ mice have smaller skeletal features and defects in skull growth [81]. Simple staining with alcian blue and alizarin red will show if *dusp6* mutant zebrafish have similar defects during the hatching period [153]. *Dusp6*$^{-/-}$ mice also exhibit larger

hearts due to increased myocyte proliferation [83]. Cardiac development and lineages have been extensively studied in zebrafish, and the size of the heart in *dusp6* mutant embryos could be examined using a marker for cardiomyocytes, such as Connexin-43. Proliferation of cardiac cells could also be monitored by BrdU labeling. The loss of *Dusp6* also causes hearing loss in mice [81]. Behavioral experiments could determine if *dusp6* mutant zebrafish exhibit any auditory or vestibular defects, and Pax2a could be used as an otic vesicle marker to confirm normal morphology. Again, these phenotypes would likely be very subtle, incompletely penetrant, and unlikely to affect viability of the individual.

In the adult *dusp6* mutants, further characterization should focus on defects in the gonads and gametes. It would be ideal to quantify changes in ERK signaling between wildtype and mutant gonads. This could be done by fixing and sectioning dissected ovaries and testes, and then immunostaining for pERK. However, this technique could be very technically challenging as the difference may be small and may only occur in a percentage of gonadal cells. Additional examination of the granulosa cells of the ovary could be done using the *TgBAC(cyp19a1a:EGFP)* or *Dr_gsdf:eGFP* lines mentioned above [136,137]. The *dusp6* loss of function allele would need to be crossed onto these lines. A comparison of the transcriptome between *dusp6*$^{+/+}$ and *dusp6*$^{-/-}$ granulosa cells could then be performed by dissecting the ovaries, cell sorting to obtain a population of granulosa cells, and performing RNA-seq. This would provide insight into the transcriptional changes caused by an increase in ERK signaling specifically in the cells controlling oocyte maturation.

To further focus on the embryos that do not survive, it would be informative to quantify the genomic DNA following the fusion of the maternal and paternal pronuclei. Numerous techniques could be used to perform this quantification, including flow cytometry, FISH, karyotyping, and qPCR [141,142]. This information would provide a genetic reason as to why these embryos are unable to develop normally. Moreover, it would be interesting to determine if the stalled embryos are able to enter a second S phase without completing the first mitosis. I suspect this is unlikely, but possible, and could be determined using BrdU labeling of one-cell embryos.

Additionally, all of the aforementioned experiments could be performed on the *dusp2* mutants, in which I was not able to identify a phenotype previously.

Why are dusp6 and dusp2 nonessential in the embryonic hindbrain?

Based on their expression patterns and the requirement for FGF signaling, I had hypothesized that *dusp6* and *dusp2* would play an important role in hindbrain development. My results clearly suggest that this is not the case. This raises the question of redundancy and compensation among negative regulators of the FGF/ERK pathway.

I intended to address this question by comparing the transcriptomes of wildtype and *dusp2*$^{-/-}$*;dusp6*$^{-/-}$ embryos by RNA-seq. However, I was unable to identify genes that were up-regulated in compensation for the loss of *dusp6* and *dusp2* or genes that were differentially-expressed and interact with the FGF/ERK pathway (Figure 2.5C-D, Figure 2.6, Table 2.5). To improve upon this

experiment, it may be more informative to construct RNA-seq libraries from mRNA isolated from dissected hindbrains, or even isolated r4 cells. It is clear that the ERK pathway is under different levels of regulation in different regions of the body, and the previous use of mRNA from whole embryos may be diluting any changes that are specific to the hindbrain. Moreover, there may be post-translational modifications required to activate other negative regulators of the pathway. Specific assays could be designed to determine if increased levels of these modifications are present despite no increase in transcription.

The most direct readout of *dusp6* and *dusp2* function in the hindbrain is immunostaining for pERK, but this technique is challenging, variable, and not easily quantifiable. It may be more informative to perform a different phosphorylation assay. Lysates from dissected hindbrains could be probed by Western blot using the same pERK antibody or using a non-antibody method of detecting protein phosphorylation, such as Tymora's pIMAGO kits. More traditional *in vitro* enzymatic assays or a phospho-specific ELISA could also be used. However, small changes may not be detectable and these techniques would not provide information regarding where in the hindbrain any pERK changes occur. Additionally, a key difference between the two phosphatases is that Dusp6 has a stronger specificity for ERK MAP kinases, while Dusp2 has been reported to target JNK and p38 in addition to ERK in certain contexts [71,72]. This begs the question of whether the activation status of JNK and p38 MAP kinases is changed in the *dusp2* mutants. Immunostaining for pJNK and

pp38 will show if these pathways are affected, but again, any differences are likely subtle as the *dusp2* mutants exhibit normal development and survival.

Are there other roles for regulators of FGF/ERK signaling in adults?

In addition to *dusp6* and *dusp2*, there may be novel roles for other modulators of the FGF/ERK pathway in the gonads or adult zebrafish. It will need to be determined where many of these proteins are expressed in the adult system. By examining the regions in which multiple regulators overlap, it may be possible to get create germ line mutant lines lacking several regulators that have more severe phenotypes.

Further investigations, both using the germ line mutants generated here and other similar lines, may provide insight into the roles of modulators of the FGF/ERK pathway in a broader context, particularly in the adult. Although much of the field focuses on embryonic development, the pathway has also been studied in adults due its association with mainstream areas of study. The FGF/ERK pathway has been shown to play vital roles in regeneration of adult tissues in the zebrafish (reviewed in [154]), especially in the fin [155] and spinal cord [156]. Glia progenitors of the adult brain, which will give rise to cells that support and insulate neurons, also require active ERK signaling to proliferate and differentiate [157]. In humans, FGF/ERK and EGF/ERK pathways have established roles in the formation and metastasis of numerous cancers, especially those of the female reproductive system (reviewed in [49,158–160]).

At this time, it is not fully understood what roles all of the pathway modulators may play in these processes.

CONCLUSIONS

In conclusion, this work establishes a role for *dusp6* in gamete maturation in female and male zebrafish. By generating germ line mutations, I show that a loss of function *dusp6* allele results in defective gametes that do not give rise to healthy offspring. Interestingly, not all gametes and embryos are affected, and my model illustrates how the loss of negative regulation normally supplied by Dusp6 results in increased signaling range and variability. This suggests that some gametes develop under normal ERK signaling conditions, while others sense excess signaling and this negatively impacts their maturation. Notably, homozygous mutant embryos from unaffected gametes develop with no overt phenotypes, leading me to believe that other ERK regulators are able to compensate during embryonic development. The FGF/ERK signaling pathway has numerous vital roles throughout embryonic and adult life, meaning our understanding of its regulation is important for the future treatment of human disorders and diseases. Further investigation of the key regulators of this pathway will continue to provide insight into redundancy, plasticity, and compensation in signaling networks.

APPENDIX A:
LOSS OF FUNCTION *spry1* DOES NOT AFFECT ERK SIGNALING IN THE EARLY ZEBRAFISH HINDBRAIN

INTRODUCTION

In addition to the Dusp family, the Sprouty (Spry) proteins also negatively regulate the ERK signaling pathway. This group is composed of the four vertebrate homologs to the singular Spry protein in *Drosophila*. Spry was originally identified as an inhibitor of the Breathless FGF receptor during tracheal development [17]. Since then, several studies have demonstrated the ability of the Spry proteins to antagonize receptor tyrosine kinase signaling, specifically the ERK pathway through FGF signaling [18–25]. Similarly to the Dusp family, Spry expression requires activation through FGF signaling, suggesting a negative feedback loop system of regulation [161,162].

Interestingly, the Spry proteins contain no conserved protein-protein interaction or catalytic motifs [23,24,163], making it difficult to determine the mechanism by which they function as part of the signaling pathway. Each member of the family contains conserved serine- and cysteine-rich protein regions. It has been shown that Spry proteins require phosphorylation on a tyrosine residue to have inhibitory activity [17] and these regions are believed to be involved in kinase interactions [18]. Due to the lack of other interaction domains or any conserved protein domain, it remains unclear with which component of the FGF signaling pathway Spry proteins interact. Early studies in *Drosophila* suggested that Spry acts on Grb2 downstream of the FGF receptor (Figure 1.1) [17–20]. Later studies performed on cultured cells reported the possibility that Spry inhibits activation of Raf or Ras (Figure 1.1) [23,24]. It is

possible that different Spry proteins act at different levels in the pathway, or that their interactions may be dependent on the cellular environment, but these precise interactions are not yet understood.

In the context of embryonic development, the Spry family has been connected to several important roles, all of which involve the negative modulation of ERK signaling. In mouse embryos, the loss of *Spry1* and *Spry2* causes an increase in the size of the otic placode as epidermal cells are recruited to the otic domain as a result of increased FGF signaling [21]. Anti-sense morpholino oligos have been used to generate *spry4* morphants in zebrafish and these embryos are dorsalized in a similar manner to embryos with up-regulated FGF/ERK signaling [22]. Work in zebrafish has also shown that Spry proteins also work cooperatively with Sef at the mid-hindbrain boundary to regulate FGF together with BMP signaling [164]. In accordance with their antagonistic effect on ERK signaling, Spry proteins have demonstrated roles in inhibiting cell differentiation and growth factor targets more broadly [23,165].

Of the four proteins in zebrafish, *spry1* shows the strongest expression in the hindbrain region. During the early segmentation stages, *spry1* is expressed in a nearly-identical pattern to that of *dusp6* and overlaps with *dusp2* expression in r4 (Figure A.1A). Additionally, *spry1* expression is also dependent FGF/ERK signaling and *spry1* is a member of the FGF-synexpression group [13,16,32]. Based on this, I hypothesized that germ line *spry1* mutants would provide new information regarding how *spry1* functions and how members of FGF-synexpression group work together to effectively control ERK signaling.

Here I used the CRISPR/Cas9 genome editing system to generate loss of function zebrafish mutants for *spry1* in a similar manner to the mutant alleles presented in Chapter II. While these mutant embryos were not subjected to intensive characterization, I do not detect any overt phenotypes or any effect on the localization or intensity of pERK.

METHODS

Zebrafish care and embryonic injections

Zebrafish were handled and injected as discussed in Chapter II.

Generation and injection of CRISPR guide RNAs

CRISPR target sites (Table A.1) were selected based on their proximity to the start and stop codons of the coding sequence of *spry1*, and also by the requirement for a protospacer adjacent motif (PAM) sequence (NGG) at the 3' end of target site (Figure A.1B). I created and annealed oligos containing a T7 promoter sequence, the target sequence, and an additional constant region to create the template for the guide RNAs (Table A.2). These templates were transcribed *in vitro* using T7 RNA polymerase (Promega) in a reaction containing transcription buffer (Promega), RNase inhibitor (Promega), and rNTPs. A linearized plasmid encoding cas9 [100] was also transcribed *in vitro* using the Sp6 mMessage mMachine Kit (Ambion). The two guide RNAs were combined

with *cas9* mRNA and phenol red, and 1-2nl of this mixture was injected into the cell of early one-cell stage embryos.

Table A.1 Characteristics of CRISPRs targeting *spry1*

CRISPR guide	Target coordinate [a]	Target sequence [b]	Strand [c]	Mutagenesis rate [d]
spry1-5'	Chr14:508885	GCGTGGGCATGCGGACCCCG	+	2/8
spry1-3'	Chr14:509658	GCTGCCGCTGCAAGAACTCC	-	

[a] Target coordinate defined by the first nucleotide of the target sequence
[b] Genomic sequence targeted by the guide RNA
[c] Strand of genomic DNA which is targeted by the guide RNA
[d] The number of F0 germ line positive founders identified out of those screened

Table A.2 Sequences of oligos to generate CRISPR guide RNAs for *spry1*

CRISPR	First oligo [a]	Second oligo [b]
spry1-5'	TTAATACGACTCACTATAGGCGTGG GCATGCGGACCCCGGGGGTTTTAG AGCTAGAAATAGCAAG	AAAAAAGCACCGACTCGGTGCCACTTT TTCAAGTTGATAACGGACTAGCCTTATT TTAACTTGCTATTTCTAGCTCTAAAAC
spry1-3'	TTAATACGACTCACTATAGGAGTTC TTGCAGCGGCAGCCGGGTTTTAGA GCTAGAAATAGCAAG	AAAAAAGCACCGACTCGGTGCCACTTT TTCAAGTTGATAACGGACTAGCCTTATT TTAACTTGCTATTTCTAGCTCTAAAAC

[a] Sequence of the first oligo used to create the guide template containing the T7 promoter sequence
[b] Sequence of the second oligo used to create the guide template containing the constant region

Identification of germ line mutations and genotyping

The embryos injected with the guide RNAs and *cas9* mRNA mixture were raised as the F0 generation. At three months of age, these fish were individually crossed to a wildtype fish. Half of each resulting clutch was raised to adulthood as the F1 generation. Genomic DNA was extracted from the embryos in the remaining half of the clutch to confirm activity of the guide RNAs. This genomic DNA was screened for deletions by PCR using primers that flank the region between the two guide RNA target sites (Figure A.1B, Table A.3). Amplification from mutant sequences containing large deletions will produce a 200-300bp product (Figure A.1C, Table A.3). In contrast, amplification from wildtype sequences with the same primer pair will produce a 1036bp product (Figure

A.1C, Table A.3). F1 adults derived from positive clutches were individually genotyped with fin clip DNA using the same PCR primers (Figure A.1D). F1 heterozygous fish were then crossed to generate homozygous mutants.

Table A.3 Primer sequences to genotype *spry1* mutants

PCR primers to genotype (F/R) [a]	Size of mutant band [b]	Size of WT band [c]
CGCTACAGATCACGGATCAA/ GTTTGTGCCTCAGGATGGTT	~263bp	1036bp

[a] Sequence of the forward and reverse primers used to detect deletion alleles
[b] Approximate expected size of the PCR band if a CRISPR-induced deletion occurred
[c] Expected size of the PCR band for the wildtype allele

Immunostaining

For whole-mount immunostaining of pERK, embryos were fixed in 4% paraformaldehyde overnight at 4°C, treated with 3% hydrogen peroxide in methanol for 1 hour on ice, and then stored in 100% methanol at -20°C. Antibody staining was then performed as described previously [166] using a rabbit anti-phospho-p44/42 MAPK ERK1/2 antibody (1:250; Cell Signaling Technology 4370) and a goat anti-rabbit IgG-HRP secondary antibody (1:1000; Abcam 6789). Signal was detected using PerkinElmer's TSA Plus Fluorescein System. Embryos stained for pERK were counter-stained using a Valentino antibody, which was generated by immunizing rabbits with a GST-tagged full-length zebrafish Valentino protein, and a goat anti-rabbit Alexa Fluor 568 secondary antibody (1:200; Molecular Probes A110011). Stained embryos were suspended in 3% methyl cellulose for imaging. Images were captured using a Leica M165 FC microscope equipped with a Leica DFC310 FX camera. All images were

imported into Adobe Photoshop and adjustments were limited to contrast, levels, and cropping; all adjustments were applied to the entire image.

RESULTS

Generation of spry1 germ line mutants

To gain a better understanding of the role of *spry1* during zebrafish development, I generated germ line mutants using the CRISPR/Cas9 genome editing system. I designed two guide RNAs – one targeted to the 5' end of the coding sequence and one targeted to the 3' end (Figure A.1B, Table A.1) – with the intention of co-injecting them to delete the sequence between the two target sites. Due to the fact that Spry proteins contain no interaction or conserved domains, I elected to delete the majority of the coding sequence to generate a null allele. For this reason, guide RNA target sequences were chosen based on their proximity to the start and stop codons, and also by the requirement for a protospacer adjacent motif (PAM) sequence (NGG) at the 3' end of each target site (Figure A.1B, Table A.1).

The activity of the guide RNAs was tested and the F0 fish were generated as described in Chapter II. Briefly, genomic DNA from pools of injected embryos was amplified using primers that anneal outside the guide RNA target sites (Figure A.1B-C). I detected bands of approximately 200-300bp, indicating the presence of large CRISPR-induced deletions. I then injected several hundred embryos with the same guide RNAs and mRNA encoding *cas9*. F0 founder fish

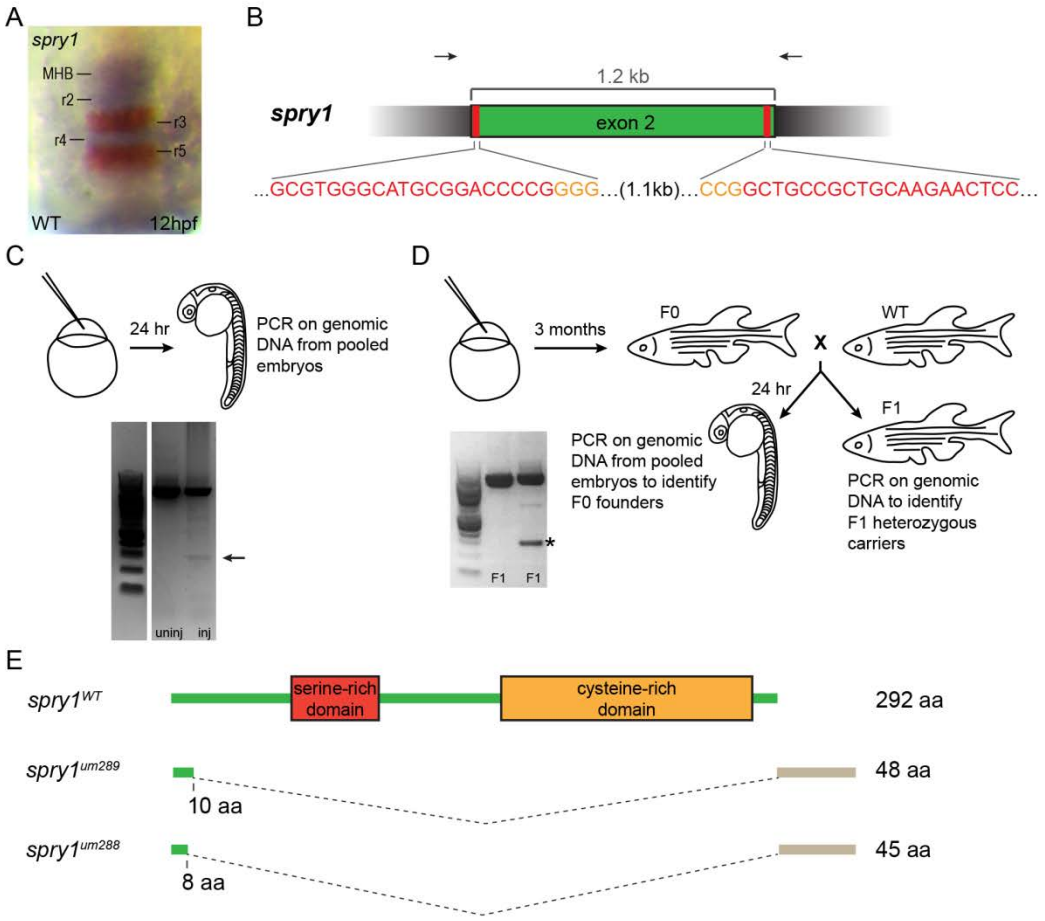

Figure A.1. CRISPR genome editing yields loss of function mutants for *spry1*
A. 12hpf wildtype embryos were assayed by *in situ* hybridization for expression of *spry1* (blue stain) and *krox20* (red stain) marking r3 and r5. **B**. Schematic of the genomic sequence for *spry1* with the length of the total coding sequence indicated. Exon 1 contains only UTR and no coding sequence. Vertical red lines and red nucleotides denote the CRISPR target sequence, and orange nucleotides indicate the PAM sequence. Arrows above the schematic indicate the approximate locations of the genotyping primers used to detect CRISPR-induced deletion alleles (see Table A.2). **C**. Identification of active guide RNAs. Genomic DNA was extracted from pools of injected embryos and PCR-amplified to detect CRISPR-induced deletions. Arrow points to PCR product resulting from successful deletions. **D**. Identification of F0 founder fish. Adult F0 fish were crossed to wildtype and the resulting offspring genotyped as in **C**. Asterisks indicate F0 fish transmitting deletions to their offspring. **E**. Predicted peptide sequences of the identified mutant alleles for *spry1*. The large dashed wedges represent the location of CRISPR-induced deletions, and the gray bars represent residues that are read out of frame prior to a premature stop codon. Amino acid numbers below each peptide sequence indicate the residue affected by the deletion, and the numbers to the right indicate the length of the peptide.

carrying germ line mutations were identified by crossing F0 fish to wildtype fish and screening the offspring for deletions with the same PCR primers (Figure A.1D). Offspring of F0 founders with germ line mutations were raised to adulthood followed by genotyping to identify heterozygous F1 carriers.

Two F0 founders with germ line mutations were identified out of eight fish tested (Table A.1). One founder carried two mutant alleles with large deletions within the coding sequence of the *spry1* gene. The first mutation (*spry1*^{um289}) contains a 766bp deletion and was transmitted to 19% of the offspring. The second mutation (*spry1*^{um288}) contains a 770bp deletion and was transmitted to 5% of the offspring. Both of these deletions appear to be the product of two double strand breaks as was expected. Conceptual translation of the remaining sequences yields short peptides containing only ten or eight residues of the wildtype protein sequence (Figure A.1E). These peptides lack the tyrosine residue that requires phosphorylation for antagonist activity, and I therefore conclude that these are likely null alleles. The second F0 founder was positive for a deletion by PCR, but I was unable to identify any heterozygous carriers from its offspring.

Loss of function spry1 allele does not affect pERK localization or intensity

Upon the generation of both *spry1*$^{um288/um288}$ and *spry1*$^{um289/um289}$ homozygous mutants, I found that these embryos are viable, survive to adulthood, and are fertile as mature adults. They appear morphologically healthy with no obvious developmental phenotype.

As with the *dusp6* and *dusp2* mutants, I wanted to determine if the loss of function *spry1* allele could affect the levels of pERK in the hindbrain. If *spry1* functions as a negative regulator of the ERK pathway, a loss of function allele should cause a change in detectable pERK in the regions were *spry1* is normally expressed. However, mutant embryos stained with an anti-pERK antibody, and counter-stained with an anti-Valentino antibody marking r5 and r6, show no differences in intensity or location of pERK within the hindbrain or other regions of the embryo compared to wildtype embryos (Figure A.2A-B). The fact that *spry1* mutants are viable also allowed for the creation of a double mutant line, *spry1*$^{um289/um289}$*;dusp6*$^{um239/um239}$. These embryos also exhibited no changes in pERK localization or intensity (Figure A.2C). I conclude that disrupting *spry1* function does not increase ERK signaling during early zebrafish embryogenesis or development of the hindbrain.

DISCUSSION

Loss of function *spry1* alleles do not cause an overt developmental phenotype and do not affect pERK, but additional regulators may be compensating and further characterization is necessary.

spry1 is not required for early zebrafish embryogenesis

Similar to *dusp6* and *dusp2*, *spry1* does not seem to be required for early embryonic growth and development. Embryos that are homozygous for either loss of function allele are morphologically healthy and survive as fertile adults.

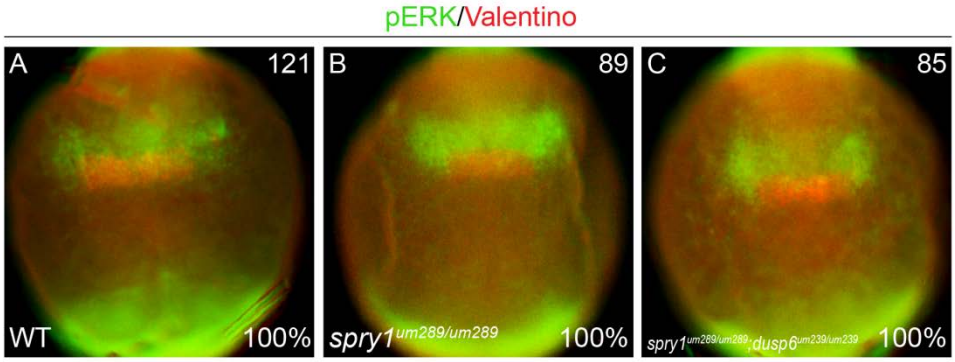

Figure A.2. Loss of function *spry1* allele does not affect pERK localization or intensity

12hpf wildtype (**A**), *spry1*$^{um289/um289}$ (**B**), and *spry1*$^{um289/um289}$*;dusp6*$^{um239/um239}$ (**C**) embryos were assayed by immunostaining for pERK in green; red counterstain detects the Valentino transcription factor in r5 and r6. All embryos are in dorsal view with anterior to the top. Numbers in top right corner of each panel indicate the total number of embryos assayed for that condition. Numbers in bottom right corner indicate percent of embryos with the phenotype shown.

This is in contrast to *Spry1*$^{-/-}$;*Spry2*$^{-/-}$ double mutant mice who die at birth [21]. Interestingly, these mutant mice have no hindbrain patterning defects, but instead exhibit increased FGF and WNT signaling domains. It is likely that these phenotypes require the loss of function of both *Spry1* and *Spry2*, and that explains why they are much more severe than what I find in the *spry1* mutant zebrafish. The *spry4* zebrafish morphant exhibits weak dorsalization and enlargement of the telencephalon during the segmentation stages [22]. While this mimics phenotypes seen by up-regulation of FGF/ERK signaling, these defects are not detected in my *spry1* mutants. It remains possible that *spry4* may have a different mechanism of action than *spry1*. At this time, there are no other loss of function *spry1* alleles in zebrafish to make a direct comparison.

Other regulators of ERK signaling may compensate for the loss of spry1

In a similar manner to the Dusp family, the Spry family members are expressed in many of the same regions of the zebrafish as the FGF ligand and are part of the FGF-synexpression group [2,13,16,32,167]. Since these proteins are present in the same regions and modulate the same pathway, it is very likely that they are able to compensate for each other when necessary. Despite the fact that they interact with different components of the pathway, their overall function is redundant. It may be necessary to generate mutant lines with more than two loss of function alleles to observe changes in signaling levels or an overt developmental phenotype.

Additional characterization of spry1 mutants is required

While *spry1* is clearly not necessary for embryonic development, it remains possible that *spry1* loss of function may cause more subtle defects that were not detected here. The same thorough analysis that was performed on the *dusp6* and *dusp2* mutants in Chapter II will need to be performed on the *spry1* loss of function mutants to identify subtle detects. This could include the examination of genes downstream of the FGF/ERK pathway (such as *pea3*, *erm*, *dusps*, and other *sprys*), genes that define hindbrain patterning (such as *hoxb1a*, *krox20*, *fgf3*, and *fgf8*), genes that control axial patterning (such as *bmp2b*, *bmp4*, *chordin*, and *noggin1*), and neuronal populations (such as the Mauthner neurons, the facial motor neurons, and the abducens motor neurons). With further characterization, these mutants may also be able to provide insight into the interactions between Spry1 and components of the FGF/ERK pathway.

APPENDIX B:
DYNAMIC LOCALIZATION OF pERK IN THE ZEBRAFISH HINDBRAIN DURING EMBRYONIC SEGMENTATION

INTRODUCTION

FGF signaling through the ERK pathway is required for proper patterning of the early hindbrain in zebrafish [47,48,93,94]. The pathway is initiated by the binding of the FGF ligand to the extracellular portion of a FGF receptor (FGFR). These receptors belong to the receptor tyrosine kinase family and the intracellular phosphorylation triggered by ligand binding recruits several adaptor proteins. These proteins, including Frs2 and Grb2, transduce the signal to the kinase cascade consisting of Ras/Raf, MEK, and finally the MAPK ERK. Phosphorylated ERK (pERK) then moves into the cell nucleus where it is able to activate transcription factors and initiate expression of downstream target genes.

Each of the four FGFRs and all of the pathway components are expressed throughout the early hindbrain [7,55,168]. Interestingly, the FGF ligands are not and have a rhombomere-restricted expression pattern during the early segmentation stages [169–171]. In zebrafish, the predominate FGF species present in the hindbrain are *fgf3* and *fgf8*, both of which are expressed exclusively in r4 at 14hpf (Figure B.1A-B) [169,170]. For this reason, r4 has been called the FGF signaling center of the hindbrain [43,54].

Despite the presence of this FGF signaling center, there is evidence that r4 does not depend on FGF signaling for its formation. When FGF signaling is blocked, either through the inhibition of the receptors by a pharmacological inhibitor or through the use of anti-sense morpholino oligos targeted to both ligands, hindbrain patterning is severely disrupted [47]. The fifth and sixth

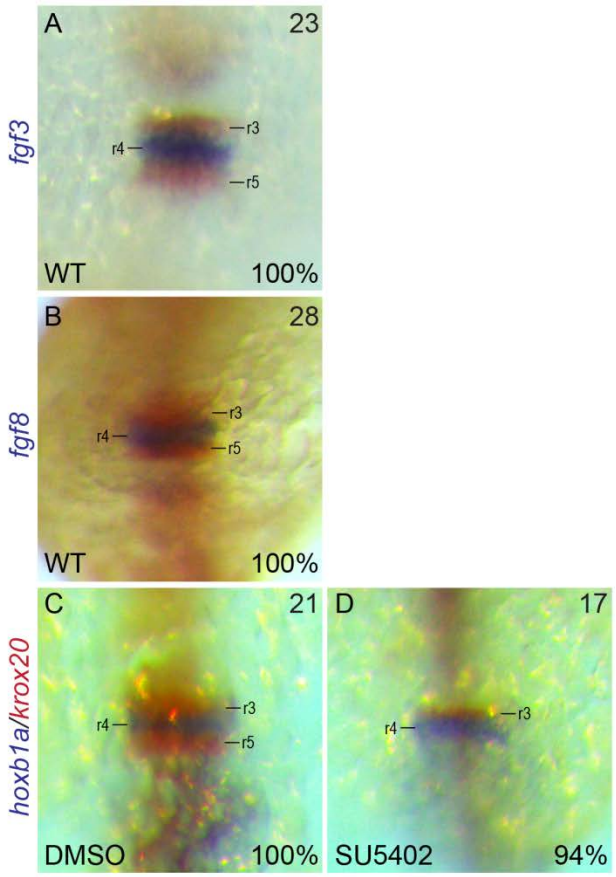

Figure B.1. r4 is the FGF signaling center of the hindbrain, but is not affected by inhibition of FGF signaling

A-B. 14hpf wildtype embryos were assayed by *in situ* hybridization for the expression of *fgf3* (**A**), *fgf8* (**B**), and *krox20* (red stain) marking r3 and r5. **C-D**. Wildtype embryos were treated with either a DMSO control (**C**) or an FGFR inhibitor called SU5402 (**D**), fixed, and assayed by *in situ* hybridization for the expression of *hoxb1a* marking r4 and *krox20* (red stain) marking r3 and r5. All embryos are in dorsal view with anterior to the top. Numbers in top right corner of each panel indicate the total number of embryos assayed for that condition. Numbers in bottom right corner indicate percent of embryos with the phenotype shown.

rhombomeres (r5 and r6), along with the neurons found in those regions, do not develop. However, r4 is not affected (Figure B.1C-D).

This suggests that despite the abundant presence of the ligands in r4, the FGF signaling pathway may actually be more active in r5 and r6. Negative regulators of the pathway may be more highly expressed in r4, as discussed in early chapters, and these may be responsible for keeping levels of active signaling in r4 relatively low. At this time, levels of active ERK signaling in each rhombomere during hindbrain patterning have not been defined.

Here I used a phospho-specific antibody to monitor the localization and intensity of pERK in the hindbrain during the late gastrula and early segmentation stages. I find that pERK is in r4 during the time of hindbrain patterning, but later becomes restricted to the mid-hindbrain boundary (MHB). I also discuss several challenges of quantifying pERK staining.

METHODS

Zebrafish care

Zebrafish were handled as discussed in Chapter II. All fish used here are from the Ekkwill wildtype line.

In situ RNA hybridization and immunostaining

For whole-mount *in situ* hybridization, embryos were fixed at the appropriate time point in 4% paraformaldehyde and stored in 100% methanol at

-20°C. RNA hybridization was performed as described and was followed by a color reaction using NBT/BCIP or INT/BCIP in 10% polyvinyl alcohol [102]. RNA probes for the following genes were produced by cloning a 900-1000bp fragment of the coding sequence into a vector and transcribing an anti-sense transcript: *fgf3*, *fgf8*, *hoxb1a*, and *krox20*.

For whole-mount immunostaining of pERK, embryos at the proper developmental time points were fixed in 4% paraformaldehyde overnight at 4°C, treated with 3% hydrogen peroxide in methanol for 1 hour on ice, and then stored in 100% methanol at -20°C. Antibody staining was then performed as described previously [166] using a rabbit anti-phospho-p44/42 MAPK ERK1/2 antibody (1:250; Cell Signaling Technology 4370) and a goat anti-rabbit IgG-HRP secondary antibody (1:1000; Abcam 6789). Signal was detected using the TSA Plus Fluorescein System (PerkinElmer). Embryos stained for pERK were counter-stained using a Valentino antibody, which was generated by immunizing rabbits with a GST-tagged full-length zebrafish Valentino protein, and a goat anti-rabbit Alexa Fluor 568 secondary antibody (1:200; Molecular Probes A110011).

For imaging, all stained embryos were suspended in 3% methyl cellulose. Images were captured using a Leica M165 FC microscope equipped with a Leica DFC310 FX camera. All images were imported into Adobe Photoshop and adjustments were limited to contrast, levels, and cropping; all adjustments were applied to the entire image.

RESULTS

pERK is localized to the central hindbrain and then shifts to the MHB

In order to examine the exact locations of ERK signaling during hindbrain development, I used a phospho-specific ERK antibody to label wildtype embryos in a time course. I chose to focus on the developmental stages when the neural tube is closing and the rhombomeres are being patterned. These stages range from late gastrula through mid-segmentation and include: 90%-epiboly (9hpf), bud (10hpf), 3-somite (11hpf), 6-somite (12hpf), 8-somite (13hpf), 10-somite (14hpf), and 14-somite (16hpf) [99]. Segmentation-period embryos were also counter-stained with a Valentino antibody to mark the location of r5 and r6.

During the late gastrula stages, I find that pERK is highly active in the central portion of the early hindbrain. At these early stages prior to the closure of the neural tube, the neural plate is wide and the presumptive rhombomeres are short in length and are arranged in a shallow chevron shape. The pattern of pERK staining observed here (Figure B.2A-B) appears broader than one rhombomere. Valentino is not yet expressed, so the size and location of the stained region is difficult to determine without a counter-stain. Additionally, pERK appears to be highly active in the posterior part of the embryo, which will later become the tailbud.

As the embryo enters the early segmentation stages and begins to develop defined somites, pERK appears to expand slightly (Figure B.2C-E). By 12hpf, there is a slight anterior expansion of the stained domain and this is

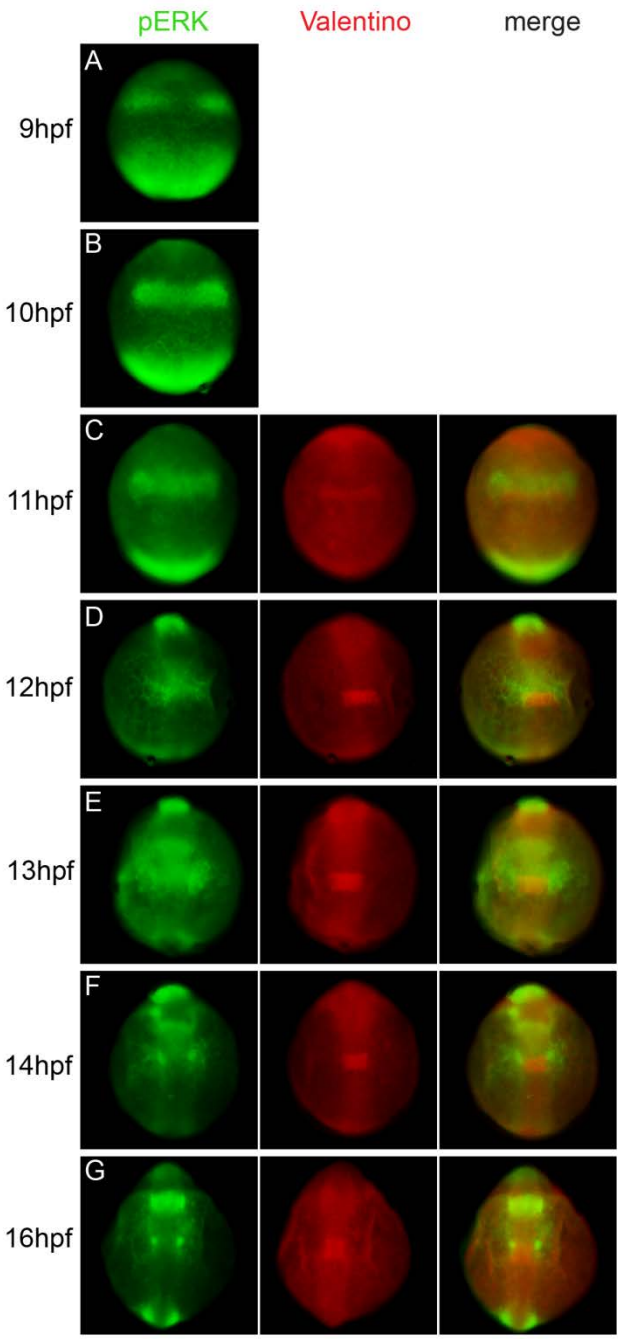

Figure B.2. ERK is active in r4 and shifts to the MHB at later stages
Wildtype embryos at 9hpf (**A**), 10hpf (**B**), 11hpf (**C**), 12hpf (**D**), 13hpf (**E**), 14hpf (**F**), and 16hpf (**G**) were assayed by immunostaining for pERK in green; red counterstain detects the Valentino transcription factor in r5 and r6. All embryos are in dorsal view with anterior to the top.

followed by a lateral expansion by 13hpf. The domain stained by Valentino, marking r5 and r6, is clearly visible directly posterior to the pERK domain. This proves that pERK is present in r4. Based on the size of both stained domains, it is likely pERK also extends into r2, r3, and also r5, as there appears to be some overlap with the Valentino stain (Figure B.2C-G).

In the following segmentation stages, there appears to be a more significant shift in the localization of pERK (Figure B.2F-G). The anterior expansion of pERK extends further to the presumptive MHB, while the pERK in the interior portion of r4 diminishes. This shift is more apparent by 16hpf, when there is high pERK at the MHB and none detectable inside the neural tube in r4.

DISCUSSION

During early hindbrain patterning, pERK is localized to r4 and the surrounding rhombomeres. As the embryo enters the segmentation stages, pERK shifts to become more active at the MHB and diminishes from r4.

ERK is highly active in r4 during hindbrain patterning

Based on the fact that r4 is not dependent on FGF/ERK signaling for its patterning and identity [47], I had hypothesized that levels of pERK might be lower in r4 relative to the surrounding rhombomeres. The results presented here indicated that this is not the case. At all the time points tested, I see high pERK in r4. Even at the stages when Valentino is not available as a marker of r5 and r6, it is likely that r4 is encompassed by the stained domain based on its size and

location. At later stages, the Valentino marker makes it clear that pERK is in r4. This indicates that despite no direct dependence of r4 identity on ERK signaling, pERK is highly active in this central region of the hindbrain.

As discussed in earlier chapters, there are many levels of regulation on the ERK signaling pathway [10–14,16]. It is possible that there are additional regulators that lie downstream of ERK. These factors could potentially interact with transcription factors or other target genes downstream of ERK. This would explain the visualization of high pERK without the resulting effects on hindbrain development. The possibility also remains that genes downstream of ERK are able to trigger effects in the surrounding rhombomeres in a non-cell autonomous manner.

ERK activity shifts from r4 to the MHB at later stages

By 13hpf, I see that the pERK domain begins to expand, anteriorly and laterally, and then eventually shifts away from r4 to the MHB. Interestingly, this shift is also seen in the expression of the FGF ligands [171]. Both *fgf3* and *fgf8* are expressed in r4 (Figure B.1A-B) first before shifting to the MHB. This provides a logical explanation for the shift in pERK localization, as the FGF ligands are required to initiate the FGF pathway and activate ERK. While FGF/ERK signaling has demonstrated roles in patterning the hindbrain, it also contributes to the formation and definition of the midbrain at later stages of development [59,172].

ERK activity is dynamic and pERK staining is variable

While antibody labeling with a phospho-specific antibody has provided novel information regarding the exact location of ERK activity, the staining technique has proven to be challenging. In many instances, embryos collected from the same clutch at the same developmental stage exhibited significantly different patterns of pERK staining. This effect manifested both in the intensity of the pERK signal (Figure B.3A-B) and in the localization or shape of the pERK signal (Figure B.3C-D), as well as at different time points. This observation brings into question the variability of ERK signaling, both cell-to-cell and embryo-to-embryo. There is evidence of cell-to-cell variability in levels of protein kinase signaling, and negative feedback regulators such as Dusp and Spry proteins are thought to act to minimize the variation [125,152]. Differences in gene expression and protein concentrations contribute to variability in signaling intensity among individual cells [126,127], and studies in various cell types and signaling pathways have identified roles for redundant regulators in reducing signal noise [128,129]. While this variability may account for some difference in pERK staining patterns, there are also technical challenges with this type of antibody labeling.

It is commonly assumed that all zebrafish embryos from a single clutch were fertilized at the same time and will be synchronized at each developmental stage. There is always the possibility that this is not the case, and embryos within a clutch can certainly vary from each other by several minutes. If slight differences in staging are able to affect the pERK staining pattern, it suggests that pERK is dynamic and can rapidly change through these developmental

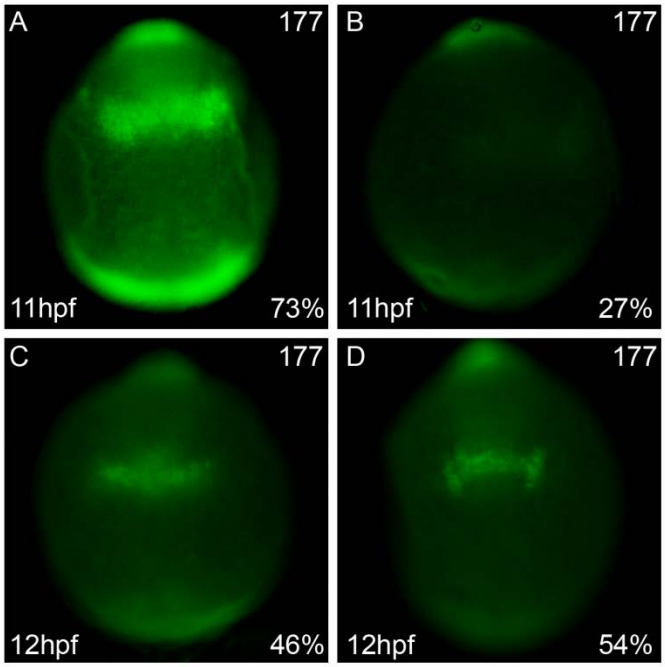

Figure B.3. ERK activity is dynamic and pERK staining is variable
Wildtype embryos at 11hpf (**A-B**) and 12hpf (**C-D**) were assayed by immunostaining for pERK. All embryos are in dorsal view with anterior to the top. Numbers in top right corner of each panel indicate the total number of embryos assayed for that condition. Numbers in bottom right corner indicate percent of embryos with the phenotype shown.

stages. While this can present a challenge to studying ERK activity, it can be overcome by analysis of embryos in a time course, as was done here.

Another explanation for the differing pERK staining patterns could simply be variability in staining. Embryos treated with an FGFR inhibitor show no pERK staining with this protocol, but despite this specificity, many clutches exhibited inconsistency in pERK staining pattern and intensity. The use of the phospho-specific antibody requires a complex protocol involving antigen retrieval and signal amplification. The tyramide used for the amplification prevents any further interactions with the primary antibody, allowing the use of a second primary antibody of the same species for the counter-stain. It is possible that a different protocol, or different antibodies, may provide better optimization and less variability in staining.

APPENDIX C:
EXPRESSION OF *dusp2* IS DEPENDENT ON FGF SIGNALING AND INDEPENDENT OF THE *hox* GENES

The data and discussion presented here will contribute to a future publication co-authored by Priyanjali Ghosh and Charles G. Sagerström.

INTRODUCTION

The *hox* genes are a family of well-conserved homeodomain-containing transcription factors that are responsible for defining the anterior-posterior axis during early vertebrate development [96,97]. In the hindbrain, *hox* genes play a key role in patterning the posterior rhombomeres [173]. A microarray screen performed by the Sagerström lab in 2011 revealed 100 hindbrain genes whose expression is up-regulated by the over-expression of *hoxb1b* [74]. Many of these genes, including *dusp2* had not been previously reported to play a role in hindbrain development. Since that time, several of the identified genes have been investigated in further detail by our lab [174] and others [175–177] revealing their roles in patterning the hindbrain and other body structures.

When we determined that *dusp2* homozygous mutants have no hindbrain defects or overt developmental phenotypes, we questioned the regulation of *dusp2* by *hoxb1b*. As previously discussed, *dusp2* is a member of FGF-synexpression group, along with *dusp6* and *spry1* [2,10–14,16,167]. Many genes in this group are expressed downstream of the FGF/ERK signaling pathway, and we questioned whether this was also the case for *dusp2* in the hindbrain.

To determine which transcription factors or signaling pathways regulate the expression of *dusp2*, we utilized germ line mutants and pharmacological inhibitors in a series of epistasis experiments. Here I demonstrate that *dusp2* is downstream of the FGF signaling pathway and is independent of *hox* gene expression. I also aimed to examine the relationship between the FGF signaling

pathway and the *hox* transcription factors, and my results indicate that these networks are independent of each other.

METHODS

Zebrafish care

Zebrafish were handled as discussed in Chapter II. The *hoxb1b* and *hoxb1a* mutant alleles, *hoxb1b*^{um197} and *hoxb1a*^{um191}*,* were generated as described previously [178].

Pharmacological inhibitor treatment

Inhibition of FGF receptors was achieved by treating embryos with SU5402 [47]. Wildtype embryos were treated with 50μM SU5402 dissolved in DMSO and diluted in egg water beginning at 7hpf. Control embryos were treated with an equal volume of DMSO diluted in egg water. The embryos remained in the treatment until fixation at 12hpf.

In situ RNA hybridization

For whole-mount *in situ* hybridization, embryos were fixed in 4% paraformaldehyde and stored in 100% methanol at -20°C. RNA hybridization was performed as described and was followed by a color reaction using NBT/BCIP or INT/BCIP in 10% polyvinyl alcohol [102]. RNA probes for the following genes were produced by cloning a 900-1000bp fragment of the coding sequence into a

vector and transcribing an anti-sense transcript: *dusp2*, *krox20*, *hoxb1a*, *fgf3*, and *fgf8*.

For imaging, stained embryos were suspended in 3% methyl cellulose. Images were captured using a Leica M165 FC microscope equipped with a Leica DFC310 FX camera. All images were imported into Adobe Photoshop and adjustments were limited to contrast, levels, and cropping; all adjustments were applied to the entire image.

RESULTS

Expression of dusp2 is absent in embryos with inhibited FGF signaling, but unaffected in hox mutants

To determine if signaling through the FGF receptor to the ERK pathway is necessary for *dusp2* expression, wildtype embryos were treated with a pharmacological inhibitor called SU5402. SU5402 interacts with the ligand binding domain of the four FGF receptors and specifically prevents all signaling through the receptor [179]. I questioned if the inhibition of FGF signaling could prevent *dusp2* expression, which normally begins at 10hpf. It has also been shown that patterning of the hindbrain depends on FGF signaling during a critical window of development between 80% epiboly and tailbud stages [47]. Considering these time points, I began treatment with SU5402 at 7hpf and continued until the embryos were fixed at 12hpf.

While embryos treated with the DMSO control exhibit normal *dusp2* expression (Figure C.1A), most embryos treated with SU5402 lack *dusp2* expression (Figure C.1B). As mentioned previously, the absence of FGF signaling will prevent the formation of r5 and r6, and this explains why only one *krox20* band (r3) is visible in the treated embryos.

In order to validate the previous report that *dusp2* is downstream of *hoxb1b*, I tested whether *dusp2* was expressed in *hoxb1b*$^{um197/um197}$ and *hoxb1a*$^{um191/+}$ mutants. These germ line mutants were generated in our lab several years ago and have hindbrain patterning phenotypes [178]. The *hoxb1b*$^{um197/um197}$ mutants survive to adulthood as a homozygous line, but *hoxb1a*$^{um191/um191}$ mutants do not, so crosses of heterozygous *hoxb1a*$^{um191/+}$ mutants were used. Interestingly, *dusp2* is expressed normally in the majority of embryos from both mutants at 12hpf (Figure C.1C-E). The *hoxb1b*$^{um197/um197}$ mutants have been shown to have a smaller r4 at 22hpf [178], but this size difference is not apparent at 12hpf.

The hox genes and FGF signaling are not dependent on each other

Since FGF signaling and the *hox* genes are two distinct drivers of hindbrain patterning, I questioned the relationship between them. Wildtype embryos treated with SU5402 have normal *hoxb1a* expression in r4 (Figure C.1F-G). Additionally, *fgf3* and *fgf8* are expressed normally in *hoxb1b*$^{um197/um197}$ and *hoxb1a*$^{um191/+}$ mutants (Figure C.1H-M). These results suggest that the *hox*

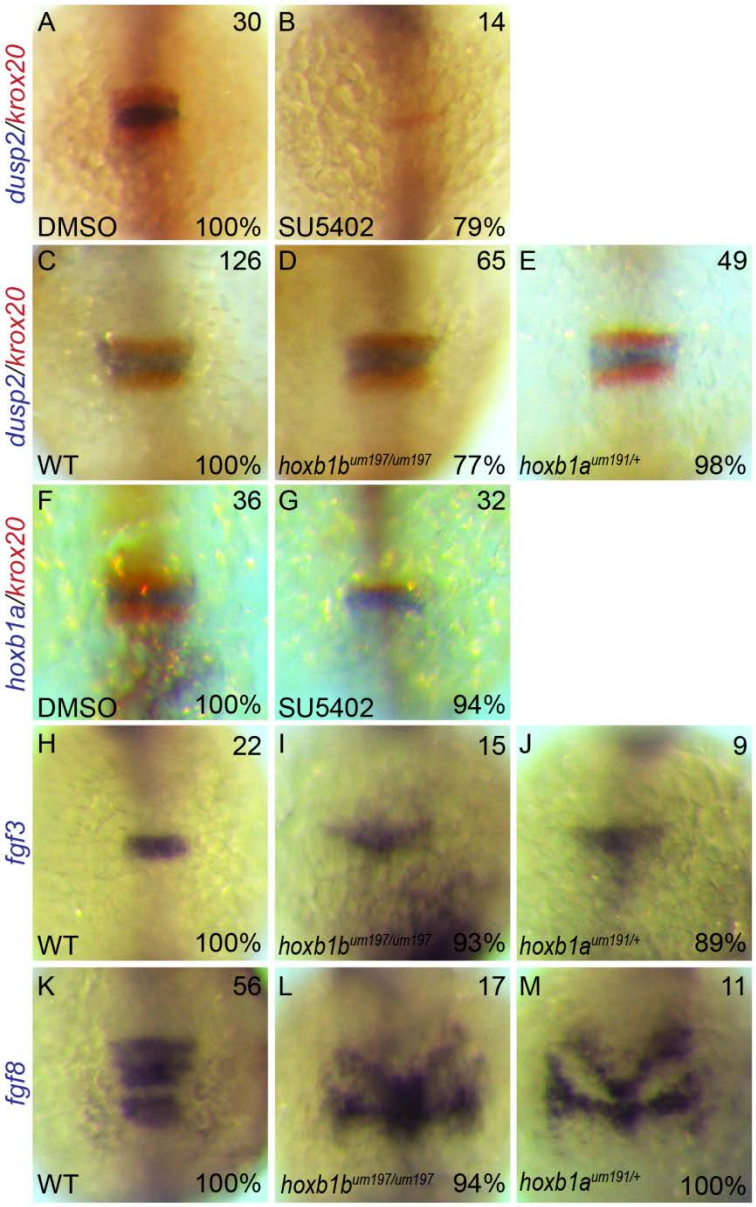

Figure C.1. Regulation of *dusp2* expression and networks in r4
Wildtype embryos were treated with either a DMSO control (**A, F**) or SU5402 (**B, G**), fixed at 12hpf, and assayed by *in situ* hybridization for the expression of *dusp2* or *hoxb1a* (blue stain) and *krox20* (red stain). 12hpf wildtype (**C, H, K**), *hoxb1b*$^{um197/um197}$ (**D, I, L**), and offspring of incrossed *hoxb1a*$^{um191/+}$ (**E, J, M**) embryos were assayed by *in situ* hybridization for the expression of *dusp2* (blue stain) and *krox20* (red stain) (**C-E**), *fgf3* (**H-J**), or *fgf8* (**K-M**). All embryos are in dorsal view with anterior to the top. Numbers in top right corner of each panel indicate the total number of embryos assayed for that condition. Numbers in bottom right corner indicate percent of embryos with the phenotype shown.

genes and FGF signaling are independent networks, and both contribute to the patterning of the hindbrain rhombomeres.

DISCUSSION

Using a series of epistasis experiments, germ line mutants, and a pharmacological inhibitor, I have demonstrated that *dusp2* is dependent on FGF signaling, but not the *hox* genes, and that the *hox* genes and FGF signaling are independent of each other.

dusp2 expression is dependent on FGF signaling and independent of hox gene expression

FGF signaling is required for the expression of *dusp2*, as *dusp2* expression is completely absent when FGF signaling is inhibited. In contrast, *dusp2* expression is normal in the absence of either *hoxb1b* or *hoxb1a*. Since *dusp2* is up-regulated when *hoxb1b* is over-expressed [74], I had expected *dusp2* expression to require the *hox* genes. Instead, it appears that FGF signaling solely drives *dusp2* expression. However, it remains possible that the *hox* genes could promote another factor capable of driving FGF signaling to up-regulate *dusp2*, rather than directly acting on *dusp2*.

FGF signaling and the hox genes are independent networks

I find that the FGF signaling pathway and the *hox* genes are independent of each other, as the expression of *hoxb1a* is not affected by the loss of FGF signaling and neither FGF ligand is affected by the loss of either *hox* gene. Interestingly, these results are not consistent with previous reports. Expression of *hoxb1a* has been reported to be lost in the presence of a dominant negative FGF receptor [59]. This report suggests that an early FGF signal is required for proper r4 patterning. While an ectopic dominant negative FGFR expressed from the one-cell stage would impact this early signal, the SU5402 treatment performed here would not as the embryos were not treated before 7hpf. This could provide an explanation as to why I find that *hoxb1a* expression is unaffected in SU5402-treated embryos, suggesting that FGF signaling is not required for *hoxb1a* expression. Additionally, it has been concluded that *hoxb1a* is required for r4-specific gene expression, as *fgf3* expression was reported to be significantly reduced in the *hoxb1b*$^{um197/um197}$ and *hoxb1a*$^{um191/um191}$ mutants [178]. This study assayed for the expression of *fgf3* at 14hpf, compared to 12hpf presented here. As discussed in Appendix B, the expression of the FGF ligands and ERK activity shift from r4 to the mid-hindbrain boundary during the segmentation stages. It is possible that the difference in stages here could account for the discrepancies in *fgf3* expression. My results show that three r4-specific genes, *fgf3, fgf8*, and *dusp2*, are all expressed at normal levels in the *hox* mutants, showing that they are independent of *hox* regulation at 12hpf.

REFERENCES

1. Krishna M, Narang H. The complexity of mitogen-activated protein kinases (MAPKs) made simple. Cell. Mol. Life Sci. 2008;65:3525–44.

2. Böttcher RT, Niehrs C. Fibroblast Growth Factor Signaling during Early Vertebrate Development. Endocr. Rev. 2005;26:63–77.

3. Widmann C, Gibson S, Jarpe MB, Johnson GL. Mitogen-activated protein kinase: conservation of a three-kinase module from yeast to human. Physiol. Rev. 1999;79:143–80.

4. Wasylyk B, Hagman J, Gutierrez-Hartmann A. Ets transcription factors: nuclear effectors of the Ras-MAP-kinase signaling pathway. Trends Biochem. Sci. 1998;23:213–6.

5. Sharrocks AD. The ETS-domain transcription factor family. Nat. Rev. Mol. Cell Biol. 2001;2:827–37.

6. Znosko WA, Yu S, Thomas K, Molina GA, Li C, Tsang W, et al. Overlapping functions of Pea3 ETS transcription factors in FGF signaling during zebrafish development. Dev. Biol. 2010;342:11–25.

7. Thisse C, Thisse B. Fast Release Clones: A High Throughput Expression Analysis. ZFIN Direct Data Submiss. 2004.

8. Roehl H, Nüsslein-Volhard C. Zebrafish pea3 and erm are general targets of FGF8 signaling. Curr. Biol. 2001;11:503–7.

9. Raible F, Brand M. Tight transcriptional control of the ETS domain factors Erm and Pea3 by Fgf signaling during early zebrafish development. Mech. Dev. 2001;107:105–17.

10. Kondoh K, Torii S, Nishida E. Control of MAP kinase signaling to the nucleus. Chromosoma. 2005;114:86–91.

11. Lemmon MA, Freed DM, Schlessinger J, Kiyatkin A. The Dark Side of Cell Signaling: Positive Roles for Negative Regulators. Cell. 2016;164:1172–84.

12. Shilo B-Z. The regulation and functions of MAPK pathways in Drosophila. Methods. 2014;68:151–9.

13. Niehrs C, Meinhardt H. Modular feedback. Nature. 2002;417:35–6.
14. Evans DRH, Hemmings BA. Signal transduction. What goes up must come down. Nature. 1998;394:23–4.

15. Tsang M, Dawid IB. Promotion and attenuation of FGF signaling through the Ras-MAPK pathway. Sci. STKE. 2004;2004:pe17.

16. Thisse B, Thisse C. Functions and regulations of fibroblast growth factor signaling during embryonic development. Dev. Biol. 2005;287:390–402.

17. Hacohen N, Kramer S, Sutherland D, Hiromi Y, Krasnow MA. sprouty encodes a novel antagonist of FGF signaling that patterns apical branching of the Drosophila airways. Cell. 1998;92:253–63.

18. Hanafusa H, Torii S, Yasunaga T, Nishida E. Sprouty1 and Sprouty2 provide a control mechanism for the Ras/MAPK signalling pathway. Nat. Cell Biol. 2002;4:850–8.

19. Casci T, Vinós J, Freeman M. Sprouty, an intracellular inhibitor of Ras signaling. Cell. 1999;96:655–65.

20. Reich A, Sapir A, Shilo B. Sprouty is a general inhibitor of receptor tyrosine kinase signaling. Development. 1999;126:4139–47.

21. Mahoney Rogers AA, Zhang J, Shim K. Sprouty1 and Sprouty2 limit both the size of the otic placode and hindbrain Wnt8a by antagonizing FGF signaling. Dev. Biol. 2011;353:94–104.

22. Furthauer M, Reifers F, Brand M, Thisse B, Thisse C. sprouty4 acts in vivo as a feedback-induced antagonist of FGF signaling in zebrafish. Development. 2001;128:2175–86.

23. Gross I, Bassit B, Benezra M, Licht JD. Mammalian sprouty proteins inhibit cell growth and differentiation by preventing ras activation. J. Biol. Chem. 2001;276:46460–8.

24. Yusoff P, Lao D-H, Ong SH, Wong ESM, Lim J, Lo TL, et al. Sprouty2 inhibits the Ras/MAP kinase pathway by inhibiting the activation of Raf. J. Biol. Chem. 2002;277:3195–201.

25. Sivak JM, Petersen LF, Amaya E. FGF Signal Interpretation Is Directed by Sprouty and Spred Proteins during Mesoderm Formation. Dev. Cell. 2005;8:689–701.

26. Caunt CJ, Keyse SM. Dual-specificity MAP kinase phosphatases (MKPs): shaping the outcome of MAP kinase signalling. FEBS J. 2013;280:489–504.

27. Patterson KI, Brummer T, O'Brien PM, Daly RJ. Dual-specificity phosphatases: critical regulators with diverse cellular targets. Biochem. J. 2009;418:475–89.

28. Camps M, Nichols A, Arkinstall S. Dual specificity phosphatases: a gene family for control of MAP kinase function. FASEB J. 2000;14:6–16.

29. Owens DM, Keyse SM. Differential regulation of MAP kinase signalling by dual-specificity protein phosphatases. Oncogene. 2007;26:3203–13.

30. Keyse SM. Protein phosphatases and the regulation of mitogen-activated protein kinase signalling. Curr. Opin. Cell Biol. 2000;12:186–92.

31. Tsang M, Friesel R, Kudoh T, Dawid IB. Identification of Sef, a novel modulator of FGF signalling. Nat. Cell Biol. 2002;4:165–9.

32. Fürthauer M, Lin W, Ang S-L, Thisse B, Thisse C. Sef is a feedback-induced antagonist of Ras/MAPK-mediated FGF signalling. Nat. Cell Biol. 2002;4:170–4.

33. Böttcher RT, Pollet N, Delius H, Niehrs C. The transmembrane protein XFLRT3 forms a complex with FGF receptors and promotes FGF signalling. Nat. Cell Biol. 2004;6:38–44.

34. Fey D, Croucher DR, Kolch W, Kholodenko BN. Crosstalk and signaling switches in mitogen-activated protein kinase cascades. Front. Physiol. 2012;3:355.

35. Itoh N, Ornitz DM. Fibroblast growth factors: from molecular evolution to roles in development, metabolism and disease. J. Biochem. 2011;149:121–30.

36. Dorey K, Amaya E. FGF signalling: diverse roles during early vertebrate embryogenesis. Development. 2010;137:3731–42.

37. Kuijk EW, van Tol LTA, Van de Velde H, Wubbolts R, Welling M, Geijsen N, et al. The roles of FGF and MAP kinase signaling in the segregation of the epiblast and hypoblast cell lineages in bovine and human embryos. Development. 2012;139:871–82.

38. Fan H-Y, Liu Z, Shimada M, Sterneck E, Johnson PF, Hedrick SM, et al. MAPK3/1 (ERK1/2) in ovarian granulosa cells are essential for female fertility. Science. 2009;324:938–41.

39. Zhang Y-L, Liu X-M, Ji S-Y, Sha Q-Q, Zhang J, Fan H-Y. ERK1/2 activities are dispensable for oocyte growth but are required for meiotic maturation and pronuclear formation in mouse. J. Genet. Genomics. 2015;42:477–85.

40. Fan H-Y, Shimada M, Liu Z, Cahill N, Noma N, Wu Y, et al. Selective expression of KrasG12D in granulosa cells of the mouse ovary causes defects in follicle development and ovulation. Development. 2008;135:2127–37.

41. Stulberg MJ, Lin A, Zhao H, Holley SA. Crosstalk between Fgf and Wnt signaling in the zebrafish tailbud. Dev. Biol. 2012;369:298–307.

42. Guillemot F, Zimmer C. From Cradle to Grave: The Multiple Roles of Fibroblast Growth Factors in Neural Development. Neuron. 2011;71:574–88.

43. Mason I. Initiation to end point: the multiple roles of fibroblast growth factors in neural development. Nat. Rev. Neurosci. 2007;8:583–96.

44. Hardcastle Z, Chalmers AD, Papalopulu N. FGF-8 stimulates neuronal differentiation through FGFR-4a and interferes with mesoderm induction in Xenopus embryos. Curr. Biol. 2000;10:1511–4.

45. Fletcher RB, Baker JC, Harland RM. FGF8 spliceforms mediate early mesoderm and posterior neural tissue formation in Xenopus. Development. 2006;133:1703–14.

46. Streit A, Berliner AJ, Papanayotou C, Sirulnik A, Stern CD. Initiation of neural induction by FGF signalling before gastrulation. Nature. 2000;406:74–8.

47. Walshe J, Maroon H, McGonnell IM, Dickson C, Mason I. Establishment of hindbrain segmental identity requires signaling by FGF3 and FGF8. Curr. Biol. 2002;12:1117–23.

48. Esain V, Postlethwait JH, Charnay P, Ghislain J. FGF-receptor signalling controls neural cell diversity in the zebrafish hindbrain by regulating olig2 and sox9. Development. 2010;137:33–42.

49. Kim EK, Choi E-J. Compromised MAPK signaling in human diseases: an update. Arch. Toxicol. 2015;89:867–82.

50. Moens CB, Prince VE. Constructing the hindbrain: insights from the zebrafish. Dev. Dyn. 2002;224:1–17.

51. Gavalas A. ArRAnging the hindbrain. Trends Neurosci. 2002;25:61–4.

52. Hébert JM. FGFs: Neurodevelopment’s Jack-of-all-Trades - How Do They Do it? Front. Neurosci. 2011;5:133.

53. Diez del Corral R, Storey KG. Opposing FGF and retinoid pathways: a signalling switch that controls differentiation and patterning onset in the extending vertebrate body axis. Bioessays. 2004;26:857–69.

54. Maves L, Jackman W, Kimmel CB. FGF3 and FGF8 mediate a rhombomere 4 signaling activity in the zebrafish hindbrain. Development. 2002;129:3825–37.

55. Ota S, Tonou-Fujimori N, Tonou-Fujimori N, Nakayama Y, Ito Y, Kawamura A, et al. FGF receptor gene expression and its regulation by FGF signaling during early zebrafish development. genesis. 2010;48:707–16.

56. Wiellette EL, Sive H. vhnf1 and Fgf signals synergize to specify rhombomere identity in the zebrafish hindbrain. Development. 2003;130:3821–9.

57. Reifers F, Böhli H, Walsh EC, Crossley PH, Stainier DY, Brand M. Fgf8 is mutated in zebrafish acerebellar (ace) mutants and is required for maintenance of midbrain-hindbrain boundary development and somitogenesis. Development. 1998;125:2381–95.

58. Wiellette EL, Sive H. Early requirement for fgf8 function during hindbrain pattern formation in zebrafish. Dev. Dyn. 2004;229:393–9.

59. Roy NM, Sagerström CG. An early Fgf signal required for gene expression in the zebrafish hindbrain primordium. Brain Res. Dev. Brain Res. 2004;148:27–42.

60. Aragon F, Pujades C. FGF signaling controls caudal hindbrain specification through Ras-ERK1/2 pathway. BMC Dev. Biol. 2009;9:61.

61. Marshall CJ. MAP kinase kinase kinase, MAP kinase kinase and MAP kinase. Curr. Opin. Genet. Dev. 1994;4:82–9.

62. Bermudez O, Pagès G, Gimond C. The dual-specificity MAP kinase phosphatases: critical roles in development and cancer. Am. J. Physiol. Cell Physiol. 2010;299:C189-202.

63. Muda M, Boschert U, Smith A, Antonsson B, Gillieron C, Chabert C, et al. Molecular cloning and functional characterization of a novel mitogen-activated protein kinase phosphatase, MKP-4. J. Biol. Chem. 1997;272:5141–51.

64. Keyse SM, Ginsburg M. Amino acid sequence similarity between CL100, a dual-specificity MAP kinase phosphatase and cdc25. Trends Biochem. Sci. 1993;18:377–8.

65. Tanoue T, Adachi M, Moriguchi T, Nishida E. A conserved docking motif in MAP kinases common to substrates, activators and regulators. Nat. Cell Biol. 2000;2:110–6.

66. Denu JM, Dixon JE. Protein tyrosine phosphatases: mechanisms of catalysis and regulation. Curr. Opin. Chem. Biol. 1998;2:633–41.

67. Rohan PJ, Davis P, Moskaluk CA, Kearns M, Krutzsch H, Siebenlist U, et al. PAC-1: a mitogen-induced nuclear protein tyrosine phosphatase. Science. 1993;259:1763–6.

68. Grumont RJ, Rasko JE, Strasser A, Gerondakis S. Activation of the mitogen-activated protein kinase pathway induces transcription of the PAC-1 phosphatase gene. Mol. Cell. Biol. 1996;16:2913–21.

69. Ward Y, Gupta S, Jensen P, Wartmann M, Davis RJ, Kelly K. Control of MAP kinase activation by the mitogen-induced threonine/tyrosine phosphatase PAC1. Nature. 1994;367:651–4.

70. Zhang Q, Muller M, Chen CH, Zeng L, Farooq A, Zhou M-M. New insights into the catalytic activation of the MAPK phosphatase PAC-1 induced by its substrate MAPK ERK2 binding. J. Mol. Biol. 2005;354:777–88.

71. Chu Y, Solski PA, Khosravi-Far R, Der CJ, Kelly K. The mitogen-activated protein kinase phosphatases PAC1, MKP-1, and MKP-2 have unique substrate specificities and reduced activity in vivo toward the ERK2 sevenmaker mutation. J. Biol. Chem. 1996;271:6497–501.

72. Jeffrey KL, Brummer T, Rolph MS, Liu SM, Callejas NA, Grumont RJ, et al. Positive regulation of immune cell function and inflammatory responses by phosphatase PAC-1. Nat. Immunol. 2006;7:274–83.

73. Lancaster GI, Kraakman MJ, Kammoun HL, Langley KG, Estevez E, Banerjee A, et al. The dual-specificity phosphatase 2 (DUSP2) does not regulate obesity-associated inflammation or insulin resistance in mice. PLoS One. 2014;9:e111524.

74. Choe S-K, Zhang X, Hirsch N, Straubhaar J, Sagerström CG. A screen for hoxb1-regulated genes identifies ppp1r14al as a regulator of the rhombomere 4 Fgf-signaling center. Dev. Biol. 2011;358:356–67.

75. Groom LA, Sneddon AA, Alessi DR, Dowd S, Keyse SM. Differential regulation of the MAP, SAP and RK/p38 kinases by Pyst1, a novel cytosolic dual-specificity phosphatase. EMBO J. 1996;15:3621–32.

76. Kim Y, Rice AE, Denu JM. Intramolecular dephosphorylation of ERK by MKP3. Biochemistry. 2003;42:15197–207.

77. Kawakami Y, Rodríguez-León J, Koth CM, Büscher D, Itoh T, Raya A, et al. MKP3 mediates the cellular response to FGF8 signalling in the vertebrate limb. Nat. Cell Biol. 2003;5:513–9.

78. Eblaghie MC, Lunn JS, Dickinson RJ, Münsterberg AE, Sanz-Ezquerro JJ, Farrell ER, et al. Negative feedback regulation of FGF signaling levels by Pyst1/MKP3 in chick embryos. Curr. Biol. 2003;13:1009–18.

79. Dickinson RJ, Eblaghie MC, Keyse SM, Morriss-Kay GM. Expression of the ERK-specific MAP kinase phosphatase PYST1/MKP3 in mouse embryos during morphogenesis and early organogenesis. Mech. Dev. 2002;113:193–6.

80. Ndong C, Landry RP, Saha M, Romero-Sandoval EA. Mitogen-activated protein kinase (MAPK) phosphatase-3 (MKP-3) displays a p-JNK-MAPK substrate preference in astrocytes in vitro. Neurosci. Lett. 2014;575:13–8.

81. Li C, Scott DA, Hatch E, Tian X, Mansour SL. Dusp6 (Mkp3) is a negative feedback regulator of FGF-stimulated ERK signaling during mouse development. Development. 2007;134:167–76.

82. Molina GA, Watkins SC, Tsang M. Generation of FGF reporter transgenic zebrafish and their utility in chemical screens. BMC Dev. Biol. 2007;7:62.

83. Maillet M, Purcell NH, Sargent MA, York AJ, Bueno OF, Molkentin JD. DUSP6 (MKP3) null mice show enhanced ERK1/2 phosphorylation at baseline and increased myocyte proliferation in the heart affecting disease susceptibility. J. Biol. Chem. 2008;283:31246–55.

84. Tsang M, Maegawa S, Kiang A, Habas R, Weinberg E, Dawid IB. A role for MKP3 in axial patterning of the zebrafish embryo. Development. 2004;131:2769–79.

85. Fürthauer M, Thisse C, Thisse B. A role for FGF-8 in the dorsoventral patterning of the zebrafish gastrula. Development. 1997;124:4253–64.

86. Kok FO, Shin M, Ni C-W, Gupta A, Grosse AS, van Impel A, et al. Reverse genetic screening reveals poor correlation between morpholino-induced and mutant phenotypes in zebrafish. Dev. Cell. 2015;32:97–108.

87. Rossi A, Kontarakis Z, Gerri C, Nolte H, Hölper S, Krüger M, et al. Genetic compensation induced by deleterious mutations but not gene knockdowns. Nature. 2015;524:230–3.

88. Stainier DYR, Kontarakis Z, Rossi A. Making Sense of Anti-Sense Data. Dev. Cell. 2015;32:7–8.

89. Gerety SS, Wilkinson DG. Morpholino artifacts provide pitfalls and reveal a novel role for pro-apoptotic genes in hindbrain boundary development. Dev. Biol. 2011;350:279–89.

90. Miraoui H, Dwyer AA, Sykiotis GP, Plummer L, Chung W, Feng B, et al. Mutations in FGF17, IL17RD, DUSP6, SPRY4, and FLRT3 are identified in individuals with congenital hypogonadotropic hypogonadism. Am. J. Hum. Genet. 2013;92:725–43.

91. Hwang WY, Fu Y, Reyon D, Maeder ML, Tsai SQ, Sander JD, et al. Efficient genome editing in zebrafish using a CRISPR-Cas system. Nat. Biotechnol. 2013;31:227–9.

92. Ochi H, Ogino H, Kageyama Y, Yasuda K. The Stability of the Lens-specific Maf Protein is Regulated by Fibroblast Growth Factor (FGF)/ERK Signaling in Lens Fiber Differentiation. J. Biol. Chem. 2003;278:537–44.

93. Weisinger K, Kohl A, Kayam G, Monsonego-Ornan E, Sela-Donenfeld D. Expression of hindbrain boundary markers is regulated by FGF3. Biol. Open. 2012;1:67–74.

94. Weisinger K, Kayam G, Missulawin-Drillman T, Sela-Donenfeld D. Analysis of expression and function of FGF-MAPK signaling components in the hindbrain reveals a central role for FGF3 in the regulation of Krox20, mediated by Pea3. Dev. Biol. 2010;344:881–95.

95. Smith TG, Karlsson M, Lunn JS, Eblaghie MC, Keenan ID, Farrell ER, et al. Negative feedback predominates over cross-regulation to control ERK MAPK activity in response to FGF signalling in embryos. FEBS Lett. 2006;580:4242–5.

96. McGinnis W, Krumlauf R. Homeobox genes and axial patterning. Cell. 1992;68:283–302.

97. Amores A, Force A, Yan YL, Joly L, Amemiya C, Fritz A, et al. Zebrafish hox clusters and vertebrate genome evolution. Science. 1998;282:1711–4.

98. Kim SC, Hahn JS, Min YH, Yoo NC, Ko YW, Lee WJ. Constitutive activation of extracellular signal-regulated kinase in human acute leukemias: combined role of activation of MEK, hyperexpression of extracellular signal-regulated kinase, and downregulation of a phosphatase, PAC1. Blood. 1999;93:3893–9.

99. Kimmel CB, Ballard WW, Kimmel SR, Ullmann B, Schilling TF. Stages of embryonic development of the zebrafish. Dev. Dyn. 1995;203:253–310.

100. Gagnon JA, Valen E, Thyme SB, Huang P, Ahkmetova L, Pauli A, et al. Efficient Mutagenesis by Cas9 Protein-Mediated Oligonucleotide Insertion and Large-Scale Assessment of Single-Guide RNAs. Riley B, editor. PLoS One. 2014;9:e98186.

101. Dolphin [Internet]. Available from: http://www.umassmed.edu/biocore/introducing-dolphin/

102. Hauptmann G, Gerster T. Multicolor Whole-Mount In Situ Hybridization. Dev. Biol. Protoc. New Jersey: Humana Press; 2000. p. 139–48.

103. Zannino DA, Sagerström CG, Appel B. olig2-Expressing hindbrain cells are required for migrating facial motor neurons. Dev. Dyn. 2012;241:315–26.

104. Zhou B, Zhang J, Liu S, Reddy S, Wang F, Zhang Z-Y. Mapping ERK2-MKP3 binding interfaces by hydrogen/deuterium exchange mass spectrometry. J. Biol. Chem. 2006;281:38834–44.

105. ZFIN The Zebrafish Information Network [Internet]. Available from: http://zfin.org/

106. PANTHER - Gene List Analysis [Internet]. Available from: http://pantherdb.org/

107. Mi H, Thomas P. PANTHER Pathway: An Ontology-Based Pathway Database Coupled with Data Analysis Tools. Humana Press; 2009. p. 123–40.

108. Mi H, Huang X, Muruganujan A, Tang H, Mills C, Kang D, et al. PANTHER version 11: expanded annotation data from Gene Ontology and Reactome pathways, and data analysis tool enhancements. Nucleic Acids Res. Oxford University Press; 2017;45:D183–9.

109. ZFIN Downloads Archive [Internet]. Available from: http://zfin.org/downloads

110. Hendzel MJ, Wei Y, Mancini MA, Van Hooser A, Ranalli T, Brinkley BR, et al. Mitosis-specific phosphorylation of histone H3 initiates primarily within pericentromeric heterochromatin during G2 and spreads in an ordered fashion coincident with mitotic chromosome condensation. Chromosoma. 1997;106:348–60.

111. Budirahardja Y, Gönczy P. Coupling the cell cycle to development. Development. 2009;136:2861–72.

112. Lee MT, Bonneau AR, Takacs CM, Bazzini AA, DiVito KR, Fleming ES, et al. Nanog, Pou5f1 and SoxB1 activate zygotic gene expression during the maternal-to-zygotic transition. Nature. 2013;503:360–4.

113. González-Fernández L, Ortega-Ferrusola C, Macias-Garcia B, Salido GM, Peña FJ, Tapia JA. Identification of protein tyrosine phosphatases and dual-specificity phosphatases in mammalian spermatozoa and their role in sperm motility and protein tyrosine phosphorylation. Biol. Reprod. 2009;80:1239–52.

114. Nagahama Y, Yamashita M. Regulation of oocyte maturation in fish. Dev. Growth Differ. 2008;50:S195–219.

115. Donaubauer EM, Law NC, Hunzicker-Dunn ME. Follicle-Stimulating Hormone (FSH)-dependent Regulation of Extracellular Regulated Kinase (ERK) Phosphorylation by the Mitogen-activated Protein (MAP) Kinase Phosphatase MKP3. J. Biol. Chem. 2016;291:19701–12.

116. Sen A, Caiazza F. Oocyte maturation: a story of arrest and release. Front. Biosci. (Schol. Ed). 2013;5:451–77.

117. Su Y-Q, Denegre JM, Wigglesworth K, Pendola FL, O'Brien MJ, Eppig JJ. Oocyte-dependent activation of mitogen-activated protein kinase (ERK1/2) in cumulus cells is required for the maturation of the mouse oocyte-cumulus cell complex. Dev. Biol. 2003;263:126–38.

118. Prochazka R, Blaha M. Regulation of mitogen-activated protein kinase 3/1 activity during meiosis resumption in mammals. J. Reprod. Dev. 2015;61:495–502.

119. Sette C, Barchi M, Bianchini A, Conti M, Rossi P, Geremia R. Activation of the mitogen-activated protein kinase ERK1 during meiotic progression of mouse pachytene spermatocytes. J. Biol. Chem. 1999;274:33571–9.

120. Di Agostino S, Rossi P, Geremia R, Sette C. The MAPK pathway triggers activation of Nek2 during chromosome condensation in mouse spermatocytes. Development. 2002;129:1715–27.

121. Di Agostino S, Fedele M, Chieffi P, Fusco A, Rossi P, Geremia R, et al. Phosphorylation of high-mobility group protein A2 by Nek2 kinase during the first meiotic division in mouse spermatocytes. Mol. Biol. Cell. 2004;15:1224–32.

122. Griswold MD. The central role of Sertoli cells in spermatogenesis. Semin. Cell Dev. Biol. 1998;9:411–6.

123. Cheng J, Watkins SC, Walker WH. Testosterone Activates Mitogen-Activated Protein Kinase via Src Kinase and the Epidermal Growth Factor Receptor in Sertoli Cells. Endocrinology. 2007;148:2066–74.

124. Almog T, Lazar S, Reiss N, Etkovitz N, Milch E, Rahamim N, et al. Identification of extracellular signal-regulated kinase 1/2 and p38 MAPK as regulators of human sperm motility and acrosome reaction and as predictors of poor spermatozoan quality. J. Biol. Chem. 2008;283:14479–89.

125. Jeschke M, Baumgartner S, Legewie S. Determinants of Cell-to-Cell Variability in Protein Kinase Signaling. PLoS Comput. Biol. 2013;9:e1003357.

126. Spencer SL, Gaudet S, Albeck JG, Burke JM, Sorger PK. Non-genetic origins of cell-to-cell variability in TRAIL-induced apoptosis. Nature. 2009;459:428–32.

127. Feinerman O, Veiga J, Dorfman JR, Germain RN, Altan-Bonnet G. Variability and robustness in T cell activation from regulated heterogeneity in protein levels. Science. 2008;321:1081–4.

128. Ferrell JE. Tripping the switch fantastic: how a protein kinase cascade can convert graded inputs into switch-like outputs. Trends Biochem. Sci. 1996;21:460–6.

129. Cheong R, Rhee A, Wang CJ, Nemenman I, Levchenko A. Information Transduction Capacity of Noisy Biochemical Signaling Networks. Science (80). 2011;334:354–8.

130. Maro B, Johnson MH, Webb M, Flach G. Mechanism of polar body formation in the mouse oocyte: an interaction between the chromosomes, the cytoskeleton and the plasma membrane. J. Embryol. Exp. Morphol. 1986;92:11–32.

131. Schmerler S, Wessel GM. Polar bodies--more a lack of understanding than a lack of respect. Mol. Reprod. Dev. 2011;78:3–8.

132. Xu B, Yang L, Lye RJ, Hinton BT. p-MAPK1/3 and DUSP6 regulate epididymal cell proliferation and survival in a region-specific manner in mice. Biol. Reprod. Oxford University Press; 2010;83:807–17.

133. Johnson KJ, Hensley JB, Kelso MD, Wallace DG, Gaido KW. Mapping gene expression changes in the fetal rat testis following acute dibutyl phthalate exposure defines a complex temporal cascade of responding cell types. Biol. Reprod. 2007;77:978–89.

134. (Yön) NDK, Aytekin Y, Yüce R. Ovary maturation stages and histological investigation of ovary of the zebrafish. Brazilian Arch. Biol. Technol. An Int. J. 2008;51:513–22.

135. Draper BW, McCallum CM, Moens CB. nanos1 is required to maintain oocyte production in adult zebrafish. Dev. Biol. 2007;305:589–98.

136. Dranow DB, Hu K, Bird AM, Lawry ST, Adams MT, Sanchez A, et al. Bmp15 Is an Oocyte-Produced Signal Required for Maintenance of the Adult Female Sexual Phenotype in Zebrafish. Mullins MC, editor. PLoS Genet. 2016;12:e1006323.

137. Gautier A, Sohm F, Joly J-S, Le Gac F, Lareyre J-J. The Proximal Promoter Region of the Zebrafish gsdf Gene Is Sufficient to Mimic the Spatio-Temporal Expression Pattern of the Endogenous Gene in Sertoli and Granulosa Cells. Biol. Reprod. 2011;85:1240–51.

138. Potapova T, Gorbsky G. The Consequences of Chromosome Segregation Errors in Mitosis and Meiosis. Biology (Basel). Multidisciplinary Digital Publishing Institute; 2017;6:12.

139. Poss KD, Nechiporuk A, Stringer KF, Lee C, Keating MT. Germ cell aneuploidy in zebrafish with mutations in the mitotic checkpoint gene mps1. Genes Dev. 2004;18:1527–32.

140. Westerfield M. The zebrafish book: a guide for the laboratory use of zebrafish. 4th ed. Eugene, OR: University of Oregon Press; 2000.

141. Kovács T, Békési G, Fábián Á, Rákosy Z, Horváth G, Mátyus L, et al. DNA flow cytometry of human spermatozoa: Consistent stoichiometric staining of sperm DNA using a novel decondensation protocol. Cytom. Part A. 2008;73A:965–70.

142. Handyside AH. 24-chromosome copy number analysis: a comparison of available technologies. Fertil. Steril. 2013;100:595–602.

143. Lu S, Zong C, Fan W, Yang M, Li J, Chapman AR, et al. Probing Meiotic Recombination and Aneuploidy of Single Sperm Cells by Whole-Genome Sequencing. Science (80-.). 2012;338:1627–30.

144. Reyes JM, Ross PJ. Cytoplasmic polyadenylation in mammalian oocyte maturation. Wiley Interdiscip. Rev. RNA. 2016;7:71–89.

145. Holt JE, Stanger SJ, Nixon B, McLaughlin EA. Non-coding RNA in Spermatogenesis and Epididymal Maturation. Adv. Exp. Med. Biol. 2016. p. 95–120.

146. Yadav RP, Kotaja N. Small RNAs in spermatogenesis. Mol. Cell. Endocrinol. 2014;382:498–508.

147. Wang L, Xu C. Role of microRNAs in mammalian spermatogenesis and testicular germ cell tumors. Reproduction. 2015;149:R127–37.

148. Rando OJ. Intergenerational Transfer of Epigenetic Information in Sperm. Cold Spring Harb. Perspect. Med. 2016;6:a022988.

149. Anderson D, Schmid T, Baumgartner A. Male-mediated developmental toxicity. Asian J. Androl. 2014;16:81.

150. Wang Y, Navin NE. Advances and applications of single-cell sequencing technologies. Mol. Cell. NIH Public Access; 2015;58:598–609.

151. Liu Q, Li Y, Feng Y, Liu C, Ma J, Li Y, et al. Single-cell analysis of differences in transcriptomic profiles of oocytes and cumulus cells at GV, MI, MII stages from PCOS patients. Sci. Rep. 2016;6:39638.

152. de la Cova C, Townley R, Regot S, Greenwald I. A Real-Time Biosensor for ERK Activity Reveals Signaling Dynamics during C. elegans Cell Fate Specification. Dev. Cell. 2017;

153. Walker MB, Kimmel CB. A two-color acid-free cartilage and bone stain for zebrafish larvae. Biotech. Histochem. 2007;82:23–8.

154. Ornitz DM, Itoh N. The Fibroblast Growth Factor signaling pathway. Wiley Interdiscip. Rev. Dev. Biol. 2015;4:215–66.

155. Wehner D, Weidinger G. Signaling networks organizing regenerative growth of the zebrafish fin. Trends Genet. 2015;31:336–43.

156. Goldshmit Y, Sztal TE, Jusuf PR, Hall TE, Nguyen-Chi M, Currie PD. Fgf-Dependent Glial Cell Bridges Facilitate Spinal Cord Regeneration in Zebrafish. J. Neurosci. 2012;32:7477–92.

157. Topp S, Stigloher C, Komisarczuk AZ, Adolf B, Becker TS, Bally-Cuif L. Fgf signaling in the zebrafish adult brain: association of Fgf activity with ventricular zones but not cell proliferation. J. Comp. Neurol. 2008;510:422–39.

158. Katoh M, Nakagama H. FGF Receptors: Cancer Biology and Therapeutics. Med. Res. Rev. 2014;34:280–300.

159. Wee P, Wang Z. Epidermal Growth Factor Receptor Cell Proliferation Signaling Pathways. Cancers (Basel). 2017;9:52.

160. Fearon AE, Gould CR, Grose RP. FGFR signalling in women's cancers. Int. J. Biochem. Cell Biol. 2013;45:2832–42.

161. Minowada G, Jarvis LA, Chi CL, Neubüser A, Sun X, Hacohen N, et al. Vertebrate Sprouty genes are induced by FGF signaling and can cause chondrodysplasia when overexpressed. Development. 1999;126:4465–75.

162. Komisarczuk AZ, Topp S, Stigloher C, Kapsimali M, Bally-Cuif L, Becker TS. Enhancer detection and developmental expression of zebrafish sprouty1, a member of the fgf8 synexpression group. Dev. Dyn. 2008;237:2594–603.

163. Guy GR, Jackson RA, Yusoff P, Chow SY. Sprouty proteins: modified modulators, matchmakers or missing links? J. Endocrinol. 2009;203:191–202.

164. Lin W, Jing N, Basson MA, Dierich A, Licht J, Ang S-L. Synergistic activity of Sef and Sprouty proteins in regulating the expression of Gbx2 in the mid-hindbrain region. Genesis. 2005;41:110–5.

165. Edwin F, Anderson K, Ying C, Patel TB. Intermolecular interactions of Sprouty proteins and their implications in development and disease. Mol. Pharmacol. 2009;76:679–91.

166. Shin M, Male I, Beane TJ, Villefranc JA, Kok FO, Zhu LJ, et al. Vegfc acts through ERK to induce sprouting and differentiation of trunk lymphatic progenitors. Development. 2016;143:3785–95.

167. Basson MA, Echevarria D, Petersen Ahn C, Sudarov A, Joyner AL, Mason IJ, et al. Specific regions within the embryonic midbrain and cerebellum require different levels of FGF signaling during development. Development. 2008;135:889–98.

168. Rohs P, Ebert AM, Zuba A, McFarlane S. Neuronal expression of fibroblast growth factor receptors in zebrafish. Gene Expr. Patterns. 2013;13:354–61.

169. Maroon H, Walshe J, Mahmood R, Kiefer P, Dickson C, Mason I. Fgf3 and Fgf8 are required together for formation of the otic placode and vesicle. Development. 2002;129:2099–108.

170. Phillips BT, Bolding K, Riley BB. Zebrafish fgf3 and fgf8 encode redundant functions required for otic placode induction. Dev. Biol. 2001;235:351–65.

171. Kudoh T, Tsang M, Hukriede NA, Chen X, Dedekian M, Clarke CJ, et al. A Gene Expression Screen in Zebrafish Embryogenesis. Genome Res. 2001;11:1979–87.

172. Miyake A, Itoh N. Fgf22 regulated by Fgf3/Fgf8 signaling is required for zebrafish midbrain development. Biol. Open. 2013;2:515–24.

173. Tümpel S, Wiedemann LM, Krumlauf R. Chapter 8 Hox Genes and Segmentation of the Vertebrate Hindbrain. Curr. Top. Dev. Biol. 2009. p. 103–37.

174. Zannino DA, Downes GB, Sagerström CG. prdm12b specifies the p1 progenitor domain and reveals a role for V1 interneurons in swim movements. Dev. Biol. 2014;390:247–60.

175. Wang X, Wang X, Yuan W, Chai R, Liu D. Egfl6 is involved in zebrafish notochord development. Fish Physiol. Biochem. 2015;41:961–9.

176. Kim YS, Jung S-H, Jung DH, Choi S-J, Lee Y-R, Kim JS. Gas6 Stimulates Angiogenesis of Human Retinal Endothelial Cells and of Zebrafish Embryos via ERK1/2 Signaling. PLoS One. 2014;9:e83901.

177. Sahu SK, Fritz A, Tiwari N, Kovacs Z, Pouya A, Wüllner V, et al. TOX3 regulates neural progenitor identity. Biochim. Biophys. Acta - Gene Regul. Mech. 2016;1859:833–40.

178. Weicksel SE, Gupta A, Zannino DA, Wolfe SA, Sagerström CG. Targeted germ line disruptions reveal general and species-specific roles for paralog group 1 hox genes in zebrafish. BMC Dev. Biol. 2014;14:25.

179. Mohammadi M, McMahon G, Sun L, Tang C, Hirth P, Yeh BK, et al. Structures of the tyrosine kinase domain of fibroblast growth factor receptor in complex with inhibitors. Science. 1997;276:955–60.